UNIVERSITÀ DEGLI STUDI DI MILANO

Department of Agricultural and Environmental Sciences

Production, Landscape, Agroenergy (DiSAA)

PhD School in Plant Biology and Crop Production

Disciplinary sector: Agricultural Genetics (AGR/07)

Genetic dissection of developmental traits in barley (*Hordeum vulgare*).

PhD program coordinator: Prof. Piero Bianco

Supervisor: Dr. Laura Rossini

Co-supervisors: Dr. Elahe Tavakol and Dr. Luigi Cattivelli

PhD candidate: Gabriele Verderio

XXVII cycle

Summary

ABSTRACT 3
1 INTRODUCTION 6
1.1 ECONOMIC IMPORTANCE 6
1.2 BARLEY PLANT ARCHITECTURE AND DEVELOPMENT, A BRIEF SUMMARY 7
1.3 ORIGIN 11
1.4 ORIGINS OF MODERN EUROPEAN CULTIVARS 11
1.5 CURRENT PERSPECTIVES IN BARLEY BREEDING 12
1.6 THE CEREAL IDEOTYPE 12
1.7 BARLEY GENOMIC STRUCTURE AND PHYSICAL MAP 14
1.8 MARKERS, GENETIC MAPS AND GENOMIC TOOLS 15
1.9 BARLEY GENETIC RESOURCES 17
1.9.1 MUTATION RESEARCH 17
1.9.2 GENETIC DISSECTION OF MENDELIAN TRAITS 18
1.9.3 GENETIC DISSECTION OF QUANTITATIVE TRAITS 19
1.9.3.1 QTL MAPPING 19
1.9.3.2 ASSOCIATION MAPPING 19
1.10 SCOPE AND OBJECTIVE 31
2. ASSOCIATION MAPPING ON TRAITS RELATED TO SHOOT ARCHITECTURE 33
2.1 INTRODUCTION 33
2.1.1 THE BARLEY PHYTOMER AND PLANT DEVELOPMENT 33
2.1.2 LEAF DEVELOPMENT 34
2.1.3 TILLERING 38
2.1.4 PLANT HEIGHT 46
2.1.5 STEM DIAMETER 47
2.1.6 FLOWERING DATE AND SPIKE DEVELOPMENT 49
2.2 SCOPE OF THE WORK 54
2.3 MATERIAL AND METHODS 54
2.3.1 PLANT MATERIALS AND PHENOTYPING 54
2.3.2 GWAS GENOTYPING 55
2.3.3 STATISTICAL ANALYSES-PHENOTYPE 60

2.3.3 STATISTICAL ANALYSIS - POPULATION STRUCTURE, LINKAGE DISEQUILIBRIUM AND GWAS ANALYSES 61
2.4 RESULTS 62
2.4.1 POPULATION STRUCTURE AND LINKAGE DISEQUILIBRIUM 62
2.4.2 PHENOTYPIC VARIATION AND GENOME-WIDE ASSOCIATION SCANS 63
2 .4 DISCUSSION 76
3. EXPLORATION OF GENETIC VARIATION FOR ROOT EXTENSION IN WINTER BARLEY 81
3.1 INTRODUCTION 81
3.1.1 BARLEY ROOT ANATOMY 81
3.1.2 GENETIC AND HORMONAL CONTROL OF ROOT DEVELOPMENT AND ARCHITECTURE 85
3.1.3 ENVIRONMENTAL FACTORS INFLUENCING ROOT DEVELOPMENT 88
3.1.4 NATURAL VARIATION 89
3.1.5 BARLEY ROOT MUTANTS 91
3.2 OBJECTIVES 92
3.3 MATERIALS AND METHODS 92
3.3.1 GENETIC MATERIALS 92
2.4.2 GREENHOUSE TRIAL EXPERIMENTAL CONDITIONS 93
2.4.3 GROWTH CHAMBER TRIAL EXPERIMENTAL CONDITIONS 93
3.5 RESULTS AND DISCUSSION 98
4. MORPHOLOGICAL CHARACTERIZATION OF *mnd6.6*, A BARLEY HIGH TILLERING MUTANT 102
4.1 INTRODUCTION 102
4.2 OBJECTIVE 105
4.3 MATERIAL AND METHODS 105
4.3.1 GENETIC MATERIAL 105
4.3.2 GARDEN EXPERIMENT 106
4.3.3 GROWTH CHAMBER EXPERIMENT 106
4.3.4 DATA ANALYSES 107
4.4 RESULTS 108
4.4.1 OVERALL PHENOTYPES OF *mnd6.6* MATURE PLANTS 108
4.4.2 DEVELOPMENTAL ANALYSIS OF THE HIGH-TILLERING PHENOYPE OF THE *mnd6.6* MUTANT 109
4.4 DISCUSSION 121
5. CONCLUSIONS 123
REFERENCES 127

ABSTRACT

Genetic dissection of developmental traits in barley (*Hordeum vulgare*).

Barley (*Hordeum vulgare*) ranks in fourth place among cultivated cereals for worldwide production and is a recognized model organism for genetic and genomic studies in the *Triticeae* tribe, which includes wheats (*Triticum* species) and rye (*Secale cereale*). Root and shoot architecture traits are key factors in plant performance, competition with weeds, adaptation and stress responses thus having an important impact on yield and yield stability. Breeders have proposed hypothetical optimal morphological parameters to improve production in relation to different environmental conditions. Leaf size and orientation are determinants of canopy transpiration and radiation interception e.g. in dry and sunny Mediterranean environments reduced size and erect orientation of the leaves can reduce water loss by transpiration and allow deeper light penetration into the canopy. Tillering influences crop performance, biomass and grain production, e.g. a reduction in tillering compensated by an increase dimension and number of kernels per spike could be a strategy of adaptation to dry climates. A reduction in plant height and an augment in stem thickness is connected to lodging resistance. Root system extension is connected to the ability of the plant to reach water.

The objectives of this project were to dissect genetic variability for shoot and root morphological traits in barley, identifying genomic regions and characterizing genes controlling these traits, and exploring how different traits influence each other. To this end, two approaches were undertaken depending on the trait(s) under study:

- the first exploited natural variation in a panel of modern and old European barley cultivars to carry out association mapping of flowering date, stem diameter, spike fertility, leaf dimension, plant height, tillering and root extension (Chapters 2 and 3);
- the second was to characterize the ontogenetic basis of increased tillering using as a case study the *many-noded dwarf6.6 (mnd6.6)* high tillering barley mutant (Chapter 4).

In the first approach, we focused on winter barley because of its agronomic interest in the Mediterranean area, where genetic improvement of drought tolerance is particularly important. We analyzed a panel of 142 European winter barley cultivars (67 two-rowed and 75 six-rowed) with a view to conduct a genome wide association scan (GWAS) for shoot and root architecture traits in two separate sets of experiments. To this end, genotyping data for 4,083 SNPs were available from previous projects of which 2,521 mapped on the POPSEQ barley reference map. PCoA results indicated the existence of two major sub-populations in our germplasm panel, corresponding to two-rowed and six-rowed barley cultivars.

In order to study shoot developmental traits (Chapter 2) the panel was phenotyped during the growing season 2012-2013 in a field trial at Fiorenzuola d'Arda, Piacenza, Italy. The experimental scheme consisted in 3 replicates (each being a plot of 24 well spaced plants) in randomized blocks. For selected traits data were integrated and analyzed together with those coming from a parallel field trial that was carried out at the University of Shiraz, Iran (data courtesy of Dr. Elahe Tavakol). Flowering date (FD) and leaf width (LW) were measured in both Italy and Iran, leaf length (LL) was measured only in Iran, plant height (PH), spike length (SL), number of fertile rachis node per spike (NFRN) tillering (T) and (SD) were measured only in Italy. Best Linear Unbiased Estimators (BLUEs) of FD, LW were calculated as the phenotypic values estimated for each genotype in a mixed linear

model, where genotypes were set as fixed factor and location, location-genotype interaction and replicates as random factors. For BLUEs calculation of all other traits only replicates were used as random factors. BLUEs were subjected to GWAS analyses, using a mixed linear model (MLM) correcting for population structure with a Q matrix (PCA first three coordinate) and for individuals co-ancestry using a K matrix (a pair-wise matrix defining the degree of genetic covariance among individuals). Significance of marker-trait associations was evaluated based on false discovery rate (FDR)-adjusted p-values (threshold value for significant association was set at 0.05). All traits except tillering exhibited good heritability. Few QTLs were detected in GWAS (five for FD, two for LW, three for LL, one for PH, two for SL, two for NFRN, one for tillering, no one for SM). Flowering date exhibited significant correlation with leaf dimension and spike length and six markers designed on *Photoperiod-H1* (*Ppd-H1*) gene (the major determinant for photoperiod response in barley) were the most significantly associated to FD, LW, LL and SL. In particular the recessive *ppd-H1* allele causing reduced photoperiod sensitivity, delayed flowering date and increased leaf dimension and spike length compared to the *Ppd-H1* allele. Three markers diagnostic for the *HvCEN* gene (which regulates flowering date independently from photoperiod) were significantly associated to FD and SL. These results suggested that genes for flowering date could have pleiotropic effects on other morphological traits that may mask other genetic effects. For this reason we tested a novel approach repeating GWAS for LW, LL and SL using flowering date as a cofactor (fixed effect) in further analyses. For SL and LW no new significant associations were found with this method, while new significant associations were uncovered for LL, including two markers on chromosome 5H mapped in a region where *narrow leaf dwarf 1a* (*nld-1a*) mutant had previously been previously mapped. Tillering and NFRN were only associated to markers diagnostic *INTERMEDIUM-C* (*INT-C*), one of the two main genes controlling row type: in our panel two-rowed genotypes had a significantly higher number of tillers and NFRN compared to six-rowed varieties, confirming the known pleiotropic effects of row-type genes on tillering and NFRN and the balancing of patterns of development by breeding practice for the particular row-type. Based on these results, we run GWAS for NFRN and tillering using row-type as covariate. With this model, we found six markers associated with NFRN on chromosome 5H, in the region hosting *HvCO12, HvCO13, HvCO15, XvCCA-1, HvLHY,* genes involved in control of flowering date. These same markers, were associated to the duration of the phase between awn primordia formation and tipping (awn arising from flag leaf) in a recently published GWAS study. Together, results from Chapter 2 provide the first evidence of the involvement of the *Ppd-H1* gene in control of leaf size and spike length. Thus few QTLs were detected that explain the phenotypic variation for our morphological traits, with some major genes having strong pleiotropic effects that mask minor genetic effects. The use of traits that appear to influence others measures as covariates in GWAS models seems to be a promising approach, although the statistical power of this strategy is still to be evaluated. Germplasm collections with uniform growth habit and row-type are an attractive alternative to prevent confounding effects and allow additional loci to be detected.

In Chapter 3, we explored natural genetic variation in root extension using the same winter barley panel as Chapter 2 in growth chamber experiments. In order to evaluate root growth we built 50 cm deep cylindrical pots (called rhizotrons) and used digital scans of the root system to measure total root extension with the winRHIZO software. Based on a series of preliminary tests, we used siliceous sand supplemented with controlled release fertilizer to analyze 4th leaf stage plants from 31 genotypes (9 plants per genotype). Root extension per se exhibited 75% heritability, while normalizing root extension on shoot dry weight resulted in low variability (22%) likely due to low

heritability of shoot dry weight in our system. These results support the validity of our protocol for evaluation of genetic variation in root extension in barley and other cereals and indicate significant variation exists in our germplasm panel. Thus, the already collected material will be analysed to phenotype the entire panel. In the future, more variability may be uncovered by exploring wild barleys (*Hordeum vulgare* spp. *spontaneum*) or landraces.

Tillering is a plastic trait affected by the complex interplay of genetic and hormonal factors with environmental conditions such as plant density/light quality and nutrient availability, which likely complicated genetic dissection of this trait in our field experiment on the winter barley panel (Chapter 2). To circumvent the limited power of the GWAS approach for this trait and understand more about the mechanisms subtending tiller formation, we decided to use the *mnd6.6* mutant as a case study to investigate the ontogenetic basis of high tillering in barley and its relation to leaf development. Mutant and wild-type plants were grown in growth in a controlled chamber under long day conditions, and dissected weekly from the emergence to anthesis, registering the development of axillary buds, leaves and tillers together with internode elongation, in relation to shoot apical meristem (SAM) stage. Results show that the mutant is not altered in timing of apical meristem development and differentiation to spike, but has a shorter phyllochron that leads to an increment in the number of leaves per vegetative axis. This in turn results in a higher number of axillary buds and a higher number of tillers. The *HvMND6* gene was recently identified and our results are consistent with the activity of the previously characterized rice homologue *PLASTOCHRON1*, indicating an evolutionarily conserved link between plastochron/phyllochron duration and tillering.

Concluding, while significant genetic variation was identified for various traits within the gene pool of our winter barley collection, variability of morphological traits as leaf dimension was subordinated to the length of vegetative period. Indeed, flowering date is one of the major factors on which breeding practice has worked to adapt barley to different environments. Beyond modern European varieties, barley breeding for new ideotypes should explore wider genetic resources as *Hordeum* spp. *spontaneum* or landraces. In any case, the existence of correlations between different phenotypes calls for careful evaluation of sources of traits to avoid undesired effects on other traits, e.g. due to the relation between tillering and phyllochrone, breeding for early plant vigour through shortening phyllochron, may have pleiotropic effects and result in increased tillering whose benefits would have to be evaluated.

1 INTRODUCTION

1.1 ECONOMIC IMPORTANCE

Barley (*Hordeum vulgare* L., Family: *Poaceae*, Tribe: *Triticeae* ranks in fourth place among cultivated cereals , after maize, wheat and rice, with a world-wide cultivated surface of 49,781,045 Ha (FAOSTAT 2013). Western Europe countries have a surface of 3,461,819.00 Ha cultivated with barley (FAOSTAT 2013). Barley is mostly used as feed grain, as a raw material for malt production and in a lower amount as food.

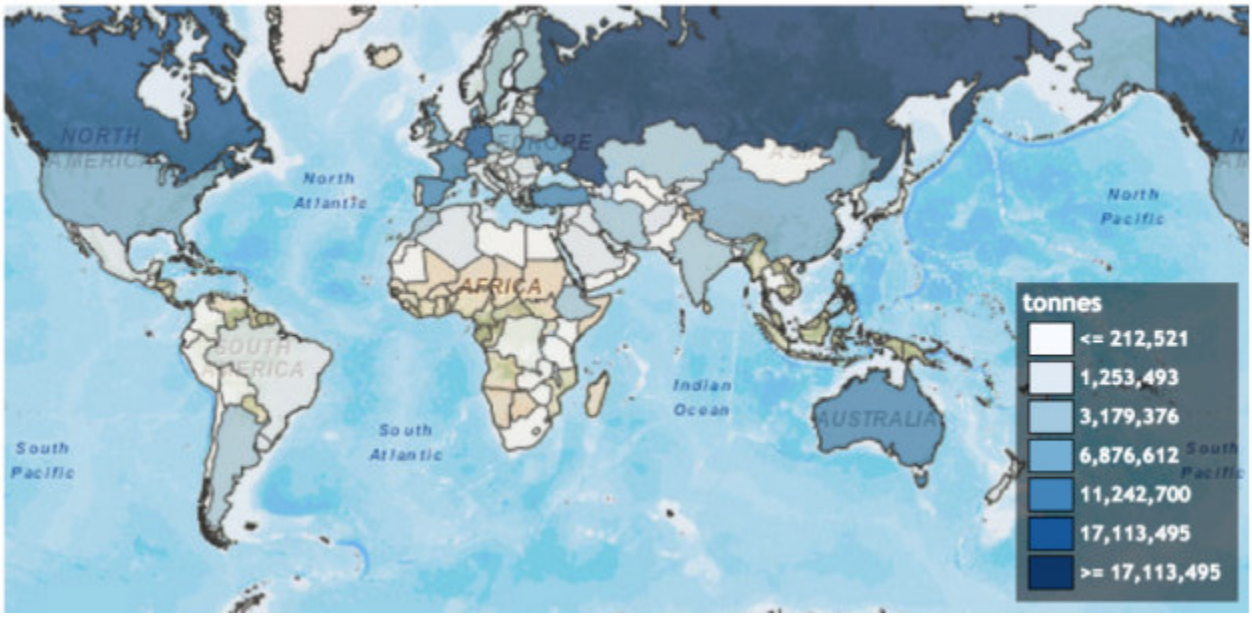

Figure 1.1 Barley world production (ton), average 1993-2013 (FAOSTAT, http://faostat.fao.org).

1.2 BARLEY PLANT ARCHITECTURE AND DEVELOPMENT, A BRIEF SUMMARY

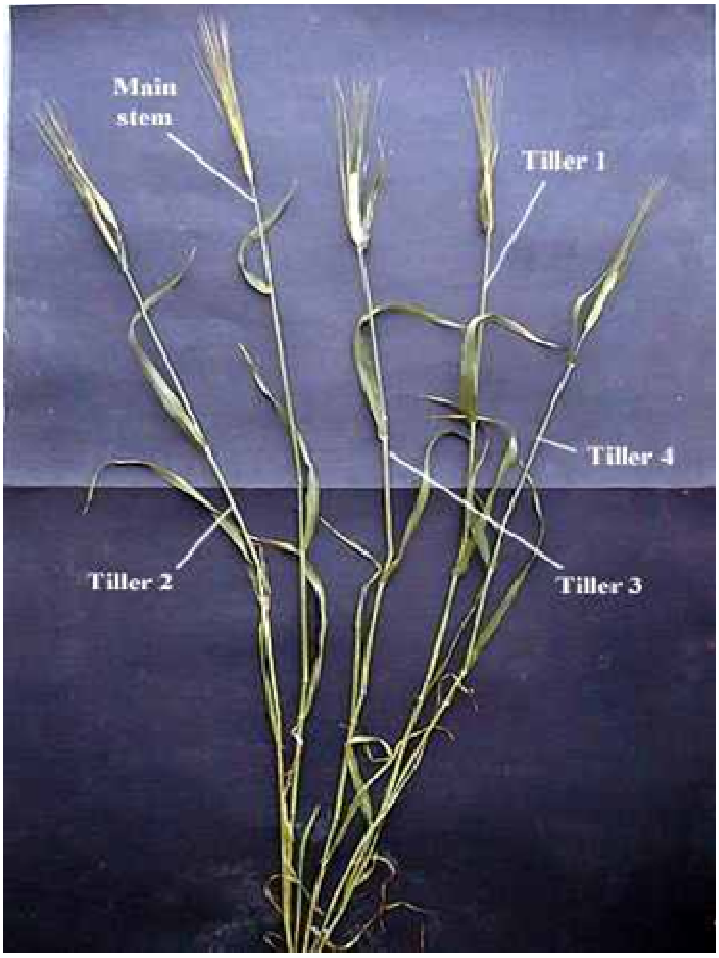

Figure 1.2 Example of barley plant (image from oregonstate.edu/instruct/css/330/five/BarleyOverview.htm)

A mature grass caryopsis contains a highly organized embryo consisting of different regions with specialized functions (MacLeod and Palmer, 1966):

- the scutellum, a structure unique to grass species that mediates release of hydrolytic enzymes and subsequently the transfer of nutrients from the endosperm during germination. The scutellum can be considered as a modified cotyledon (Rudall et al., 2005).
- the radicle with the root apical meristem (RAM) protected by the coleorhiza;
- the epicotyl comprising the shoot apical meristem (SAM) and leaf primordia enclosed by the coleoptile;
- the hypocotyl: the nodal region between the epicotyl and the radicle.

The barley SAM, seems to be structured in tunica (L1, one layer) and corpus (L2), although a three-

layer organization cannot be excluded (Döring et al., 1999). In dicots and many grasses, the tunica is structured into an epidermal L1 layer and a subepidermal L2 layer(Clark and Fisher, 1988)

Intersecting these layers, three zones can be distinguished to describe the radial patterning of the SAM:

- the peripheral zone is characterized by high cell division rates and is the site of lateral organ formation,
- in the central zone is constituted by a group of slowly-dividing pluripotent stem cells responsible for the maintenance of the meristem,
- the rib zone originates stem tissues.

The architecture of a plant can be seen as the reiteration of a basic module called phytomer, consisting of an internode (stem segment), a node, a leaf and an axillary bud (Figure 1.3).

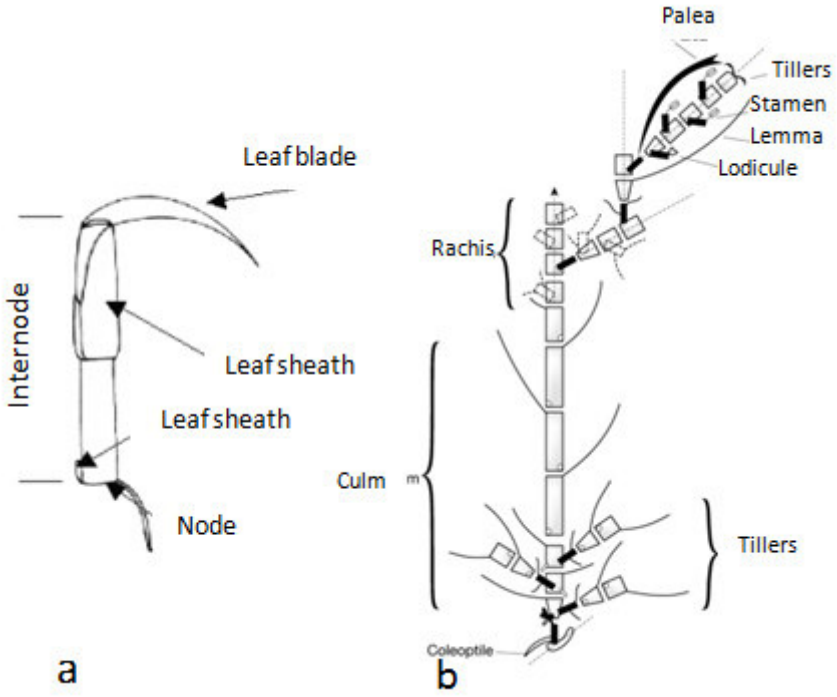

Figure 1.3. a) The barley phytomer based on Weatherwax (1923) and Sharman (1942), image modified from Bossinger et al., (1992). b) Phytomeric structure of barley plant, image from Forster et al. (2007).

This reiteration is carried out by the continuous production and differentiation of cells produced by the meristematic activity of the SAM from the In an adult barley plant each fully grown stem, or culm, consists of a series of cylindrical hollow internodes separated at the nodes (joints) by transverse septa (Briggs, 1978). Barley is characterized by a distichous arrangement of leaves and

spikelets on culms and inflorescence axes (rachis), respectively. The leaf is joined to the stem at the node, with its basal part (sheath) surrounding the internode participating to stem stability, while the distal lamina projects out from the stem to maximize light capture. Leaves are strap-shaped with parallel veins and a prominent midrib. The blade and sheath are separated by the ligule, a membranous outgrowth which is flanked by two ear-like projections called auricles. The basal internodes are the shortest and normally each internode is longer than the one below it. Axillary buds from basal unelongated phytomers (collectively called crown) can grow out into lateral culms (tillers) that often develop spikes contributing to plant biomass and grain yield (Kirby and Aplleyard, 1987).

Roots extend by cell divisions, which take place at the apex, and the subsequent growth and differentiation of the new cells. The apex is continually being pushed forward into the soil. The apex consists of two sets of meristematic cells. The outer set, or calyptrogen, divide to produce the root-cap (calyptra). This structure protects the apex as it is forced through the soil. It also contains cells rich in starch grains which may act as statoliths. The cells at the generative centre of the root divide and subsequently extend to create the root cylinder. When the seed germinates 5-7 seminal roots grow out from the coleorhizae (Briggs, 1978). In the soil they extend and branch, forming a fibrous, branched mass of root. During germination, the coleoptile reaches the soil surface and forms a “canal” through which the first leaf emerges (Briggs, 1978). Concurrently seminal roots are growing and branching (Hackett, 1969). Gradually leaves, either preformed in the embryo or generated later, grow rolled up from the tube formed by the leaf sheaths of earlier leaves. The leaf blade unfolds after emerging from the ligule of the previous leaf.

At the four leaves stage, secondary stems (tillers) start to form on the main stem. Adventitious roots develop from nodes of the main stem and tillers (Figure 1.4), at first many of these roots extend horizontally in the soil. They are thicker, and are less branched than seminal roots. Tillers physically separated from the plant can grow supported by adventitious roots only. Sometimes in drought or starvation stress the adventitious roots do not develop and seminal roots spread faster leading the plant to maturity by themselves. In very deep soils roots may descend to 1.8-2.1 m(Hackett, 1969). The deepest roots are usually of seminal origin, these roots at the upper layers of the soil tend to be packed with adventitious roots.

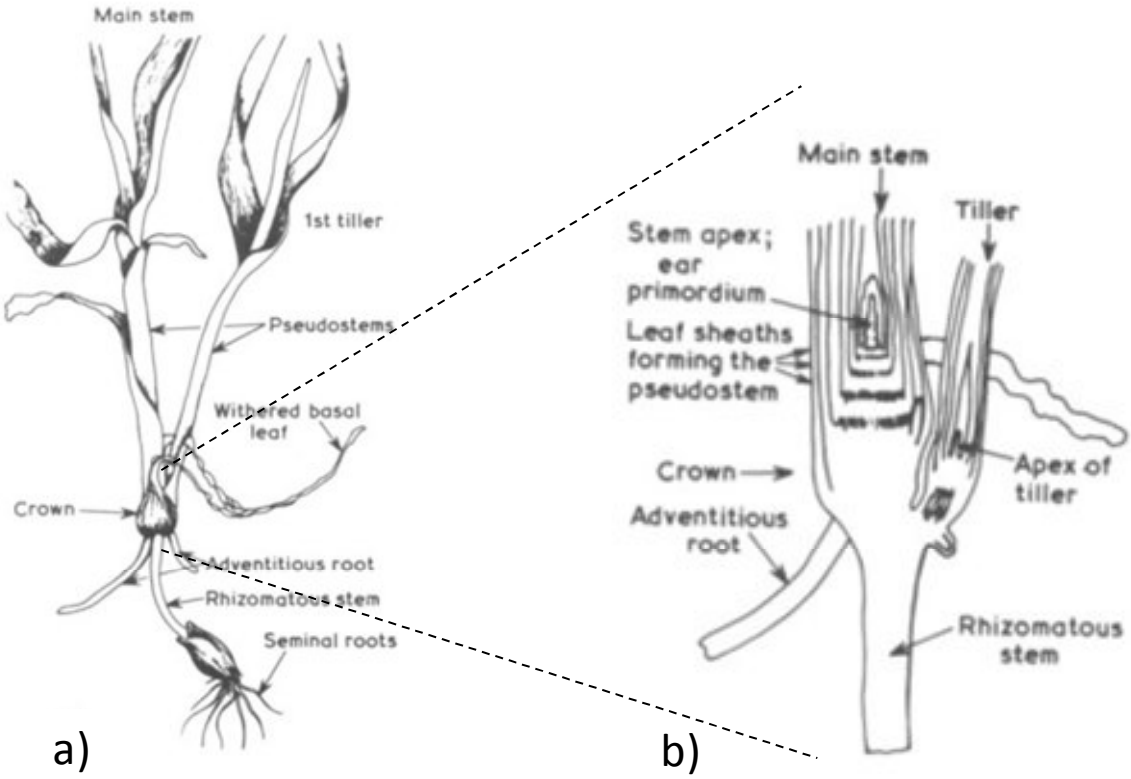

Figure 1.4. Representation of a barley seedling (left) with a focus on the section of the crown (right) (Image from Briggs, 1978).

Upon transition from the vegetative to the reproductive phase (after 8-9 leaves per main stem have been produced, the shoot apical meristem ceases to produce leaves and generates an ear primordium (Kirby and Riggs, 1978).

At this stage, internodes, that till now have remained short and not visible, start to elongate from intercalary meristems at the base of internodes emerging from leaf sheaths; normally only the upper (6-7) internodes elongate, while the basal ones remain at ground level (Kirby and Aplleyard, 1987). By the time the stems have fully elongated the seminal and coronal root systems are at or near their greatest size and the root system reaches its maximum size at anthesis (Briggs, 1978). The apex of each fertile tiller carries an ear. As the stem shoots are elongated the ear is carried upwards. The last, “flag” leaf generally contains the ear within its sheath, which swells, and is called the 'boot'. When the spike is fully developed it has already emerged from the “flag” leaf and flowering occurs. Barley flowering is cleistogamic, with > 97% self pollination (Baldoni and Giardini, 2000).

During grain ripening the mature leaves progressively senesce: the older basal leaves first loose their green colour, becoming brownish, brittle and withered (Briggs 1978). Gradually the whole plant dries out until full maturity, when the grain is ripened (June/July).

1.3 ORIGIN

Barley was one of the first crops to be domesticated in the "Fertile Crescent" at least 10,000 years ago (Fischbeck, 2002). Based on variability of AFLP linked to the non-brittle rachis gene (Komatsuda et al., 2004), (Morrell and Clegg, (2007) proposed that a second domestication occurred 1500-3000 km further East of "Fertile Crescent". non-brittle rachis and 6-rowed spike are key traits selected in barley domestication (Morrell and Clegg, 2007; Sakuma et al., 2011) Spread of barley cropping out of its place of origin implied mutations and recombination events to develop reduced vernalization requirement and reduced sensitivity to photoperiod (Salamini et al., 2002). Barley has then evolved to adapt to a wide range and climates: it is normally cultivated from temperate (winter and spring planting) to semi-arid subtropical (winter planting) climates; the range of cultivation goes from Nordic European countries (with barley cultivars showing more cold resistance than oat and rye) to the Maghreb area, where it benefits from a higher drought and salt tolerance than durum-wheat (Ullrich, 2010).

1.4 ORIGINS OF MODERN EUROPEAN CULTIVARS

Contemporary European spring and winter varieties descend from a small number of successful European landraces selected around 100 years ago (Bothmer and Fischbeck, 2003). European spring varieties (most of them two-rowed) trace back to European landraces from Bavaria (southern-Germany), Moravia (today Czech Republic), Sweden and the United Kingdom (Ullrich, 2010). Cycles of cross-breeding between these landraces led to the release of first cultivars like Isaria (1924) and Kenia (1931),(Ullrich, 2010). Later more exotic material like *Hordeum levigatum* and arabishe where inserted in breeding programs as source of disease resistance leading to the release of cultivars carrying mildews resistance e.g. Aramir (1974) and Apex (1983) (Ullrich, 2010). Breeding programs of two-rowed spring varieties proceeded focusing on acquisition of malt quality and resistance to disease such as scald (*R.secalis*), leaf rust (*P. hordei*) and yellow mosaic

viruses, such as Barley Mild Mosaic Virus BaMMV and Barley yellow mosaic viruses BAyMV (Ullrich, 2010).

Modern European winter varieties descend from two sources of six-rowed landraces, one from the Netherlands and one from the Canadian winter type Mammuth (Ullrich, 2010). Subsequent breeding cycles based on crossing between six-rowed winter varieties and both two-rowed and six-rowed spring varieties led to a series of important varieties e.g. Dea and Dura carrying resistance against mildews and BaMMV (Ullrich, 2010) Over 100 years of breeding activity, grain yield was more than doubled with an estimated genetic contribution to this increase of about 30–50% (Schuster et al., 1997).

1.5 CURRENT PERSPECTIVES IN BARLEY BREEDING

With the human population projected to hit 9.6 billion people by 2050 (United Nation report, www.un.org/apps/news/story.asp?NewsID=45165#.VIMLGvtc7C0) it is estimated that the planet's demand for food and feed crops will almost double by 2050 (Foley et al., 2011). Furthermore effects of climate change are becoming increasingly evident:Europe is expected to face a general increase of winter rainfalls and loss of snow accumulation that provides springtime water; Northern regions will see warmer and wetter weather, leading to an increase in fungal pathogen infections and plant diseases, whereas Southern regions will suffer from more frequent and severe droughts (Durack et al., 2012). Beside a continued need to improve yields and pathogen resistances, important targets in barley breeding will be the increase of crop stability through higher tolerance to abiotic stresses (Blum, 1988; Lieth, 2009). Crop performance under drought conditions is a highly complex phenomenon because of the multiple physiological and genetic mechanisms involved, partly dependent on the timing, intensity and duration of water limitation and the interactions with other abiotic and biotic factors (Reynolds et al., 2006).

1.6 THE CEREAL IDEOTYPE

Donald (1968) first introduced the ideotype concept, proposing that breeding should seek to develop a model plant based on an understanding of the morphological, phenological, physiological and genetic components that subtend crop performance and "efficiency" in relation to available resources. Thus ideotype breeding involves three steps: define the traits that will lead to increased yield, quality etc., define the goals for those traits and select directly on those traits (Rasmusson, 1987). Ideotype breeding was first proposed by Donald, (1968) to increase wheat

yield in a high input environment: fixed some characteristic should had been achieved by breeding practice in wheat: his model wheat plant had a short and robust stem to prevent lodging; narrow and erect leaves to maximise light capture, based on the concept that in a dense community near-vertical leaves should permit adequate illumination of a greater leaf surface area preventing overshadowing of lower leaves from upper leaves;a single culm to maximize vigour and yield of the only spike, avoid competition between main culm and tillers, and synchronize development of the canopy facilitating mechanical operations. Donald's ideotype was a weak competitor relative to its mass, and thus would have been less affected by crowding, making a minimum demand on resources per unit of dry matter produced (Donald, (1968). Nevertheless heavy nutrient supply was a cardinal feature of the environment of this ideotype. A proof-of-concept for ideotype breeding came with the Green Revolution when cereal yields and harvest indexes were increased by selecting for semidwarf lodging resistant wheat and rice cultivars (Khush, 2001).

With time, new ideotypes have been proposed in relation to changes in crop practices and problems. For Rasmusson (1991) the choice of traits to include in an ideotype model depends on environmental conditions. For example, under continuing water stress, traits that improve water-use efficiency deserve priority. In this case, he proposed a model adjusting the length of the vegetative and grain-filling periods, and projecting small leaves. In contrast, when water supply is ample and energy capture becomes more important as a yield-limiting factor, traits that alter canopy profile become a priority. Rasmusson formulated his ideotype based on analyses of historical data of yield increments achieved by barley breeding in relation to morphological traits,. In contrast to Donald's model, he proposed that increased leaf width together with an erect bearing should be advantageous for high input conditions. In addition, he auspicated an increase in kernel number per spike along with a wider stem diameter for lodging resistance.

In the last years efforts have been focused on water use efficiency and some attention has been focused on optimizing rooting systems (Rich and Watt, 2013) In this respect, deeper root distribution could help, since root length density (root length per unit volume of soil) is often below a critical threshold for potential water and nitrate capture of around 1 cm/cm^3 (Gregory et al., 1978; Barraclough et al., 1989) at lower depths in the rooting profile (Ford et al., 2006; Reynolds et al., 2006). In a context of limited water availability (Mediterranean environments), reduction of leaf dimension together with erect bearing could also reduce water loss by

transpiration and allow a deeper light penetration in the canopy (Geller and Smith, 1982; Welander and Ottosson, 1997; Horton, 2000).

Based on the considerations above, understanding the genetic mechanism regulating morphological traits is expected to support breeding of resilient crops in a changing climate.

From this point of view barley, due to its diploid genome and relatedness with other Triticeae crops (Linde-Laursen et al., 1997), is an important model organism for the dissection of the genetic and molecular bases of morphological traits.

1.7 BARLEY GENOMIC STRUCTURE AND PHYSICAL MAP

Barley is an annual diploid self-pollinating species with 2n = 14 chromosomes with a genome size of 5.1 Gbp (The International Barley Genome Sequencing Consortium, 2012). The 7 barley chromosomes (1H-7H) share homeology with other Triticeae crops, such as wheat species (Linde-Laursen et al., 1997).

The International Barley Sequencing Consortium (IBSC) is a multinational collaboration that was established with the objective of obtaining the whole sequence of the barley genome (Schulte et al., 2009). A milestone in this direction was the assembly of a barley physical map anchored to a high-resolution genetic map and enriched by dense sequence information of the barley gene-space (The International Barley Genome Sequencing Consortium, 2012). The physical map of the barley genome is based on high information content fingerprinting (HICF) of 571.000 BAC clones (from cultivar Morex), deriving from 5 different BAC libraries and covering 13x the genome size (The International Barley Genome Sequencing Consortium, 2012). After assembly the physical map comprised 9,265 BAC contigs and a cumulative length of 4.98 Gb, covering over 95% of the barley genome. A total of 1,136 Mb of genomic sequences are integrated directly into the physical map, allowing the anchoring of genetic maps on the physical map. Also publicly available barley full-length cDNAs and RNA-seq data generated by the IBSC project were used for structural gene calling of the genomic sequences anchored on the map. Characteristic of the barley genome is the abundance of repetitive DNA (Wicker et al., 2009), approximately 84% of the genome is comprised of mobile elements or other repeat structures (The International Barley Genome Sequencing Consortium, 2012).

The transcribed complement of the barley gene space was annotated by mapping 167 Gb of RNA-seq reads obtained from eight stages of barley development, together with 28,592 barley full-length cDNAs (Matsumoto et al., 2011) to the whole-genome shotgun assembly. Out of 79,379 transcript clusters, 95% were anchored to the whole-genome shotgun assembly. Based on a gene-family-directed comparison with the genomes of *Sorghum*, rice, *Brachypodium* and *Arabidopsis*, 26,159 of these transcribed loci fall into clusters and have homology support to at least one reference genome and then they were refined as high confidence. Comparison with a data set of metabolic genes in *Arabidopsis thaliana* (Zhang, 2005) indicated a detection rate of 86%, allowing the barley gene set to be estimated as approximately 30,400 genes .

1.8 MARKERS, GENETIC MAPS AND GENOMIC TOOLS

Many marker sets and genetic maps have been produced during the last decades - their amount growing together with the evolution of sequencing and genotyping technologies.

Early sequencing efforts in barley were based on Expressed Sequence Tags (ESTs), short sequences (500-800 nucleotides), derived from single sequencing reactions performed on randomly selected clones from cDNA libraries (Parkinson and Blaxter, 2009). Due to the facility in obtaining EST sequences and their informativeness (coding sequences), ESTs have been extensively used in plant genomics. A large barley EST database is the HarvEST database (http://harvest.ucr.edu/) containing six EST assemblies, where EST sequences have been assembled into contigs that represent hypothetical gene coding sequences (“unigenes”).

Based on ESTs from the barley HarvEST database and PCR amplicon resequencing, Close et al., (2009) identified 4,596 single nucleotide polymorphism (SNP) markers and developed two Illumina GoldenGate oligonucleotide pool assays (Fan et al., 2006), called BOPA1 and 2 each including 1520 SNPs. The BOPAs were used to genotype four mapping populations and build a reference consensus map containing 2,943 SNP markers(Close et al., 2009).

Later Comadran et al., (2012) developed an Illumina 9K SNP chip (http://bioinf.hutton.ac.uk/iselect/app/) based on polymorphisms identified from RNA sequencing (RNA-seq, Wang et al., 2009) data from ten diverse cultivated barley genotypes and including markers designed in Close et al., (2009). They then used this platform of 7,864 SNP markers to

genotype a population of 360 recombinant inbred lines (RILs) from a cross between the cultivars Barke and Morex to construct a robust genetic framework of 3,973 genetically ordered markers. The chip developed by Comadran works on Illumina Custom Infinium iSelect HD tool, which is able to genotype 24 samples for 3,000-1,000,000 SNP markers per run (http://support.illumina.com/array/array_kits/iselect_24x1hd_beadchip_kit.html).Recently a new genetic map was produced, the POPSEQ map (Mascher et al., 2013). In this case SNP detection was carried out by whole genome sequencing of 90 individuals of a population of recombinant inbred lines (RILs) (from a cross between barley cultivars Morex and Barke (the same used on Comadran et. al 2012) and 82 duble haploid lines from OWB Oregon Wolfe Barley (OWB) population. Sequence information was used for gene calling and anchoring to the barley physical map. The new POPSEQ map was built through segregation analyses and integration into the high-density SNP-based genetic map of the same population constructed by array-based genotyping (Comadran et al., 2012).Genomic sequences, and gene annotation data, as well as physical/genetic map integration are available through the MIPS barley genome database (http://mips.helmholtz-muenchen.de/plant/barley/). The database hosts also the so-called "genome zippers" datasets of chromosome-anchored barley gene sequences arranged in a putative linear order based on colinearity with already sequenced cereal genomes (Mayer et al., 2011). These were obtained from shotgun sequencing of isolated barley chromosomes and chromosome arms and filtering for sequences matching HarvEST barley ESTs.Finally sequence data sets were aligned against complete model grass genomes of Rice, *Brachipodium* and sorghum to estimate sinteny with these species. These analyses predict a hypothetical gene number of 32.000, and allowed ordering of 86 % of these hypothetical genes along the seven barley chromosomes (Mayer et al., 2011). Genome zipper tables are then useful tools that anchor together and order barley genetic markers and coding sequences against Rice, *Brachipodium* and sorghum. Another important resource connected to the MPIS web site is the Barley IPK BLAST server (http://webblast.ipk-gatersleben.de/barley/) that allows to align input sequences against different barley sequence databases, e.g. to the barley phisycal map (The International Barley Genome Sequencing Consortium, 2012) and the POPSEQ map (Mascher et al., 2013).

More recently DNA sequencing techniques (e.g. Illumina Hiseq 2000 and exome capture) and bioinformatic tools allowed barley scientists to create and manipulate large dataset accelerating progresses in barley genetics. (Mascher et al., 2013a) developed an hybridization-based sequence

capture platform that selectively enriches for coding sequences (exome capture): this constitutes an important tool for genomic studies in barley, allowing to focus on the protein-coding fraction of the genome excluding repetitive non-coding regions. The exome-capture barley tool finds ample applications in characterization of genetic diversity in barley germplasm and genetic mapping. In this context, mapping-by-sequencing has emerged as a powerful technique for genetic mapping in several plant and animal species. This approach was used to clone the barley *mnd6* mutant by Mascher et al., (2014). Using as a starting point an F2 population derived from a cross between the *mnd6* mutant and the wild type, DNAs from 18 mutant plants and 30 randomly selected wild-type plants were combined into two pools, which were subjected to exome capture and subsequent sequencing on the Illumina HiSeq2000, yielding 82 million and 70 million 2 × 100 bp read pairs for the mutant and wild-type pools, respectively. Reads were mapped on the barley physical map and SNPs were detected. They position of the mutated gene was detected observing allele frequencies at SNP positions along the physical and genetic map of barley: the gene was positioned in a region where the frequency of the mutant allele increased to over 95% and dropped to about 30% in the wild-type pool (Mascher et al. 2014).

In summary, ever-growing barley genomic resources provide an unprecedented platform for Triticeae scientific research and crop improvement.

1.9 BARLEY GENETIC RESOURCES

Genomic tools described in the previous paragraph are applyied to dissect large genomic resources, that have been constituted during years. Large mutant collection allowed to isolate genes with mendelian heritance basing on segregation analyses, while natural variation (also of wild barleys) have been used to map QTLs responsible for continuous variation of traits of agronomic importance. Natural variation is exploited through constitution of segregant population deriving from parents with phenotype of interest (QTL mapping) or through the dissection of pre-existing germplasms, e.g. collections of cultivars, landraces or *H. vulgare ssp. spontaneum* (association mapping).

1.9.1 MUTATION RESEARCH

Barley mutation research started in 1928 when Stadtler demonstrated that ionizing radiation could increase the mutation frequency in barley and that the induced mutations were transmitted to subsequent generations (Stadler, 1928). Indeed barley is one of the best studied models in plant

mutation research for its diploid genome, and generated considerable basic understanding about fundamental processes of plant morphology, physiology, and development (Druka et al., 2011). The barley research community actively characterized mutant lines into collections that grew to contain thousands of accessions. One of the most important barley mutant collections is that of the Scandinavian mutation research program that contains 10,000 different characterized mutants stored at the NordGen genebank (http://www.nordgen.org/). The corresponding genes can be identified through positional cloning, of which the abovementioned mapping-by-sequencing approach is a new development.

1.9.2 GENETIC DISSECTION OF MENDELIAN TRAITS

Positional cloning starts from the assembly of a high density genetic map of the genomic region containing the locus of interest (Jander et al., 2002). The first step is to find two tightly linked markers flanking the target locus (Tanksley et al., 1995) and anchor them to a physical map or genome sequence to identify the genomic region harbouring the gene of interest. Annotation of this region leads to identification of one or more candidate gene for the target locus (Tanksley et al., 1995).

In barley, morphological mutants have been used to isolate genes involved in a range of domesticantion and developmental process, such as the gene responsible for the floral bract phenotype *Hooded* (*Kap1*, Müller et al., 1995), plant height genes *UZU DWARF* (*UZU*; (Chono, 2003) and *SLENDER1* (Chandler et al., 2002), the row-type genes *SIX-ROWED SPIKE1, SIX-ROWED SPIKE4* (*VRS1*,*VRS4*;(Komatsuda et al., 2007; Koppolu et al., 2013), the cleystogamy gene *Cly1* (Nair et al., 2010) also involved in spike density, the hull adhesion gene *NAKED CARYOPSIS* (*NUD*; Taketa et al., 2008).

A milestone in genetic analysis of barley mutants was the work of Druka et al., (2011), that is the base for many further mutant research investigations. They produced a series of independent introgression lines containing mutant alleles by recurrent backcrossing of mutant lines with the recurrent parent Bowman followed by selfing, with phenotypic selection for the mutant phenotype in each cycle. In this way they obtained 979 Bowman isolines that were genotyped with

3,072 SNPs of the Close et al (2009) map, allowing to define the position and width of introgressed segments containing the mutant loci.

1.9.3 GENETIC DISSECTION OF QUANTITATIVE TRAITS

1.9.3.1 QTL MAPPING

In mutant research traits are defined by a binomial distribution (mutant, wild type), and positional cloning is based on frequency of cosegregation of the phenotype with markers. Investigating natural variation, traits are more commonly defined by a continuous scale of intensities and are regulated by multiple genes, often with additive effects, i.e. quantitative trait loci (QTLs). QTL mapping involves three main steps: 1) the development of a segregant population by crossing parental lines with contrasting phenotypes; 2) the construction of a genetic map of molecular markers; 3) phenotyping experiments on the population in multiple years/environments. The goal of QTL mapping is to find markers associated with phenotypic variation. Basic QTL mapping involves the simple interval mapping (SIM) method that makes use of linkage maps and analyses intervals between adjacent pairs of linked markers along chromosomes: this methods produces a profile of the likely sites for a QTL between adjacent linked markers (Lander and Botstein, 1989). More sophisticated analyses have been developed over the years to accommodate normally and non-normally distributed traits and take into account the effects of co-factors, leading to more precise identification of QTLs and their phenotypic effects.

1.9.3.2 ASSOCIATION MAPPING

An alternative approach to QTL mapping is the “association mapping” or “linkage disequilibrium mapping” approach (Goldstein and Weale, 2001). The advantage of association mapping is that it exploits variation inside a pre-existing natural population. The principle is that over multiple generations of recombination during historical evolution of populations, only correlation with markers tightly linked to the trait of interest will remain. Association mapping is based on Linkage Disequilibrium.

Linkage disequilibrium.

In an "ideal population" where mating and allele segregation have occurred randomly, the frequency of a haplotype (pattern of alleles at different loci) is equal to the product of frequencies of single alleles at different loci: this is a situation of linkage equilibrium. When something interferes with random mating and/or allele segregation, there is a situation of Linkage Disequilibrium (LD), i.e. a non-random association between two markers or two genes (Lewtonin, 1965)(Figure 1.5) .

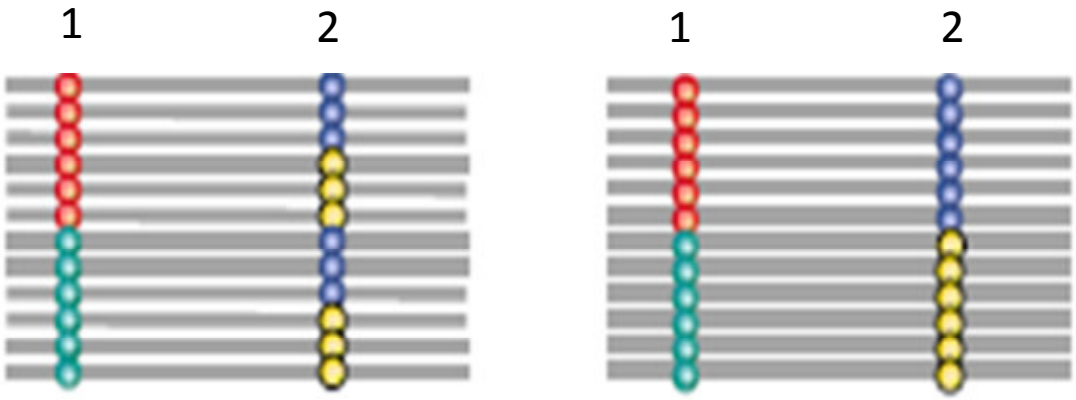

Figure 1.5. Schematic explanation of linkage disequilibrium. Loci 1 and 2 are in linkage equilibrium on the left, loci 1 and 2 are in total linkage disequilibrium on the right.

LD can be measured with different formulas the first is: D = p (AB) - p (A) p (B) (Lewtonin, 1965). Where p(AB) is the frequency of gametes carrying allele A and B at two loci; p (A) and p (B) are the frequencies of the allele A and B, respectively. In other words D is the difference between the observed gametic frequencies of haplotypes and the expected Hardy-Weinberg gametic frequencies of the same haplotype. In a situation of linkage equilibrium, D=0. D is limited because its range is determined by allele frequencies. The two most utilized statistics for LD are D' (Lewontin, 1964) and r^2 (Hill and Robertson, 1968), both varying from 0 to 1. These two parameters reflect different aspects of LD and perform differently under various conditions. They are calculated as follow:

$D' = |D| / D_{max}$

$D_{max} = \min [p(A)\,p(b) , p(a)\,p(B)]$ if $D > 0$;

$D_{max} = \min [p(A)\,p(B) , p(a)\,p(b)]$ if $D < 0$

$r^2 = D^2 / [p(A)\ p(a)\ p(B)\ p(b)]$

Where A/a and B/b refer to the two alleles at two different loci.

While D' measures only recombination differences, r^2 summarizes recombination and mutation history (Figure 1.6). Also r^2 is indicative of how markers might be correlated with QTL of interest, so that for association studies, often r^2 is preferred (Abdallah et al., 2003). Typically, r^2 values of 0.1 or 0.2 are often considered the minimum thresholds for significant association between pairs of loci and to describe the maximum genetic or physical distance at which LD is significant (Zhu et al., 2008).

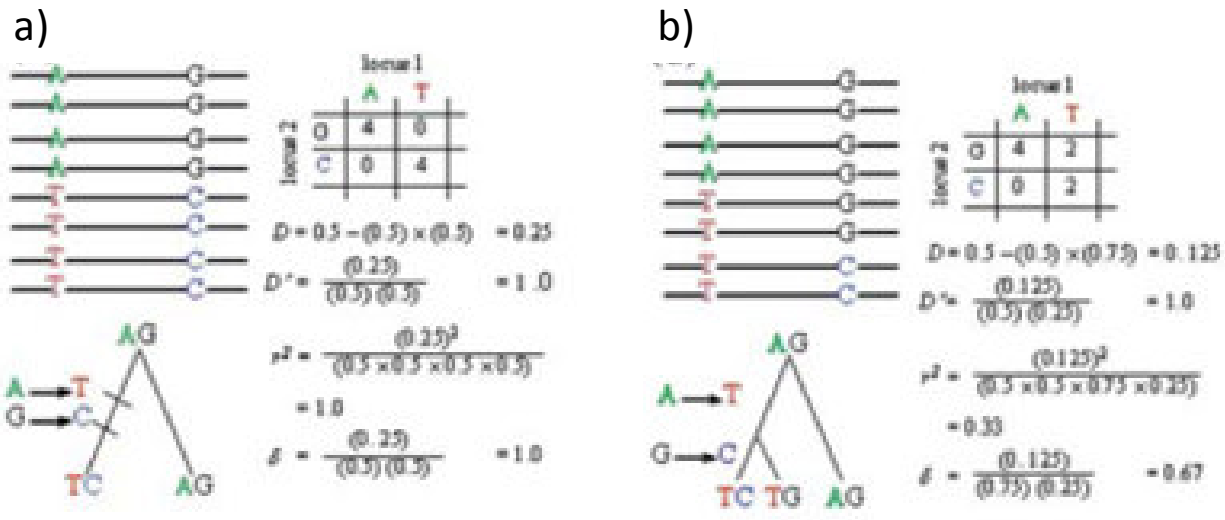

Figure 1.6. Diagrammatic representation of linkage disequilibrium (LD) between two SNPs showing the behavior of D' and r^2 statistics under the following conditions: (A) No recombination (mutations at two linked loci not separated in time) (B) No recombination (only mutations separated in time) (image from Gupta et al., (2005)).

LD and linkage are two different things: linkage refers to the correlated inheritance of loci through the physical connection on a chromosome, whereas LD refers to the correlation between alleles in a population (Flint-Garcia et al., 2003). In fact, even if physical linkage between two loci is the main determinant of their LD in a population, it's common to find a significant LD between pairs of loci located far from each other or even in different chromosomes (Flint-Garcia et al., 2003).

These long stretched LD or LD between unlinked loci indicate the existence of other LD generating factors than linkage itself.

Summarizing, LD extent depends on different factors:

- Mating system has strong effects on LD (Myles et al., 2009). Self crossing augments the extent of LD: as recombinational events are reduced in self-pollinated species such as rice (*Oryza sativa*), Arabidopsis (*Arabidopsis thaliana*), barley (*Hordeum vulgare*) hexaploid wheat (*Triticum aestivum*)(Nordborg, 2000; Garris, 2004; Zhang et al., 2010), LD extends much further as compared to outcrossing species such as maize (*Zea mays*), grapevine (*Vitis vinifera*) and rye (*Secale cereale*) (Tenaillon et al., 2001; Myles et al., 2009, Li et al., 2011).

- The germplasm as results of historical recombination events, and the level of genetic diversity captured by the population under consideration. In general the larger the genetic variation, the more LD is reduced. The population sample effect is evident in maize (*Zea mays*) where LD decays within 1 kb in landraces, approximately doubles (~ 2kb) in diverse inbred lines and can extend up to several hundred kb in commercial elite inbred lines (Jung et al., 2004).
- Selection. Positive selection will increase LD between a favourable locus and an adjacent locus, even if the second locus is neutral: this phenomenon is called genetic hitchhiking, LD level between the these two loci will remain constant over time depending on the genetic distance, the recombination rate and the effective population size (Slatkin, 2008). Mosaics of large LD blocks are observed, especially in regions carrying agronomic-related genes. In contrast if a particular haplotype is favourable LD can persist indefinitely (Lewontin, 1964).
- The effect of genetic drift in a small population results in the consistent loss of rare allelic combinations which increases LD level (Flint-Garcia et al., 2003). LD can also be created in populations that have experienced a reduction in size (called a bottleneck) with accompanying extreme genetic drift (Flint-Garcia et al., 2003).
- The population structure (existence of distinctly clustered subdivisions in a population) and population admixture are the main factors to create LD between unlinked loci. This primarily happens due to the occurrence of distinct allele frequencies with different ancestry in an admixed or structured population (Slatkin, 2008). Theoretically, relatedness generates LD between linked loci, but it might also generate LD between unlinked loci pairs when predominant parents exist in germplasm groups (Slatkin, 2008)

In maize, an out-crossing species, LD decays under short distances. In Yan et al., (2009) a maize Illumina GoldenGate Assay with 1,229 SNPs from 582 loci was used to genotype a highly diverse global maize collection of 632 inbred lines from temperate, tropical, and subtropical public breeding programs. The LD decay distance differed among chromosomes and ranged between 1 to 10 kb.

In rice, a selfing species, Mather et al., (2007) used unlinked SNPs to determine the amount of background LD in each population, and found and that the extent of LD is greatest in temperate japonica (probably 500 kb), followed by tropical japonica (150 kb) and indica (75 kb) types. Garris et al.,(2003) examined the LD surrounding disease resistance locus Xa5 using 21 SSRs in a survey of 114 rice accessions. They determined strong LD within 100 kb with $r^2 = 0.1$.

In hexaploid wheat, an almost completely self-pollinating species, strong LD was detected along regions of 1-5 cM of length on chromosome 2D and a centromeric region on 5A: analyzing a panel of 95 winter wheat cultivars that were genotyped with 36 SSR markers (Breseghello and Sorrells, 2006). In Chen et al., (2012) 90 winter wheat accessions were analyzed with 269 SSR markers distributed throughout the wheat genome. The maximum LD decay distance, estimated by curvilinear regression, was 17.4 cM ($r^2>0.1$), with a whole genome LD decay distance of approximately 2.2 cM ($r^2>0.1$, $P<0.001$). In Würschum et al., (2013) 172 elite European winter wheat cultivars were genotyped for 518 SNP and 91 SSR and LD was estimated to decay within approximately 5–10 cM.

Association mapping methodology

Association mapping is an LD-based approach that seeks to find statistical association between allelic (or haplotype) variation at a locus and the phenotypic value of a trait across a large sample of accessions coming from a natural population (Figure 1.7).

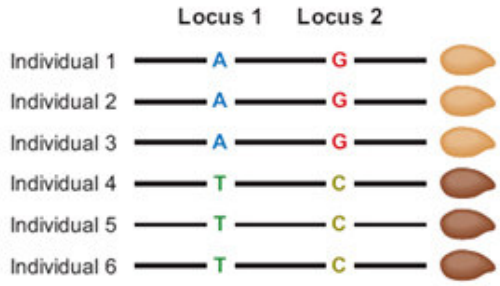

Figure 1.7. Principle of association mapping: Locus 1 and Locus 2 are in total LD. Significant covariance with the seed colour phenotype indicates that the gene responsible for color of seed is near or between the two markers (Braulio and Cloutier, 2012).

Originally this method was developed for genetic studies of human hereditary diseases. The classical methodology of association mapping is the "case-control" approach that identifies alleles causative of diseases based on the comparison of allele frequencies in a sample of unrelated affected individuals (cases) and a sample (of the same size) of un-affected individuals (controls) (Abdurakhmonov and Abdukarimov, 2008). The Pearson chi-square test, Fisher's exact test, or Yates continuity correction can be used to test the association between alleles and disease co-frequency (Ohashi et al., 2001; Schulze and McMahon, 2002).

In case of quantitative traits as those studied in plants, the covariance between allele variation and phenotypic variation is statistically tested. Having two alleles (A/a) at one locus the three different genotypes are considered as three different levels of the same treatment, and the effect of this treatment on phenotypic variation can be tested through ANOVA or linear regression (Figure 1.8, Balding, 2006). In either case, tests require the trait to be approximately normally distributed for each genotype, with a common variance.

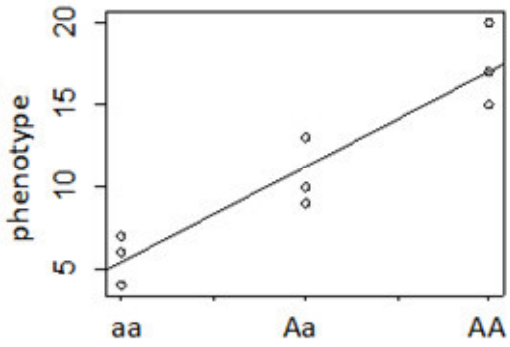

Figure 1.8 Example of linear regression test for a single SNP association with a continuous outcome.

A simple linear regression model is the so-called general linear model (GLM), that accounts for additive effects, while for dominant/recessive effect an ANOVA method is preferred.

GLM model can be described as y=ax+q (Figure 1.8) where y is the phenotypic score, x is the genetic marker with number of levels equal to three (in case of biallelism), a is the regression slope (increase of phenotypic value corresponding to variation of allelic status, q is the intercept) A genome wide association scan (GWAS) indicate a set of linear regressions tests whose number is equal to the number of markers tested.

Population structure and false positives

One problem associated with the GLM is the detection of false positive associations due to population structure. The population structure is the existence of distinctly clustered subdivisions in a population, expressed by the presence of a systematic difference in allele frequencies between subpopulations, structure origins from a nonrandom mating between groups, often due to their physical separation e.g. geographical origin but in case of crops, also to breeding selection (Braulio and Cloutier, 2012). False positives arise when phenotype intensities are not equally distributed between sub-populations, so that any markers whose alleles distribution match with the distribution of individuals between sub-populations, can be wrongly associated with the trait (Schulze and McMahon, 2002) (Figure 1.9).

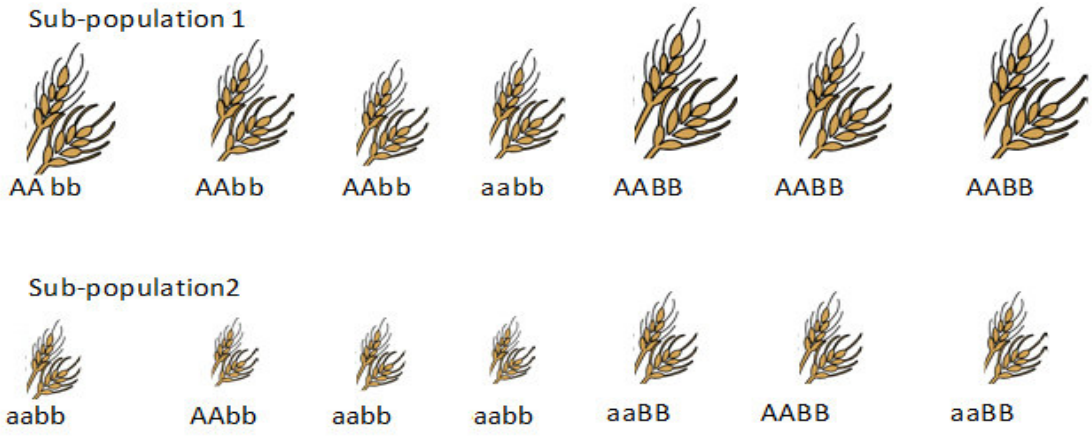

Figure 1.9. Example of how a false positive arises. Sub-population 1 is characterized by producing large spikes and a high frequency of allele A, therefore association analyses will associate the A/a locus with spike dimension even if actually it is not responsible for the trait. Locus B alleles have the same frequencies within the two sub-populations and effectively allele B causes an increase in spike dimension, but locus B is not detected as responsible for the trait, because its effect is masked by the effect of population structure.

Several statistical instruments have been developed to correct models for population structure. Yu et al., (2006) developed a mixed linear model (MLM) that accounts for population structure and relatedness between individuals by integrating two matrices in the model. In a Q matrix, each column represents a fixed factor with number of levels equal to number of individuals; it can be calculated in two radically different ways: the first is by STRUCTURE software (http://pritchardlab.stanford.edu/structure.html), which (based on marker genotypes) infers the presence and calculates the number of distinct populations by a Bayesian approach and assigns individuals to each populations (Hubisz et al., 2009); another kind of Q-matrix is the principle component analyses (PCA) matrix, which, based on genotypes, calculates correlation between individuals and finds the main axes of variation inside the population. - In a PCA matrix columns represent axes of variation, reported values are the position of individuals along the axes (Ringner, 2008). Each marker allele is inside a genetic background (an individual), alleles are expressed with an intensity that varies depending on genetic background, two related individual (co-ancestry) have similar genetic background, this is a cause of non independence of data and then of false positives. K matrix is an n x n matrix (n=number of individual) that report coefficient of relatedness between individuals accounting, random factor due to co-ancestries of individuals is then accounted by the model Yu et al., (2006); simplifying, kinship matrix is calculated based on similarity between genotypes based on the proportion of alleles mismatches at each SNP between pairs of genotypes. Although computationally intensive, the MLM approach is effective in removing the confounding effects of population structure in association mapping (Yu et al., (2006). MLM can be described by the following formula: Phenotype= M+Q+K+e in which M and e denote the genotypes at the marker and residuals, respectively.

As association mapping is based on LD, once a marker is detected to be associated with a trait, one expects that the locus actually responsible for the trait would be in LD with the marker (in cases the marker itself would correspond to the locus). For this reason, the extend of LD in a populationis a key factor in effectiveness of GWAS (Abdurakhmonov and Abdukarimov, 2008). In populations with high LD level, GWAS does not require a large number of markers, but the resolution will be low and this implies more efforts to clone candidate genes. In contrast GWAS on populations with small extent of LD require a larger number of markers to the genome at high density, but this higher resolution enables more accurate fine mapping and potentially facilitates the cloning of candidate genes.

The choice of genetic materials is therefore the most important step in GWAS (Breseghello and Sorrells, 2006; Flint-Garcia et al., 2003; Yu et al., 2006).

Genetic diversity, extent of genome-wide LD, and relatedness within the population determine the mapping resolution, marker density, statistical methods, and mapping power. In comparison to QTL mapping in biparental segregating progenies, GWAS has the potential to afford a higher genetic resolution (Figure 1.10) (Zhu et al., 2008). For example, Tommasini et al., (2007) reported that LD on chromosome 3B extended up to 0.5 cM in 44 varieties or 30 cM in 240 RIL populations of winter wheat. Normally plant GWAS collections consist of breeding lines, landraces or samples from natural populations: as these germplasm panels derived from many events of crossing and recombination, they lead to a suitable level of genetic diversity and linkage disequilibrium (Zhu et al., 2008).

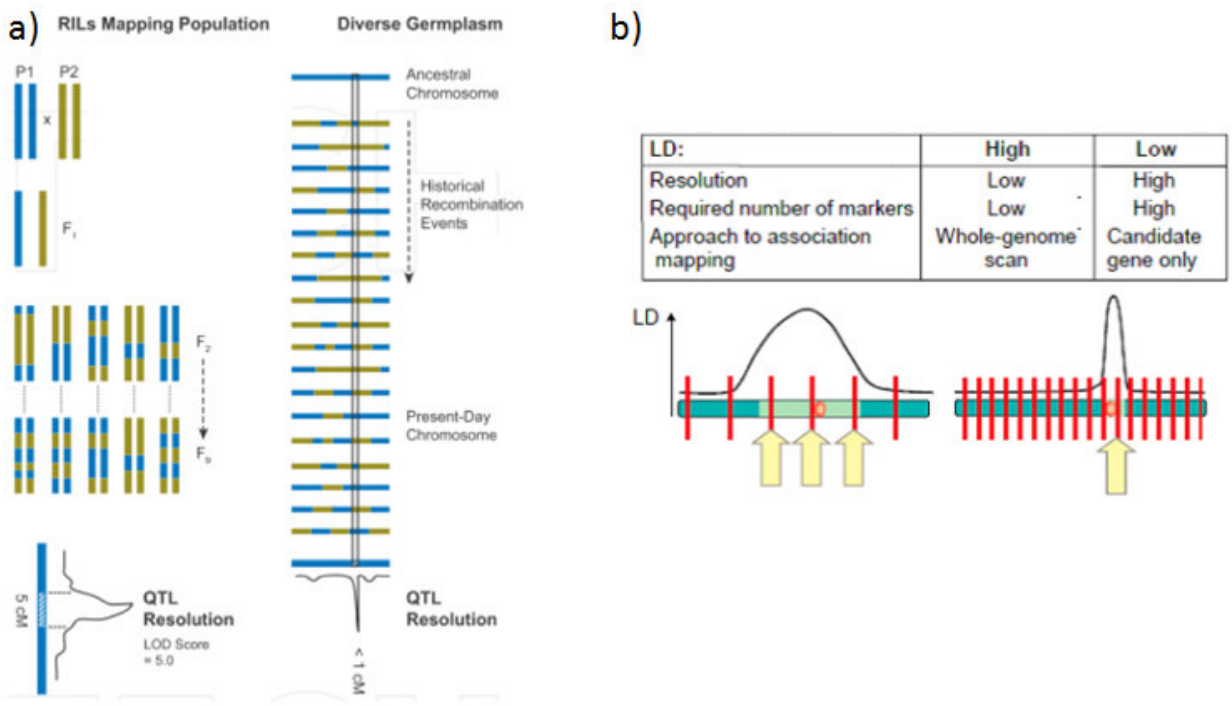

Figure 1.10. a) Schematic comparison of QTL mapping with bi-parental derived segregant population (left) and association mapping with diverse collections (right) (from Braulio and Cloutier, 2012). b) Effect of LD size on mapping resolution (from Rafalski, 2010).

The assembly of a GWAS population is often a compromise between the width of genetic-phenotypic variation and statistical power. For example, a GWAS population of highly genetically diverse individuals (e.g. from distant geographical areas) would exhibit high phenotypic variability but likely it would be strongly structure; in contrast an assembly of related individuals (e.g.

varieties from one breeding program) could be analyzed with simple models but would not exhibit high phenotypic variation (Zhu et al., 2008). Normally locally adapted material is used for GWAS. In case of barley, row-type, growth habit (spring/winter), origin (European, North American, Asian, Australian…) are the main coordinates through which barley germplasms are diversified, and the tendency is to assemble GWAS populations that do not cross these categories (Table 1.1).

Recently barley populations with large phenotypic variability and low population structure have been developed. Nice, et al. (2013) developed a multiparental advanced backcross population with 25 wild barley accessions backcrossed to the same recurrent parent (the cultivar Rasmusson): this population of 798 BC2F6 lines has almost no structure, as on average 85-99% of the genome of each line came from the recurrent parent, while the small introgressed regions from wild barley parents are source of an high variation (Nice, et al., 2013), this procedure is also called "nested association mapping" (NAM). Another population design with high variability and low population structure is represented by multiparent advanced intercross (MAGIC) populations that are created by inter-crossing n lines for n/2 generations until all founders are combined with equal proportions in the inter-crosses, RILS are derived immediately or with additional rounds of self-mating (Huang et al., 2012). In these populations, genomes from founders are mixed in equal proportions within individuals so that population structure is absent. The number of recombination events is enough to get a suitable LD extent. A barley MAGIC population has been developed at CRA (Fiorenzuola d'Arda, Italy) by inter-crossing four old and four modern six-rowed winter barley varieties, differing for yield related traits but with small differences in developmental and phenological traits. Phenotyping and genotyping are in progress in the frame of the EU Whealby project.

Phenotyping

Association mapping analyses require collection of phenotype data from replicated trials on large numbers of accessions across multiple years and locations. Efficient field design, appropriate statistical methods (e.g., nearest neighbor analysis and spatial models), and consideration of QTL × environmental interaction should be explored to increase the mapping power, particularly if field conditions are not homogenous (Eskridge, 2003).

Furthermore relationships between different traits should be evaluated , e.g. flowering date, lodging and susceptibility to pathogens could influence other traits under field conditions (Zhu et al., 2008).

Multiple testing

GWAS analyses normally employ from hundreds till thousands markers, implying that hundreds or thousands p-values are calculated. To evaluate significance of marker-trait associations a threshold p-value must be established. If n SNPs are tested and the tests are approximately independent, the appropriate per SNP significance level α' should satisfy $\alpha = 1 - (1 - \alpha')^n$, which leads to the Bonferroni correction $\alpha' = \alpha / n$. For example, to achieve $\alpha = 5\%$ over 1 million independent tests means that we must set $\alpha' = 5 \times 10^{-8}$. However, at high marker densities markers are tightly linked, so that tests are less independent and Bonferroni correction is too conservative leading to ignore true associations (Balding, 2006).

An alternative approach to establish a significance threshold is based on false discovery rate (FDR), which is the proportion of false positives over the total of positives. It consists in ordering for increasing P-value from i = 1 to i = n and setting the significance threshold at the highest P-value at which the inequality P-value ≤ α x m / n (where α is the threshold level of significance, n is the number of tests and m is the ordering number) holds true, establishing that this and all smaller P-values correspond to significant comparisons. If the inequality never holds true, no comparison is established as significant (Benjamini and Hochberg, 1995).

Association mapping in Barley (*Hordeum vulagare*).

Barley is a self-pollinating species and has, as well as other crop plants, undergone a severe population bottleneck during domestication (Tanksley and McCouch, 1997); furthermore contemporary European spring and winter varieties descend from a small number of successful European landraces selected around 100 years ago (Bothmer and Fischbeck, 2003). This have impacted the patterns of variation within cultivated European barleys and strong LD has been observed along chromosomal regions up to 212 kb in length (Piffanelli et al., 2004; Caldwell et al., 2006). In landrace accessions, LD decayed over 90 kb and in wild barley (*Hordeum vulgare* ssp. *spontaneum*) LD did not extend beyond the genic regions (Piffanelli et al., 2004). Kraakman et al (2004) performed GWAS using 123 mapped AFLP markers in modern two-rowed spring barley varieties and observed LD between markers as far apart as 10 cM. In Rostoks et al., (2006) 91

European spring and winter cultivars were genotyped with 612 SNPs, finding that the extent of LD was strongly affected by population structure. Highly significant intrachromosomal LD (r^2= 0.5) extended over 60 cM with a mean of 3.9 cM. In the combined set of European spring and winter barley 20.4% of all significant associations were interchromosomal. In the spring two-row subset, LD extended only up to 15 cM (mean 1.53 cM) and the proportion of interchromosomal associations was reduced to 2%.

Due to the large extent of linkage disequilibrium, providing a well-defined haplotype structure from which marker-trait associations can be identified, barley is particularly suited for GWAS. Several GWAS studies were made during the last decades, some of them are reported in Table1.1.

Table 1.1 Examples of GWAS in barley.

Number of individuals	Type of population	Type and number of marker	Trait	New genes cloned	Reference
516	UK barley cultivars	1536 SNP	Yied, malting traits		(Wang et al., 2012)
429	Modern spring, winter European cultivars	129 SAP	Vernalization requirement		(Cockram et al., 2008)
192	Spring and winter European 2-rowed old and modern cultivars	1307 SNP	Frost tolerance		(Visioni et al., 2013)
500	UK barley cultivars	1426 SNP	Antocyanin pigmentation	ANT-2	(Cockram et al., 2010)
95	Winter German varieties	1915 Dart+ 72 SSR	Heading date, lodging, plant height, yeld,brekling, neckling.		(Lex et al., 2014)
224	Spring cultivar	985 SNP	Heading date, plant height, thousand grain weight, starch content, protein content		(Pasam et al., 2012)
329	Winter North American cultivar	3072 SNP	Resistance to: powdery mildew, leaf rust, net blotch, spot blotch.		(Berger et al., 2013)
426	Winter and spring barley cultivar	5213 SNP	Heading date	EPS2/EAM6	(Comadran et al., 2012)
192	American and European cultivars	4608 SNP	Row-type	Int-c	(Ramsay et al., 2011)
216	Spring 2-rowed cultivar	5213 SNP	Resistance to lodging, breackling, neckling.		(Tondelli et al., 2013)
318	Wild barley accessions	588 DArT, 2878 SNP	Resistance to spot blotch		(Roy et al., 2010)

Cockram et al. (2010) used a collection of 500 elite UK barley lines genotyped with 1536 SNP markers to identify the causal polymorphism for *ANT-2*, a major gene governing anthocyanin production in barley. Ramsay et al. (2011) analysed 192 American / European elite cultivars genotyped with 4608 SNP markers to identify the candidate gene for *INT-C*, one of the genes controlling barley spike morphology. The candidate gene was then validated using a collection of well-characterized mutant stocks. Comadran et al. (2012) used a genome-wide scan for divergent selection footprints in 216 spring and 207 winter two-rowed barley genotyped with 5323 SNPs to identify the candidate gene for *EARLINESS PER SE 2* (*EPS2*), a locus associated with flowering date (independently from vernalization and photoperiod response). The candidate gene was validated by re-sequencing the historical collection of early flowering barley mutants.

These studies highlight the power of GWAS for genetic dissection of natural phenotypic variation, discovery of genes controlling agronomic traits and identification of sources of useful variation from “exotic” materials (landraces, Crop Wild Relatives, CWRs). The resulting information is being applied to contemporary breeding efforts along with other genomics-based approaches.

1.10 SCOPE AND OBJECTIVE

Root and shoot architecture traits are key factors in plant performance, competition with weeds, adaptation and stress responses thus having an important impact on yield and yield stability. In formulating cereal ideotypes, breeders proposed hypothetical optimal morphological parameters that were modelled in relation to different environmental conditions. Understanding and manipulation of morphological traits is key in view of breeding improved crops for future agriculture.

The objective of this project was to identify and characterize genomic regions or genes controlling root and shoot architecture in barley and how different traits are influencing each other. To this end, two approaches were undertaken depending on the trait(s) under study:

- the first exploited natural variation in a panel of modern and old European barley cultivars to carry out association mapping of flowering date, stem diameter, number of fertile rachis nodes per spike, spike length, leaf dimension, tillering and root extension (Chapters 2 and 3);
- the second was to characterize the ontogenetic basis of increased tillering using as a case study the *many-noded dwarf6 (mnd6)* high tillering barley mutant (Chapter 4).

In the first approach, we focused on winter barley because of its agronomic interest in the Mediterranean area, where genetic improvement of drought stress is important. We analyzed a panel of 142 European winter barley cultivars (67 two-rowed and 75 six-rowed) with a view to conduct a genome wide association scan (GWAS) for shoot and root architecture traits in two separate sets of experiments: one field experiment where shoot architecture traits were measured on fully developed plants, and one experiment in controlled condition of growth chamber, where we phenotyped for root extension on plants collected at early stages. To GWAS, genotyping data for 4,083 SNPs were available from previous projects of which 2,521 mapped on the POPSEQ barley reference map.

The second approach aimed at gaining insight into the ontogenetic mechanisms of barley tillering using as a model the high tillering *mnd6* mutant. Morphological development of *mnd6* and wild-type lines were compared in detail from germination till maturity in relation to shoot apical meristem stage.

2. ASSOCIATION MAPPING ON TRAITS RELATED TO SHOOT ARCHITECTURE

2.1 INTRODUCTION

2.1.1 THE BARLEY PHYTOMER AND PLANT DEVELOPMENT

The aerial part of the plant body is organized as a series of repeated units call phytomers (Figure 2.1), where each phytomer consists of a node, an internode, a leaf and an axillary bud (Weatherwax, 1923; Sharman, 1942). In barley and other grasses, the node displays meristematic activity giving rise to internode (stem) elongation, axillary bud and adventitious root formation (Figure 2.1, Weatherwax, 1923; Sharman, 1942). The architecture of reproductive organs and paired structures present at branching points (eg floral bracts stamen and pistils) can be explained by an adaptation of this model (Figure 2.1 Bossinger et al., 1992; Forster et al., 2007). Thus, development of the main stem is a continuous process of organogenesis carried out by the shoot apical meristem (SAM) where phytomers are produced one upon the other by the differentiation of cells produced by the meristematic activity of the SAM. In barley and other grasses, lateral shoots called tillers develop from vegetative axillary meristems (AXMs) present in the axils of leaves at the base of the plant (crown) (McSteen and Leyser, 2005). An axillary bud, consists of an AXM with young leaf primordia enclosed by the prophyll, a leaf-like organ that may be seen as the first leaf of the lateral shoot (Bossinger et al., 1992). Axillary buds can then develop with the same pattern described before for the SAM, producing a new series of phytomeric units which constitute the tiller (Bossinger et al., 1992; Forster et al., 2007). Each tiller develops other AXMs that may in turn develop secondary tillers and so on according to a reiterative pattern (Kirby and Aplleyard, 1987). Shoot architecture is then determined by the activity and determinacy of the SAM and AXMs (Wang and Li, 2008). In the following paragraphs the development of different lateral organs and structures will be discussed in more detail.

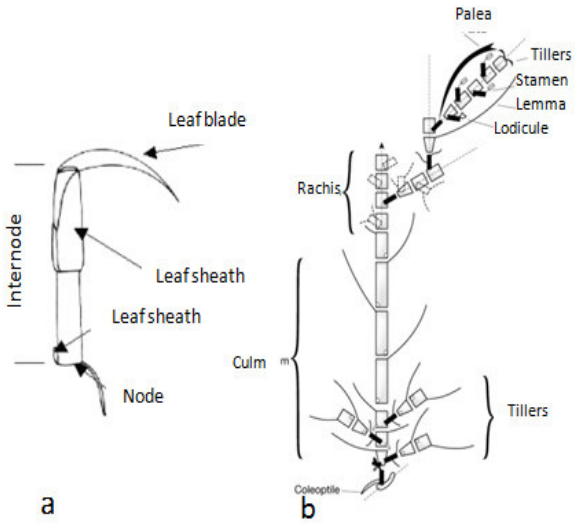

Figure 2.1. a) The barley phytomer based on Weatherwax (1923) and Sharman (1942), image modified from Bossinger et al., (1992). b) Phytomeric structure of barley plant, image from Forster et al. (2007).

2.1.2 LEAF DEVELOPMENT

Leaves absorb light radiation and convert it into energy for the plant through photosynthesis (Barber, 2009; Zhu et al., 2010). Photosynthetic efficiency derives from a complex balance between light absorption, CO2 assimilation and water transpiration, and depends on a number of canopy architectural and physiological features that are also influenced by the interaction with the environment. In barley and other cereals leaf size and orientation are determinants of canopy transpiration and radiation interception (Poorter et al., 2012). Large leaves tend to have a high leaf mass per unit area to counter leaf bending (Poorter et al., 2012). In dry and sunny Mediterranean environments reduced size and erect orientation of the leaves can reduce water loss by transpiration (because of a lower number of stomata), and allow deeper light penetration into the canopy so that radiation can be intercepted and utilized by lower leaves (Geller and Smith, 1982; Welander and Ottosson, 1997; Horton, 2000). Conversely, Farooq et al., (2010) analyzing plant growth in green-house under water stress condition of on rice lines characterized by different leaf size, found that lines with broader leaves had higher biomass, less stomatal conductance, and higher transpiration efficiency under drought than lines with narrow and shorter leaves.

At the same time it should be considered that in rice and other cereals, the top 2 leaves on the stem produce more than 80% of the photosynthates that go to fill the grains (Tomoshiro et al., 1983; Gladun and Karpov, 1993a; Gladun and Karpov, 1993b). Understanding the genetic control of leaf dimension is the first step for manipulating these traits.

In *Arabidopsis* the mechanisms underlying leaf formation and growth are well characterized. The process can be divided in partially overlapping steps with coordinated patterns of cell proliferation and expansion along the developing leaf resulting in its final shape and size (Figure 2.2). Following initial developmental stages when all the cells of the primordium are proliferating, proliferation ceases at the tip of the leaf, giving way to cell expansion; in intermediate stages cell proliferation continues at base of the growing leaf while more distal cells in the proliferating zone start expanding; in later stages mitosis ceases completely and cell expansion continues till reaching the final leaf dimension (Gonzalez et al., 2012).

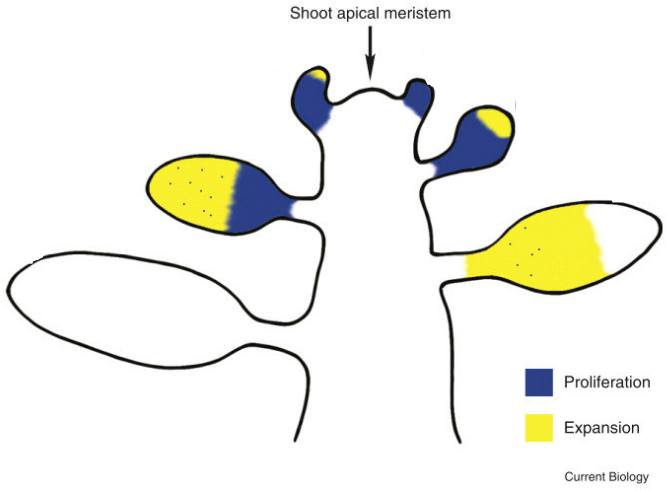

In *Arabidopsis* leaf growth occurs through the following steps:

- Initiation phase: the leaf primordium is initiated at the periphery of the SAM and grows out like a protrusion where dorsal and ventral domains are defined. The SAM size seems to be related to plastochron (i.e. the time interval between the initiation of two successive leaves) and possibly to leaf area (Chaudhury et al., 1993; Werner et al., 2003; Higuchi et al., 2004; Kwon, 2005), although only one mutant was reported where the number of cells of the leaf primordium affected final leaf size (Autran et al., 2002).
- Cell proliferation: cells increase in numbers while maintaining a small size. A direct correlation was found between the total amount of cells produced in this step and leaf size (Korner et al., 1989; Meyerowitz, 1997). The final number of cells was found to be

proportional to cell division rate, but above all it is depends on the duration of the cell proliferation phase (Gonzalez et al., 2012).

- Cell expansion and differentiation: when cells stop dividing, leaf growth occurs through turgor-driven cell expansion and differentiation of different tissues (Cosgrove, 2005). Between mitosis and cell expansion, some cells undergo endoreduplication (Breuer et al., 2010), where ploidy level increases without subsequent mitosis; correlation between cell size and ploidy level, cell size and leaf size were reported (Gonzalez et al., 2012).
- Meristemoid division: during cell expansion and differentiation, so-called meristemoid cells continue to duplicate to form specific cell types, like stomatal guard cells, pavement cells and vascular cells (Peterson et al., 2010). Pavement cells play an important role in leaf size (Gonzalez et al., 2012).

Grasses have a different leaf architecture from dicotiledons, but some patterns of leaf formation are similar (Powell and Lenhard, 2012). A grass leaf is typically divided into three regions along the longitudinal axis (Itoh et al., 2005): the blade is the distal region of leaf, projecting out from the stem and playing the major role in photosynthesis; the leaf sheath is the proximal portion of the leaf directly connected to the node and surrounding the stem and the shoot apex; the junction between blade and sheath is organized in three parts: 1) the lamina joint which binds the leaf blade toward the abaxial side, 2) the ligule, a thin membranous outgrowth that develops on the adaxial side of the blade-sheath boundary and is flanked by 3) the auricles, two ear-like protrusions that form on the leaf margins at the base of the blade (Figure 2.3).

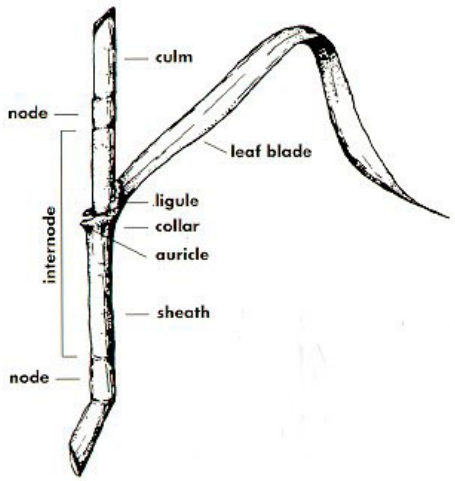

Figure 2.3. Schematic representation of a grass leaf (http://www.fsl.orst.edu/forages/projects/regrowth/print-section.cfm?title=Grass%20Structures).

Leaf formation in rice follows a series of steps partly similar to *Arabidopsis* (Itoh et al., 2005). Leaf development can be described by six stages.

- Stage P1: formation of the leaf primordium as a crescent-shaped protrusion the flank of the SAM.
- Stage P2: the primordium exhibits a hood-like shape, the differentiation of vascular bundles starts.
- Stage P3: formation of ligule primordium, the leaf margins overlap and surround the SAM, the boundary between sheath and blade is formed; in this stage cell proliferation at the tip ceases and formation of vascular bundles proceed basipetally. Differentiation of sclerenchymatous cells and initiation of epidermal specific cells occur.
- Stage P4: rapid elongation of leaf blade due to the activity of intercalary meristem situated at the base of leaf blade. Differentiation of specific epidermal cells (bulliform cells, silica cells, cork cells and stomata) occurs.
- Stage P5: rapid elongation of leaf sheath. The maturation of epidermal tissue and formation of lacunae occur. The leaf blade tip emerges from the sheath of the P6 leaf (the time interval between the appearance or emergence of two leaves is called phyllochron).
- Stage P6: mature leaf. The leaf becomes mature and growth is completed. Leaf blade bending occurs at the lamina joint.

Despite these progresses, information on the genetic control of leaf size in important cereal species such as barley is still lacking. In barley some mutations, causing altered leaf development were identified and partially mapped (Druka et al., 2011):

- *broad leaf1* (*blf1*): Plants are somewhat lighter green than normal. All leaf blades are very broad, about twice normal width, and markedly crinkled, especially at the margins. The mutant is mapped on the long arm of chromosome 5H (Lundqvist and Franckowiak, 1996; Druka et al., 2011)
- *gigas2* (*gig2*) mutant plants are tall and robust. Most plant organs including leaves are larger and spikes have 4 to 8 more fertile spikelets compared to wild-type. Flowering is delayed by two or three weeks in the mutant and plants lodge easily. The gene is not mapped (Lundqvist and Franckowiak, 1996; Druka et al., 2011).

- *macolosus-3* (*mac.3*): mutant leaves are wider than wild-type, the gene is not mapped (Druka et al., 2011).
- *narrow leaf dwarf-1* (*nld.1*): mutant plants have narrow dark green leaves, which are erect with well developed midribs; the mutant locus maps on chromosome 5HL (Lundqvist and Franckowiak, 1996; Druka et al., 2011).
- *granum-a* (*gra-a*) was mapped on chromosome 3HL, *gra-a* plants have numerous, thin tillers with narrow leaves and short internodes (1/2 of normal plant height) (Druka et al., 2011).
- *many node dwarf 6* (*mnd6*, 5HL) and *many node dwarf 1* (*mnd1*, 4HL) mutants have an accelerated phyllochron and a higher number of internodes, tiller and leaves compared to wild-type while leaves are smaller (Lundqvist and Franckowiak, 1996; Druka et al., 2011).

Among these one the only gene to be cloned was *mnd6* (see chapter 4, Mascher et al., 2014).

2.1.3 TILLERING

Tillering in grasses is the process through which buds formed at leaf axils in basal nodes of the culm germinate and produce lateral branches (tillers) that in turn can produce roots and reproductive organs, so that the mature plant can be considered as a composition of tillers derived from the main culm (Skinner and Nelson, 1992).

Tillering is one of the main factors influencing crop performance, biomass and grain production (Sakamoto and Matsuoka, 2004; Sreenivasulu and Schnurbusch, 2012). It is a plastic trait and the plant can modulate the number of tillers in response to environmental conditions and plant density, optimizing the use of resources, maximizing soil surface coverage, competing with weeds and increasing the number of reproductive organs (Donald, 1968; Seavers and Wright, 1999; Agusti and Greb, 2013). However, senescence of tillers before maturity can reduce yield by dissipating resources that could be invested in increasing production of productive tillers; indeed the domestication of many crops, such as maize (*Zea mays* ssp. *mays*), foxtail millet (*Setaria italica*) and sunflower (*Helianthus annuus*), implied total or partial loss of branching (Doebley et al., 2006; Doust and Kellogg, 2006). Control of tiller number is an important objective of crop breeding, especially with respect to adaptation to environments with severe water limitation (Donald, 1968; Islam and Sedgley, 1981). Relation between drought stress and tillering have been well study in wheat. Typically, wheat seedlings tend produce a large number of tilllers early in the

season developing a large leaf area, prior to initiation of the reproductive structures (Duggan et al., 2005). While this may be an advantage to control weeds (by covering the soil quickly), there is a consume of water so high that crops exhaust soil water before the completion of grain filling. Reducing demand for water at the beginning of season should increase availability of water for post-anthesis crop growth (Richards and Townley-Smith, 1987). Restricted tillering has been proposed as a trait for reducing leaf area development, thereby slowing canopy growth early in the season (Islam and Sedgley, 1981; Yunusa and Sedgley, 1992). Islam and Sedgley (1981) demonstrated that manually de-tillered wheat consumed less water in pre-anthesis to leave more water for post-anthesis growth. However, Duggan et al. (2005) and Yunusa and Sedgley (1992) compared different reduced and free-tillering near-isogenic lines, and observed either no difference in leaf area index (LAI), or an even greater LAI in reduced-tillering lines. Both these researchers and others (Marshall and Boyd, 1985; Richards, 1988) have reported that the larger individual leaf size of reduced-tillering lines compensated for fewer tillers and therefore water use may not be conserved for use during grain filling (Yunusa and Sedgley, 1992). The tiller inhibition (*tin*) mutant of wheat has most of the features of a high yielding ideal wheat plant for both favourable and dry environments as proposed by Donald (1968). It has few tillers, enlarged aboveground organs including thick leaves and stem, a large spike, more and larger grains per spikelet and a higher harvest index (Atsmon and Jacobs, 1977). In the northern Australian wheat belt, it was observed that *tin* gene when introgressed in the Silverstar genetic background produced a reduced LAI (Mitchell, 2010), in part because the warmer environment accelerates development and therefore the 'compensation' by leaf size for reduced tiller number was reduced. (Mitchell et al., 2013) compared yields of a three *tin* introgressed-Silvestar isogenic line (two restricted tillering, and one semi-restricted tillering), with other three Silverstar free tillering near-isogenic lines and their recurrent Silverstar parent under field normal and drought condition at normal density sowing. While in irrigated condition *tin* lines exhibit a lower yield than free tillering isolines, because of a reduced number of spikes, under drought condition *tin* lines yield was major because of a higher kernel weight and greater number of kernel per spike. The higher kernel weight of the *tin* lines under stress conditions was associated with greater anthesis biomass and increased stem water-soluble carbohydrates, ensuring more assimilate for later translocation to filling grain.

Tiller development occurs through 3 different phases: 1) the establishment of an AXM at the leaf

axil, 2) the formation of an axillary bud and finally 3) the outgrowth of a bud to form a tiller (Schmitz and Theres, 2005). The first two steps are mainly genetically controlled, while bud outgrowth is regulated by complex interactions between genetic factors, hormones and environmental cues (Kebrom et al., 2013). While sharing these major developmental stages, tillers differ from side branches in dicots in that they can produce adventitious roots and grow independently from the main culm, and aspects of the molecular mechanisms involved in tiller formation appear to be distinct from those of dicot model species such as *Arabidopsis*, tomato and petunia (Kebrom et al., 2013). Genetics and molecular studies of tillering have been particularly intense in rice and the following paragraphs present a summary of the current knowledge of the genes involved in the three main phases of tiller development.

AXM establishment.

The genetic mechanism underlying AXM formation have been partially clarified in rice (Figure 2.4). *MONOCULM 1* (*MOC1*) is the main gene responsible of AXM formation and axillary bud maintenance, with loss of function mutants lacking AXMs and consequently tillers; conversely, enhanced *MOC1* expression results in high tillering and reduced plant height (Li et al., 2003). The *TILLERING AND DWARF1 TAD1/TE* gene encodes a suppressor of the MOC1 protein, and loss of function mutants have similar phenotypes of plants over-expressing *MOC1* (Lin et al., 2012; Xu et al., 2012). After AXM formation, the *LAX PANICLE* genes *LAX1* and *LAX2* are involved in maintenance of both vegetative and reproductive AXMs , as shown by analysis of loss of function mutants that are characterized by decreased tillering and reduced rachis branches and spikelets (Komatsu et al., 2001; Komatsu et al., 2003; Oikawa and Kyozuka, 2009; Tabuchi et al., 2011).

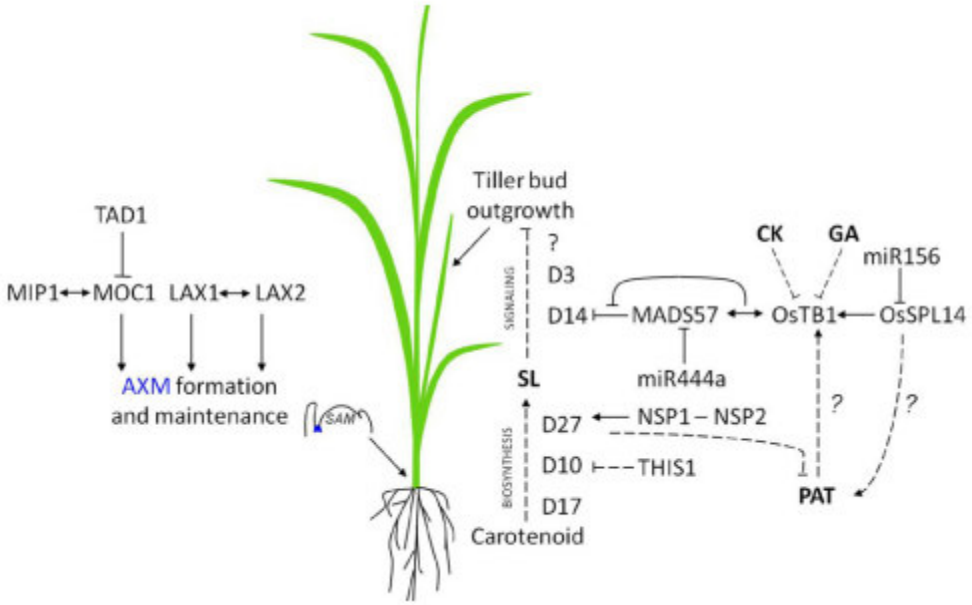

Figure 2.4. Key interactions among genes controlling rice tiller number. Left: genes involved in axillary meristem (AXM) initiation and establishment. Right: genes involved in axillary bud outgrowth through the strigolactone (SL) pathway and its interactions with auxin (Aux), gibberellic acid (GA), and cytokinin (CK). Arrows indicate positive regulation, blunt-ended lines indicate negative regulation, dashed lines indicate multiple steps or indirect effects, and double-headed arrows represent protein–protein interactions (image from Hussien et al., 2014).

Axillary bud establishment and outgrowth: the role of hormones. Apical dominance is the repressive action of the shoot apex on outgrowth of axillary buds and is mediated in part by auxin produced by young expanding leaves and actively transported basipetally through the stem (Agusti and Greb, 2013a). Polar auxin transport (PAT) through the stem is mediated by integral membrane proteins of the PIN family (Zazimalova et al., 2010) and increased tillering has been associated with under/over-expression of *OsPIN1b* and *OsPIN2*, respectively, indicating divergent roles for *PIN* genes in rice. Another player in this pathway is *ABERRANT SPIKELET AND PANICLE1* (*ASP1*) a gene encoding a corepressor acting in auxin signallig, with pleiotropic effects on tillering, phyllotaxis and panicle branching (Yoshida et al., 2012). In addition, *TLD1* (*increased number of Tillers/ enlarged Leaf angles/Dwarfism*) is a gene encoding an auxin-inactivating protein, and gain of function *tld1-D* mutants show enhanced tillering (Zhang et al., 2009).

Beside auxin, other hormones are involved in controlling bud outgrowth also in response to environmental cues (Figure 2.4). Cytokinins (CKs) regulate many plant development processes, for example stimulating cell division, activating axillary buds, inhibiting root growth and retarding

senescence (Werner et al., 2003). CKs are produced in roots and transported to the shoot through xylem, and CK synthesis is regulated by nutrient and water availability (Krouk et al., 2011; Ha et al., 2012).

Gibberellin (GA) synthesis is regulated by apically produced auxins, and together these hormones regulate stem elongation (O'Neill, 2002). GAs positively regulate germination, stem and root elongation, flower development, and repress *OsTB1* (*Oriza sativa Teosinte branched1*) 1, a key repressor of tiller outgrowth: rice mutants which over-synthesize GA are semi-dwarf with enhanced tillering and enhanced adventitious root growth (Lo et al., 2008).

Brassinosteroids (BR) are hormones that together with GA control plant height, and rice mutants with altered BR biosynthesis or signal transduction such as *DLT (DWARF AND LOW-TILLERING)* exhibit shorter stature and reduced tillering (Hong, 2003; Booker et al., 2004; Tong et al., 2009).

Strigolactones are hormones derived from carotenoids (Matusova et al., 2005), they are produced in roots and transported acropetally (Wang and Li, 2006), and are inhibitors of side branching in plants (Gomez-Roldan et al., 2008; Umehara et al., 2008). Rice *DWARF* genes *D17*, *D10* and *D27* are involved in different steps of strigolactone synthesis and loss of function mutants exhibit an increment in tiller number and a decrease of plant height (Lin et al., 2009).

Research in this area is revealing complex cross-talks among different hormonal pathways with some factors integrating different signals/pathways, such as *TEOSINTE BRANCHED1 (TB1)* (Studer et al., 2011), a TCP transcription factor first identified in maize. In wild-type maize lateral branching is suppressed, and axillary buds only develop few short internodes terminating with a spike (female inflorescence); in *tb1* mutants buds develop long primary branches terminating with a tassel (male inflorescence) indicating that *TB1* acts to inhibit lateral branching and specifies female identity (Doebley et al., 1997). The homologous gene in rice, *OsTB1* seems to play a similar role (Lukens and Doebley, 2001; Takeda et al., 2003) as shown by its loss of function mutant *fine culm1* (*fc1*), which exhibits increased tillering (Minakuchi et al., 2010). Interestingly, *fc1* mutants are insensitive to exogenous SL application and have an epistatic interaction with *d17* (Minakuchi et al. (2010) suggesting that *OsTB1* acts downstream of SL. Additional evidence that CK and GA are negative regulator of *OsTB1* (Lo et al., 2008) led to the hypothesis that *OsTB1* coordinates different pathways involved in tillering (Minakuchi et al., 2010).

Environmental Factors Influencing Axillary Bud Overgrowth

Tillering is strongly affected by planting density (Doust and Kellogg, 2006). Studies in maize and rice showed that this phenomenon is mediated by light quality through modulation of *ZmTB1* and *OsTB1* effects: the wild-type grown in high planting densities reduce the number of developed tillers, without affecting the number of produced axillary meristems, while mutants grown in the same condition don't exhibit reduction in tillering (Lukens and Doebley, 2001; Takeda et al., 2003). Thus, *TB1* plays a role in the shade avoidance response (Schmitt et al., 2003; Kebrom et al., 2013), which consists of stem elongation of plant internodes and suppression of branching when a plant is overshadowed by other plants. Plants perceive this shadowing through the phytochrome pathway as the light that reaches them has a low red/far-red ratio (due to the absorption of red light by the canopy, Sawers et al., 2005). In *Sorghum* the expression of *SbTB1* (the orthologue of *ZmTB1*) was correlated to bud outgrowth suppression in *Sb-phyB-1* null mutants that constitutively expressed a shade avoidance response. These results were confirmed by the fact that wild-type plants grown in far-red light condition exhibited shade avoidance responses. It was then hypothesized that active phyB suppresses the expression of the *SbTB1* gene, thereby inducing bud outgrowth, whereas environmental conditions that inactivate phyB allow increased expression of *SbTB1*, thereby suppressing bud outgrowth (Kebrom et al., 2006).

Barley tillering mutants

Several barley mutants exhibiting tillering abnormalities have been identified and characterized providing some initial insight into the genetic and hormonal regulation of tillering in the Triticeae (Dabbert et al., 2009). They can be divided into three classes:

1) A mutant unable to develop lateral buds is *uniculm2* (*cul2*), which develops a single culm with altered phyllotaxis or absence of the spikelets at the distal end of the spike. AXMs are formed but they do not establish buds and flowering time is delayed compared to wild-type (Babb and Muehlbauer, 2003). This mutant has been crossed with low or high tillering mutants showing epistatic effects on the other genes (Babb and Muehlbauer, 2003). The *cul2* locus was positioned on chromosome 6H near the centromeric region, but no candidate gene has been identified (Okagaki et al., 2013). Trascriptome analysis (Close, 2004) indicated that *Cul2* is involved in coordination of signaling pathways and stress response and their integration into AXM development (Okagaki et al., 2013).

2) Recessive mutants which produce axillary buds but have reduced number of tillers include *absent lower laterals1 (als1), low number of tillers1 (lnt1), uniculme4 (cul4), uzu* and *intermedium-b (int-b)*.

The *als1* mutant exhibits a reduced number of tillers, and fails to develop lateral spikelets at the base of the inflorescence (Dabbert et al., 2009): plants develop axillary buds that originate primary tillers, but these one do not develop secondary buds (Dabbert et al., 2009). The gene was mapped on chromosome 3 HL-BIN3 (Dabbert et al., 2009). Double mutants of *als-1* mutant and high tillering mutants *gra-a* or *den-6* show the same phenotype of *als1*, demonstrating that the low tillering gene has an epistatic effect on the other genes (Dabbert et al., 2009).

The *low number of tillers 1* (*lnt1*) mutant (locus mapped on 3HL, Bin 11) develops 2 or 3 tillers because of a reduction in primary axillary buds and the absence of secondary buds, although it is still unclear if this inhibition occurs at meristem establishment or in the following stages (Dabbert et al., 2009). Microarray analyses on the mutant identified a transcript whose presence is decreased in all plant organs compared to wild-type: this encodes JuBEL2, a protein with a BEL-like homeodomain previously identified as an interactor of the KNOX transcription factor encoded by the *Hooded* (*Kap1/BKn3*) gene (Muller et al 2001). Allelic comparisons and segregation analyses suggest that the *lnt1* phenotype could be caused by a mutation in the *JuBel2* gene. The homologous gene in Arabidopsis, *BLR*, has many roles in plant development and is involved in the establishment of axillary meristems (Long and Barton, 2000). Double mutant between *lnt1* and high tillering mutants exhibit the same phenotype of *lnt1*, indicating an epistatic effect of *lnt1* on the other genes (Dabbert et al., 2009). Conversely *lnt1-int-b* double mutants have no tillers suggesting a combined effect of the 2 mutations; *lnt1:int-m* double mutant exhibit few tiller more than *lnt1* suggesting an additive effect of the two mutations. These results suggest that *lnt1, int-b* and *int-m* operate in distinct pathways (Dabbert et al., 2009).

uniculm4 (*cul4*) mutants develop 1-4 tillers that are twisted and kneeling at the nodes. Spikes have elongated peduncles and elongated rachis internodes, ligules are absent and leaf sheath margins show abnormal outgrowths of auricle-like tissue indicating that the *Cul4* gene is involved in tiller development, leaf and inflorescence patterning (Babb and Muehlbauer, 2003). Expression analyses identified 308 transcripts differntially expressed between mutant and and wild-type, 20% of these genes were implied in stress response and carbohidrates methabolism. A notable group

included genes involved in response tojasmonic acid suggesting a possible interaction between the jasmonic acid pathway and the branching process (Bilgic et al., 2007). The gene has been mapped on chromosome 3 HL (Pozzi et al., 2003).

The *uzu* mutant allele causes reduced plant height and slight decrease in tiller number (Babb and Muehlbauer, 2003): it is widely used in asian breeding programs to confer lodging resistance (Hoskins and Poehlman, 1971; Tsuchiya, 1976; Saisho et al., 2004; Zhang et al., 2009). The gene, localized on chromosome 3HL, was cloned and found to encode a putative BR receptor HvBRI1 establishing an additional link between the BR pathway and tillering (Chono, 2003).

Plants carrying recessive mutations at the *intermeedium-b* locus *(int-b* chromosome 5HL) exhibit a slightly decreased tillering than wild-type.The spike appears similar to the six-rowed spike, but developmental irregularities occur commonly in the lower portion of the spike. All lateral spikelets are reduced in size, and the lemma awn is short or reduced to a pointed tip (Lundqvist and Franckowiak, 1996).

3) High tillering mutants include *granum-a (gra-a), many noded dwarf1 (mnd1), many noded dwarf 6(mnd6),* and *semidwarf1 (sdw1/denso)*.

The *gra-a* (3HL) mutant shows a semidwarf phenotype with an excessive number of tillers (Druka et al., 2011), due to increased numbers of AXMs and axillary buds, and the occasional appearance of two shoot apical meristems (Babb and Muehlbauer, 2003).

Recessive alleles at the *mnd1* (4HL) and *mnd6* (5HL) loci result in high tillering, semi-dwarf plants, where both the main stem and the primary tillers exhibit a higher number of leaves and branches develop both from non-aerial and aerial internodes (Druka et al., 2011). The *MND6* gene was recently cloned, and found to encode a protein belonging to the CYP78A subfamily of cytochrome P450 enzymes (Mascher et al., 2014), that will be better described in chapter 4.

sdw1/denso (3H), is an agronomically important dwarfing gene with pleiotropic effects leading to higher tillering (Jia et al., 2009). Even if allelic, the two mutations exhibit different phenotypic effects. A barley GA 20-oxidase gene (*Hv20ox2*) has been proposed as a candidate for *sdw1/denso* (Jia et al., 2009). Compared with wild-type, *Hv20ox2* expression is reduced four and 60 fold in the *denso* and *sdw1* mutants, respectively. These data indicate that low expression decreased plant

height while increasing tillering (Jia et al., 2009) and are consistent with a negative correlation between GA and tillering observed in rice.

Natural variation for tillering

Quantitative trait loci (QTLs) associated with tiller number have been mapped using a wild barley introgression population (Gyenis et al., 2007). Although the amount of phenotypic variation explained by genetic variance was small (Gyenis et al., 2007), three QTLs for tiller number were mapped on chromosomes 2H bin 3, 5H bin 6-8 and 6H bin 10-11, respectively (Gyenis et al., 2007). Moreover, Baum et al. (2003) detected four QTLs for tiller number on 1H, 2H, 3H, and 4H in a cross of a Syrian barley line, Arta, with a wild barley (*H. vulgare* ssp. *spontaneum*). A major tiller number QTL coinciding with the row type gene *VRS1* (see below) has been mapped in a recombinant inbred line population derived by crossing low-tillering six-rowed barley cultivar Morex to the high-tillering two-rowed cultivar Golden Promise, demonstrating that the recessive allele *vrs1.a* can have strong epistatic effect in reducing tillering (Druka et al. unpublished, reviewed in Rossini et al., 2014). In contrast, recessive alleles of the row type gene *INT-C* seem to promote tillering (Ramsay et al., 2011). The comparable increase in tillering due to *Int-c.a* in six-rowed cultivars would, however, be masked by the strong reduction in tiller number associated with 6-rowed *vrs1.a* alleles (Ramsay et al., 2011). Together these data suggest that different row type genes may have strong effects on reproductive and vegetative development as well.

2.1.4 PLANT HEIGHT

Plant height is another key factor in crop performance, as was demonstrated by the use dwarf varieties in rice breeding during the Green Revolution that allowed to strongly increase yields due to increased harvest index and lodging resistance. Rice *semidwarf*-1 (sd-*1*) and wheat *Reduced height-1(Rht-1)* semidwarf mutants were used to breed this trait during the Green Revolution. The rice *Sd-1* gene encodes GA20ox2, a key gene in GA biosynthesis and loss-of-function alleles cause partial deficiency in GA resulting in defects in cell and internode elongation. Four *GA20ox* genes are present in rice and their redundant action explains the specific and relatively mild phenotypes of *sd-1* mutants (Jia et al., 2009). In the case of wheat, semidwarf varieties have been selected from mutations in DELLA transcription factors that act as repressors of GA responses: GAs act by targeting DELLA proteins for degradation thereby releasing GA responses (Pearce et al., 2011). Wheat *Rht-B1* and *Rht-D1* are semidominant mutant alleles of DELLA-coding genes leading to reduced plant height due to GA-insensitive activity of DELLA proteins and constitutive repression

of GA responses (Pearce et al., 2011). Other mutations affecting hormonal synthesis or signaling were found to affect plant height with some examples of agronomic interest.

In barley, *uzu* is a semidwarf mutant used in breeding (described in the previous chapter). Barley breeding in Europe, North America and Australia deployed *sdw1/denso* alleles (described in the previous chapter). *ari-e* (5HL) is another semidwarfed mutant (Thomas et al., 1984) that has been used widely in barley cultivar development to reduce the severity of lodging (Ellis et al., 2002) and exhibits reduced internode length, short awns, a together with a moderate salt tolerance and a susceptibility to different fungal pathogens. The semidwarf mutant *short culm (hcm1)* has been proposed to be the allele used to reduce plant height in Upper Midwestern US malting varieties (Franckowiak, 2000). Other height mutants were genetically characterized even if they have no agronomic interest. Dominant mutations in the *Slender1* (*Sln1*) locus result in a dwarf phenotype due to GA insensitivity (Chandler et al., 2002), while a recessive mutations result in spindly plants as an effect of a constitutive GA response. Isolation of the *Sln1* gene revealed that it encodes a DELLA protein similar to the proteins encoded by wheat *Rht* genes (described above) (Peng et al., 1999; Chandler et al., 2002). The recessive GA 3-insensitive dwarfing genes *Rht-H1* and *Dwf2* were mapped on the centromeric region of chromosome 2H (Borner and Korzun, 1996), and on the short arm of 4H (Ivandic et al., 1999), respectively.Gyenis et al. (2007) used a BC_2 population derived from a cross between the wild barley OUH602 and the elite two-rowed malting variety Harrington and identified four QTLs for plant height on chromosome 1H, 2H, 3H and 7H. These QTLs appear to have been identified in many previous studies (Hayes et al., 1993; Borém et al., 1999; de la Pena et al., 1999; Marquez-Cedillo et al., 2001).

2.1.5 STEM DIAMETER

Relatively few studies have been dedicated to the genetic dissection of stem diameter, although this is generally recognized as an important trait in crop performance improvement. Rasmusson (1992) for example included stem diameter in the target traits to constitute a barley ideotype. Doley, 1983) found a positive correlation between stem diameter and kernel per head and postulated that enlargement of stem thickness could have a positive effect on yield. In addition, a field experiment with five barley cultivars revealed a positive correlation between stem diameter/cell wall thickness and lodging resistance (Dunn and Briggs, 1989). In agreement with this previous study, a field analysis of twelve barley crosses found a strong positive correlation between stem diameter at second internode and lodging resistance (Milhova et al., 2006).

Correlation between lodging and stem diameter were also found in oat (Norden and Frey, 1970) and rice (Ookawa et al., 2010). In particular Ookawa et al., (2010) carried out a detailed genetic analysis of lodging resistance in rice identifying a major QTL associated to culm diameter, called *STRONG CULM2 (SCM2)*. Comparison of the lodging resistant cultivar Habataki and normal cultivars showed that the greater physical strength of Habataki was due to a larger diameter and stem wall thickness, despite the lower lignin and cellulose contents relative to other lodging susceptible cultivars. Using a set of chromosome substitution lines from a cross between Habataki and another lodging susceptible cultivar (Ando et al., 2008), two different QTLs were detected, *SCM1* and *SCM2*, with the Habataki allele for *SCM1* increasing culm wall thickness, and the semidominant Habataki allele for *SCM2* increasing stem diameter (Ookawa et al., 2010). As larger culm diameter was more effective in enhancing lodging resistance then cell wall thickness, they focused further analyses on *SCM2*: line NIL-SCM2, carrying the *SCM2* Habataki allele, also exhibited a larger number of spikelets per panicle and consequently a larger production. Positional cloning and sequencing of *SCM2* revealed that the gene is identical to *ABERRANT PANICLE ORGANIZATION1* (*APO1)*, which encodes an F-box protein orthologous to Arabidopsis *UNUSUAL FLORAL ORGANS (UFO*, Wilkinson and Haughn, 1995). In a detailed analysis of *apo1* mutants (Ikeda-Kawakatsu et al., 2009), APO1 was found to regulate the cell proliferation rate in the inflorescence meristem. In NIL-SCM2, *APO1* expression in the inflorescence apex was 2-3 fold higher, the size of the inflorescence meristem was larger and the number of parenchyma cells in the basal internode was about 38% higher, resulting in an increased number of spikelets compared to the background (Ookawa et al., 2010). In NIL-SCM2 increased cell division in the inflorescence meristem also impacts the diameter of the basal part of the inflorescence meristem, as a consequence, culm diameter is also affected because culm cells are produced from differentiation of cells produced by the basal part of inflorescence meristem (Kawahara et al., 1968) . Thus, any increase in the cell proliferation rate in the inflorescence meristem led to an increase in the spikelet number and culm diameter, both of which were favourable traits in terms of crop productivity.

In barley, knowledge about genetic control on stem thickness is very poor. Chen et al., (2014) studied this trait in a segregant population derived from a cross between parents with opposite susceptibility to lodging, individuating ten QTLs influencing stem diameter and cell wall thickness at different internodes: cell wall thickness showed a weak but significant correlation to lodging

resistance; cell wall thickness and stem diameter of different internodes showed a strong correlation with spike weight.

2.1.6 FLOWERING DATE AND SPIKE DEVELOPMENT

Spike morphology

The mature barley spike consists of a rachis (floral stem) and floral units called spikelets. Spikelets consist of a floret subtended by two bracts called glumes. Each rachis node bears three spikelets. The spikelet axis is called rachilla and bears two bracts: the lemma with its distal extension called awn and the palea subtending two lodicules, three anthers, and two stigmas. In wild barley and two-rowed cultivars only the central spikelet is fertile, while the lateral spikelets do not develop; in six-rowed barley cultivars all three florets mature to produce grains (Kirby and Aplleyard, 1987; Komatsuda et al., 2007). The double ridge stage marks the transition from the vegetative to the reproductive phase. A detailed description of the histogenesis and sequence of floral organ differentiation can be found in (Bossinger et al., 1992). The apex continues to initiate new spikelet meristems until awn primordia are formed: at this stage the final number of spikelet primordia is defined, and all the structures of the spike are organized (Kirby and Aplleyard, 1987). After this stage, the spike undergoes further differentiation and growth. These processes together with fertilization, caryopsis development and grain filling, determine the number and size of grains produced per spike (Sreenivasulu and Schnurbusch, 2012).

Genetic control of floral induction

Barley varieties can be classified as winter or spring types. Winter (autumn-sown) barleys require vernalization and usually exhibit strong promotion of flowering in response to long days. This is typical of *H. vulgare* ssp. *spontaneum* (wild barley) suggesting that this is the ancestral condition (Szucs et al., 2007). Spring barleys lack vernalization requirement and show weak or strong response to long days depending on whether they have been selected for long or short growing seasons, respectively (Szucs et al., 2007). In long growing seasons, as in Western Europe and much of North America, reduced response to photoperiod allows spring-sown plants to extend the period of vegetative growth and accumulate additional biomass that supports higher yields.

In wild and winter cultivated barley, the transition to the reproductive stage occurs only after the requirement of vernalization is satisfied. *Vrn-H1, Vrn-H2* (Danyluk et al., 2003; Dubcovsky et al., 2005; Karsai et al., 2005; Yan et al., 2005; von Zitzewitz et al., 2005; Trevaskis, 2006; Cockram et

al., 2007; Szucs et al., 2007; Cockram et al., 2008), and *Vrn-H3* (Yan et al., 2006; Campoli et al., 2012a) are the key genes involved in the vernalization pathway. Wild-type *Vrn-H2* is a repressor of *Vrn-H3* (Yan et al., 2006), which is induced by *HvCO1* in long days and up-regulates *Vrn-H1* (Figure 2.5): Vrn-H1 activity determines the transition to the reproductive stage, but its transcription reaches a sufficient level only after vernalization (Hemming et al., 2008; Li and Dubcovsky, 2008) (Figure 2.5 and 2.6). In wild or autumn-sown winter barley, after germination when days are still long, *Vrn-H3* is repressed by high levels of *Vrn-H2*, preventing the induction of *Vrn-H1* (Hemming et al., 2008) (Figure 2.5 and 2.6). *Vrn-H1*, initially transcribed at very low levels in leaves and apices, is gradually upregulated during the short, cold days of winter, and gradually downregulates *Vrn-H2* (Trevaskis, 2006). The low levels of *Vrn-H2* transcripts in leaves allow the up-regulation of *Vrn-H3* by long days in the spring, and Vrn-H3 is exported to the shoot apex where it further promotes Vrn-H1 transcription above the threshold levels required for the induction of flowering (Trevaskis, 2006).

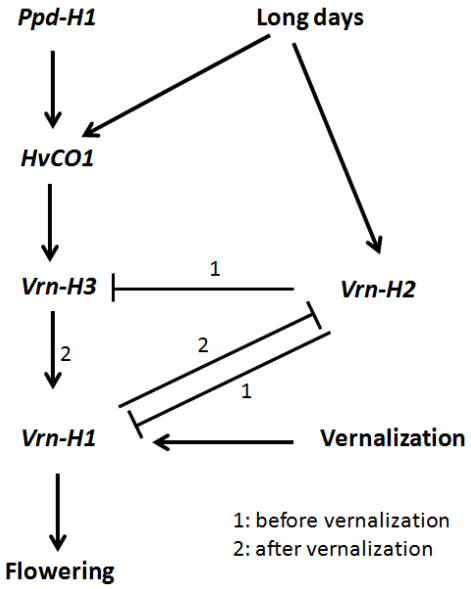

Figure 2.5. Genetic control of flowering in barley based on coordination of vernalization and photoperiod response, the explanation is in the text.

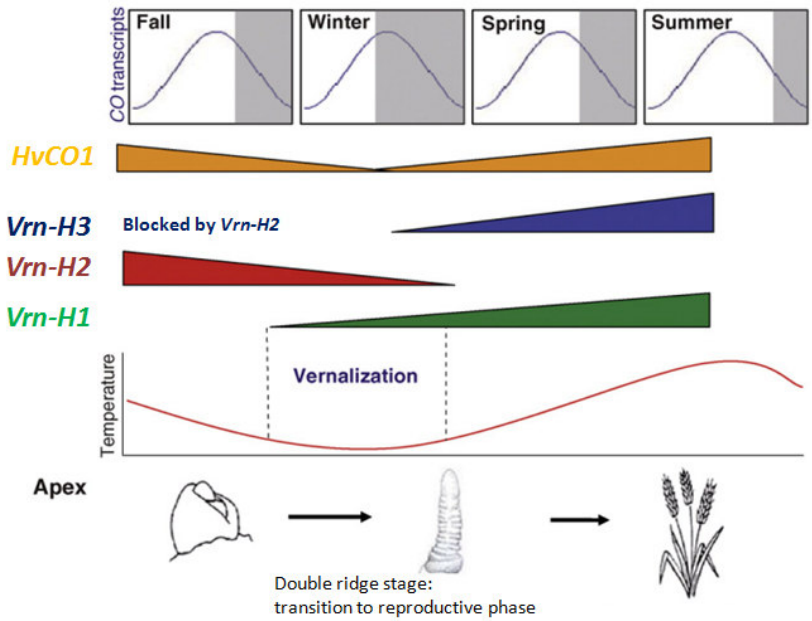

Figure 2.6. Regulation of vernalization and photoperiod genes by photoperiod and vernalization in barley, the explanation is in the text (image modified from Distelfeld et al., 2009).

Mutations in the regulatory regions of *Vrn-H1* result in dominant alleles, which are expressed with or without vernalization conferring a spring growth habit (von Zitzewitz et al., 2005). Thus the epistatic interaction between *Vrn-H1* and *Vrn-H2* determine the growth habit of varieties: winter varieties require winter alleles (recessive) at *Vrn-H1* and winter (dominant) alleles and *Vrn-H2* loci; spring growth habit is determined by the presence of spring alleles at *Vrn-H1* loci, independent of *Vrn-H2* allelic state; a third facultative growth habit is determined by the presence of winter alleles at *Vrn-H1* locus and spring alleles (mutated) at *Vrn-H2* (Takahashi and Yasuda, 1971). *Vrn-H1* and *Vrn-H2* loci were characterized and mapped on chromosome 5HL and chromosome 4HL respectively (Danyluk et al., 2003; Dubcovsky et al., 2005; Karsai et al., 2005; Yan et al., 2005; von Zitzewitz et al., 2005; Trevaskis, 2006; Cockram et al., 2007; Szucs et al., 2007; Cockram et al., 2008). *Vrn-H3* has recently been mapped on 7HS and identified as an orthologue of the Arabidopsis *FT* gene (Yan et al., 2006).

Photoperiod-H1 (*Ppd-H1,* 2 HS) is the major determinant for photoperiod response in barley, and as a component of the circadian clock it regulates the circadian timing of *CONSTANS* (*HvCO1* in barley): under long day conditions the wild-type dominant *Ppd-H1* promotes *HvCO1* expression that upregulates *Vrn-H3* promoting flowering, in contrast, a nonfunctional mutation in the CCT domain of *Ppd-H1* limits the induction of *Vrn-H3* by long days resulting in a late flowering recessive

ppd-H1 allele (Turner, 2005; Campoli et al., 2012b) Other genes whose mutants cause circadian defects accelerating flowering under long and short days: *Eam7* on 6HS (Stracke and Börner, 1998), *Eam8* on 1HL (Faure et al., 2012), *Eam9* on 4HL (Franckowiak, 1997;Lundqvist et al., 1997) and *Eam10* on 3HL (Campoli et al., 2013) (Börner et al., 2002).

There are some genes that have effect on flowering independently from vernalization or photoperiod, they are considered earliness per se genes: eps2S on 2HS (or Eam6), eps3L on 3HL, eps4L on 4HL, eps5L on 5HL, eps6L.1 and eps6L.2, both on 6HL, eps7S on 7HS and eps7L on 7HL (Laurie et al., 1995; Comadran et al., 2012).

Moreover QTLs for heading date, whose positions do not seem to coincide with these genes or loci, have been found in other barley populations (Hayes et al., 1993; Bezant et al., 1996; Baum et al., 2003; Li et al., 2006)(e.g. Hayset al., 1993; Bezant et al., 1996; Tinker et al., 1996; Baum et al.,2003; Li et al., 2006). QTLs for heading date usually have an effect on other important agronomic characters such as yield, height, resistance to diseases, quality traits, etc (Hayes et al., 1993; Bezant et al., 1996; Baum et al., 2003; Li et al., 2006), in accordance with the fact that heading date is a key trait for adaptability (Borràs-Gelonch et al., 2010).

Genetic control of spike morphology

As explained before, the number of grains produced per inflorescence is determined in early stages of reproductive development, during floral stem differentiation. This is the stage where manipulation of floral architecture can occur. Interesting examples of natural variabilty in which the spike bears a higher number of spikelets are known in *Triticum turgidum* L. convar. *compositum* (L.f) A. Filat, where first-order branches develop with additional, completely fertile spikelets at the base of the spike (Shitsukawa et al., 2009). A similar phenotype also occurs in the *compositum* mutants of barley where two independent loci have been identified.In the *compositum2 (com2)* mutant (2HS) the rachilla is converted into a rachis so that the basal rachis nodes till half of the spike are branched. In *compositum1 (com1)* (4HL) branching also starts from the rachillae at the base of the spike. In both *com* mutants spike branching is enhanced by favourable environmental conditions (Druka et al., 2011).

The two/six-rowed trait is under control of the *six-rowed spike 1 (VRS1)* gene which encodes a HD-ZIP1 homeobox transcription factor (Komatsuda et al., 2007). The wild-type allele (*Vrs.1b*) is expressed in lateral spikelets inhibiting their outgrowth (Komatsuda et al., 2007). Six-rowed cultivated varieties are loss of function *vrs.1a* mutants (Komatsuda et al., 2007). The *INTERMEDIUM-C* (*INT-C*, 4HL) gene is an orthologue of maize *TEOSINTE BRANCHED1*, and allelic variation at this locus modifies lateral spikelet development in relation to *VRS1* allelic state (Ramsay et al., 2011). Two-rowed genotypes *Vrs1.b:Int-c.a* exhibit enlarged, partially male fertile, lateral spikelets, while the presence of *int-c.b* in six-rowed cultivars (*vrs1.*a:*int-c.b*) results in the development of smaller lateral spikelets. Cultivated two-rowed carry the *Vrs1b:int-c.b* haplotype where *int-c.b* suppresses anther development in lateral spikelets. Cultivated six-rowed varieties carry the *vrs-1a:Int-c.a* haplotype (Ramsay et al., 2011). Three other independent loss of function mutation *vrs2, vrs3, vrs4* confer different degree of lateral spike fertility (Druka et al., 2011). Six-rowed spike4 (Vrs4). Recently *vrs4* was mapped on chromosome 3HS, cloned and characterized, its phenotype is that of the six-rowed spike, but also rachis nodes bear one or two additional spikelets; expression analyses showed that the gene works upstream of *Vrs1* (Koppolu et al., 2013).

The number of spikelets per spike can be manipulated by altering the duration of the spikelet initiation phase. Recently the *Eam6* gene, also called *EARLINESS-PER-SE 2* (*EPS2*) or *HvCEN*, was mapped on chromosome 2HL and cloned exploiting natural variation in modern barley cultivars: it controls flowering time and life cycle independent of environmental cues (Sameri et al., 2011; Comadran et al., 2012). Compared to wild-type, *eam6/mat-c* mutant alleles confer earlier flowering, decreased internode length, number of spikelets, spike length and grain yield (Lundqvist and Franckowiak, 2002). Thus this gene could be involved in controlling the duration of the spikelet initiation phase. Other early flowering *eam* and *mat* mutants exhibit similar phenotypes to *eam6*: their effect is independent from vernalization and photoperiod develop short spikes (Lundqvist and Franckowiak, 2002; Druka et al., 2011). The *gig2* barley mutant is delayed in flowering time by 2-3 weeks and produces four to eight more spikelets per spike then the wild-type, suggesting that the spikelet initiation phase might be extended (Lundqvist and Franckowiak, 2002; Druka et al., 2011).

Recently interest has been focused on stem elongation phase: lengthening the duration of the stem elongation phase has been associated to increases in the number of grains/m^2 (Slafer et al.,

2001; Slafer, 2003), which in turn could increase yield potential of small-grain cereals (Fischer, 2007; Miralles and Slafer, 2007; Fischer, 2008). The stem elongation phase occurs between terminal spikelet initiation and anthesis, and the length of this period influences the number of spikelet primordia that reach maturity in wheat and barley (Fischer, 1985; Kirby, 1988; Siddique et al., 1989; Miralles et al., 2000; González et al., 2003). It seems that the duration of the stem elongation (SE) and leaf and spikelet initiation (LS) phases should be under different genetic control. Borràs-Gelonch et al., (2010) in a QTL mapping experiment detected a QTL modifying SE/SL: variation at this QTL allowed to lengthen SE by shortening SL without altering heading. The QTLs responsible for a different control of LS and SE did not seem to correspond to any major gene reported in the literature.

2.2 SCOPE OF THE WORK

The traits described in this chapter define plant architecture and are key factors for crop production and adaptation to different environments. We explored natural variability through a genome wide association scan (GWAS) on a panel of winter European barley cultivars, to detect QTLs or genes that regulate these traits.

2.3 MATERIAL AND METHODS

2.3.1 PLANT MATERIALS AND PHENOTYPING

A panel of 142 European winter barley cultivars (67 two-rowed and 75 six-rowed) released between 1921 and 2006 (Table 2.1) were evaluated at two experimental field stations in Fiorenzuola d'Arda, Piacenza, Italy, (44°55'N and 9°53'E) and at the University of Shiraz, Iran (29°50'N and 52°46'E) (N.B. for latter the experiment, management and data collection were carried out by Elahe Tavakol) during the growing season 2012-2013. The experimental fields were organized in a randomized complete block design with 3 replicates; each plot consisted of 4 rows of 2 m with 40 cm spacing between rows and 30 cm between plants within a row. Seeds were sown in the middle of October and the beginning of November 2012 in Italy and Iran, respectively.

Flowering date (FD) was recorded when 60% of spikes were at anthesis stage (Zadoks stage 68) (ZADOKS et al., 1974) Leaf width (LW) and leaf length (LL) were measured on three to five most vigorous mature plants/plot. For each plant, the largest leaf of a culm (normally was the first one under the flag leaf) was measured for a total of 3-5 culms per plant. LW was measured at the

widest point of the blade and LL was measured from the ligule to the tip of the blade. LL was measured only in the experiment carried out in Iran. In the Italy field trial only, at harvesting stage the 3-5 most vigorous plants per plot were harvested and the following traits were registered:

- productive tiller number (T): all tillers carrying a totally developed spike were counted, thus excluding unproductive tillers formed in late stages of the crop cycle (e.g. during ripening);
- plant height (PH) as the length of the highest culm per plant, from the base till the spike peduncle;
- stem diameter (SD), measured in the middle of the thickest internode, that normally is that one under the node subtending the flag leaf; depending on homogeneity 3-5 internodes (from the three thickest culm) per plant were measured using a caliber;
- spike length (SL) of the 3-5 most developed spike per plant;
- number of fertile rachis nodes (NFRN) of the 3-5 most developed spikes per plant.

2.3.2 GWAS GENOTYPING

The germplasm panel used in this thesis project had been previously genotyped in the context of a collaboration between our group and the EXBARDIV project (http://www.eracaps.org/joint-calls/era-pg-funded-projects/2006-sub-call/genomics-assisted-analysis-and-exploitation-barley) using a set of 7,864 high-confidence gene-based SNPs incorporated in the illumina iSELECT Chip (Illumina Inc.) (Comadran et al., 2012). A total of 6,810 SNPs were successfully assayed in the 142 genotypes.

We filtered these data to exclude SNPs with > 5% missing data and < 10% Minimum Allele Frequency (MAF), and a total of 4,083 SNPs were employed for all following analyses: 2,521 of these markers have been mapped on the POPSEQ reference map (Mascher et al., 2013).

The population was genotyped by Alessandro Tondelli for functional variation at the two vernalization genes *Vrn-H1* and *Vrn-H2* (Table 2.1). *VRN-H1* and *VRN-H2* genotypes were tested for marker-trait associations (without filtering for MAF) together with the SNP panel.

BK_12, BK_14, BK_15, BK_16, BOPA2_12_30871 and BOPA2_12_30872 are markers included in the iSelect assay that are designed on the Photoperiod Response gene 1 (*Ppd-H1*), and they can be

considered as diagnostic for the allelic state at the *Ppd-H1* locus (Kilian et al. personal communication).

Table 2.1. The panel of 142 winter European cultivars used in GWAS.

GENOTYPE	Year of release	Row type	Country	Pedigree	*Vrn-H1* *	*Vrn-H2* **	PGH***	Ppdh1 ****
ABONDANT		6	France	Fannie x Cabro	W-1A	W	Winter	Ppd-H1
ACI	1994	2	Italy	[Alpha x (Alpha x Sonja)]x[Capri x (Okos x 273cat.)]	W-1A	W	Winter	Ppd-H1
AGER	1963	6	France	(Bordia x Kenia) x Linea 259-7110	W-1A	W	Winter	Ppd-H1
AIACE	2002	2	Italy	(Opale x HJ54111 x Alpha x Tipper x Alpha) x Katy x HJ54-30 x Igri x Arda x Baraka	S	W	Spring	ppd-H1
AIRONE	1999	2	Italy	(Gitane x Tipper) x Arda	W-1A	W	Winter	Ppd-H1
ALCE	2004	2	Italy	(Tipper x Igri x Igri x Igri) x Tipper x Alpha x Sonia x W117118	W-1A	S	Alternative	Ppd-H1
ALDEBARAN	2003	6	Italy	Rebelle x Jaidor	W-1A	W	Winter	Ppd-H1
ALFEO	1993	2	Italy	Tipper x Igri	W-1A	W	Winter	ppd-H1
ALISEO	1998	6	Italy	(Gerbel x Plaisant) x Express	W-1A	W	Winter	Ppd-H1
ALPHA	1972	2	France	Ager x (Ager x Ceres)	W-1A	W	Winter	Ppd-H1
AMILLIS	1995	2	France	Baraka x Mosar	W-1A	W	Winter	Ppd-H1
AQUARELLE	2003	2	Germany	Regina x BAU 623/94	W-1A	W	Winter	Ppd-H1
ARCO	1991	2	France	Marinka x Sel. 7761 gh	W-5C	W	Winter	Ppd-H1
ARDA	1985	2	Italy	Igri x HJ 51-15-3	W-1A	W	Winter	Ppd-H1
ARMA	1976	6	France	Manon x Ager x Hauter x Ares	W-5C	W	Winter	Ppd-H1
ASSO	1993	2	Italy	Barberousse x Tipper	W-1A	W	Winter	Ppd-H1
ATHENE	1977	6	Germany	(Herfordia x Hord.sp.nigrum H204) x (Mädru x Weissenhaus-Stamm)	W-1A	W	Winter	ppd-H1
AYDANHANIM	2002	2	Turkey	GK Omega x Tarm	W-1A	W	Winter	Ppd-H1
BALAKI	1996	6	France	Express x 3169 LH2	W-5C	W	Winter	ppd-H1
BALDA	1998	6	Italy	(Borwina x Express) x 75	W-1A	W	Winter	Ppd-H1
BALKAN	1994	6	France	Express x Vr 503	W-1A	W	Winter	Ppd-H1
BARAKA	1986	2	France	[(Midas x Ribari 33) x Alpha] x Barberousse	S	S	Spring	Ppd-H1
CANORO	1992	6	Italy	Katja x Barberousse	W-1A	W	Winter	ppd-H1
CARAT	2002	2	United Kingdom	Volley x Cabrio	W-1A	W	Winter	Ppd-H1
CAROLA	1998	6	Germany	(SG 402085 x Franka) x GW 1307	W-5C	W	Winter	Ppd-H1
CLARA	2001	2	Germany	Babylone x Anthere	W-1A	W	Winter	Ppd-H1
CLARINE	1988	2	France	Igri x Mogador	W-1A	S	Alternative	Ppd-H1
CRIMONT	1975	6	Belgium	Hauters x Ager	W-1A	W	Winter	Ppd-H1
CRITER	1984	6	France	Hop x Ager	W-1A	W	Winter	ppd-H1
DASIO	1999	2	Italy	Tipper x Arupos	W-1A	W	Winter	Ppd-H1

DEA	1953	6	Germany	((Ragusa x Peragis12) x (Heils Franken x Frw.Berg)) x ((Mahnd.Viktoria) x (Ragusa x Bolivia))	W-1A	W	Winter	Ppd-H1
DIADEM	1999	2	France	29194 x Marianne	W-1A	W	Winter	Ppd-H1
DJEBHEL		6			W-1A	W	Winter	Ppd-H1
DOLMEN	2001	2	France	Labea x MH 387	S	W	Spring	Ppd-H1
DUCHESSE	1996	2	France		W-5C	W	Winter	Ppd-H1
DUET	1995	2	United Kingdom	Marinka x Torrent	W-1A	W	Winter	ppd-H1
DURA	1961	6	Germany	(Friedrichswerther Berg x Ragusa) x Doria	W-1A	W	Winter	ppd-H1
ESTEREL	1996	6	France	7761 x Plaisant	W-5C	W	Winter	Ppd-H1
ETRUSCO	1981	6	Italy	Perga x Feder LO 20	W-1A	W	Winter	Ppd-H1
EXPRESS	1990	6	France	Robur x Athene	W-5C	W	Winter	Ppd-H1
FANFARE	1995	2	United Kingdom	Torrent x Finesse	W-1A	W	Winter	ppd-H1
FEDERAL	1994	6	France	(Capri x Bison) x Melusine	W-1A	W	Winter	Ppd-H1
FIGHTER	1991	2	United Kingdom	RPB 77-5155 x Marinka	W-1A	W	Winter	Ppd-H1
FINESSE	1988	2	United Kingdom	Igri x Maris Otter	W-1A	W	Winter	Ppd-H1
FJORD		2	Denmark	9186 GH 2 x Magie	W-1A	W	Winter	Ppd-H1
FRANKA	1980	6	Germany	((Vogels.Gold x Senta) x (Dura x Dea)) x Vogels.Gold	W-1A	W	Winter	Ppd-H1
FRIDERICUS	2006	6	Germany	Carola x LP 6-564	W-1A	W	Winter	Ppd-H1
FROST	1988	6	Sweden	Pella x Astrix	W-1A	W	Winter	ppd-H1
GAIANO	1998	6	Italy	L630 x GAZ 98	W-1A	W	Winter	Ppd-H1
GERBEL	1977	6	France	(Ager x Jumbo) x FDE 244/95(Ager x Asterix x Mana)	W-1A	W	Winter	Ppd-H1
GLEAM	1996	2	United Kingdom	Torrent x Puffin	W-1A	W	Winter	Ppd-H1
GLENAN	1988	6	France	Thibaut x Robur	W-1A	W	Winter	ppd-H1
GOTIC	1992	6	France	(Robur x Athene) x FD6 7926-17	W-1A	W	Winter	ppd-H1
GRETE	1989	6	Germany	(641003 x Tocka) x Vogels.Gold x (Pella x Dura)	W-1A	W	Winter	ppd-H1
HALCYON	1968	2	United Kingdom	Warboys x Maris Otter	W-1A	W	Winter	Ppd-H1
HASSO	1980	6	Germany	Dura x 12563 (Weissenhaus 6448 x Hauter x D5)	W-1A	W	Winter	Ppd-H1
HATIF DE GRIGNON	1937	6	France		W-1A	W	Winter	Ppd-H1
HELIGAN	1998	2	United Kingdom	Tosca x Intro	W-1A	W	Winter	ppd-H1
HERFORDIA	1950	6	Germany	Peragis-Stamm x Schladener I	S	W	Spring	ppd-H1
HOPPEL	1970	6	France	(Hybrid 456 x Feebar) x Hatif de Grignon	W-1A	W	Winter	Ppd-H1
ISA	1985	6	Belgium	Bosquet x Hoppel	W-1A	W	Winter	ppd-H1
ISACCO		6	Italy	Hop x Ager	W-1A	W	Winter	Ppd-H1
JAIDOR	1981	6	France	((Rika x Balaldi 16) x (33 x Emir) x (Ema 1038 x Robur)	W-1A	W	Winter	Ppd-H1
JEWEL	1997	2	United Kingdom	Clarine x Firefly	W-1A	W	Winter	ppd-H1

KASKADE	1981	2	Germany	Carsten x Union x Emir x Malta	W-1A	W	Winter	Ppd-H1
KELIBIA	1990	2	France	Nika x Igri	W-1A	W	Winter	Ppd-H1
KESTREL	2003	2	United Kingdom	Intro x Sunrise	W-1A	W	Winter	Ppd-H1
KETOS	2002	6	France	(Gotic x Orblonde) x (12813 x 91H595)	W-5C	W	Winter	Ppd-H1
LABEA	1992	2	Germany	Br.269 c x LBP 5906	W-5C	W	Winter	Ppd-H1
LAVERDA	2006	6	Germany	(Ludmilla x Nord 1836) x Merlot	W-5C	W	Winter	Ppd-H1
LEONIE	2000	2	Germany	Labea x 87585/6	W-1A	W	Winter	Ppd-H1
LETIZIA	1998	6	Italy	(Plaisant x Gerbel) x (Jaidor x Barberousse)	W-1A	W	Winter	ppd-H1
LOMBARD	1991	2	France	(Japon 51-2-43-15 x Marinka) x FDO 8106-21-0	W-5C	W	Winter	Ppd-H1
LONNI	2005	6	Denmark	Aviron x Carola	W-1A	W	Winter	Ppd-H1
LORENA	1993	6	Germany	Mr Kanada x Eng.50-8	W-1A	W	Winter	Ppd-H1
LUDMILLA	1999	6	Germany	Hasso x (Banteng x Venus)	W-1A	W	Winter	Ppd-H1
LUTECE	2003	6	France	Nikel x Rebelle	W-1A	W	Winter	Ppd-H1
MAGIE	1983	2	France	LBP 1911 x Alpha	W-1A	W	Winter	Ppd-H1
MAJESTIC	1994	6	France	(Express x Robur) x (Platen x Eldorado)	W-1A	W	Winter	Ppd-H1
MALTA	1968	2	Germany	((Carstens 2-Row x Aurea) x Dea) x Herfordia	W-1A	W	Winter	Ppd-H1
MALWINTA	2004	2	Denmark	Opal x Labea	W-1A	W	Winter	Ppd-H1
MANITOU	1988	6	France	1055 x Gerbel	W-1A	W	Winter	Ppd-H1
MANOLIA	2001	2	France	Labea x Astrid	W-1A	W	Winter	Ppd-H1
MARADO	2003	6	France	Nikel x 1523	W-1A	W	Winter	Ppd-H1
MARINKA	1985	2	Netherlands	(Alpha x SvP 674) x Malta	W-1A	W	Winter	Ppd-H1
MARIS OTTER	1965	2	United Kingdom		W-1A	W	Winter	ppd-H1
MARIS TROJAN	1975	2	United Kingdom		W-1A	W	Winter	ppd-H1
MATTINA	1998	6	France	(Friberga x Express) x (L40km x 43)	W-1A	W	Winter	ppd-H1
MELANIE	1993	2	Germany	BR301a x LBP5907	W-1A	W	Winter	Ppd-H1
MICUCCIO	1974	6	Italy	Local Population x Arig 7	W-1A	W	Winter	ppd-H1
MIRCO	1981	6	Italy	Selection from local population not identified	W-1A	W	Winter	ppd-H1
MIRRA	1972	6	Germany	6109 x Herfordia	W-1A	W	Winter	ppd-H1
MURCIE	2002	2	France	Sunrise x Labea	W-1A	W	Winter	ppd-H1
MUSCAT	1996	6	United Kingdom	Plaisant x Gaulois	W-1A	S	Alternative	Ppd-H1
NAOMIE	2003	6	Germany	(Julia x NS.90517/16) x Carola	W-1A	W	Winter	ppd-H1
NIKEL	1996	6	France	Express x Tasso	W-1A	W	Winter	Ppd-H1
NURE	1998	2	Italy	(Fior 40 x Alpha) x Baraka	W-1A	W	Winter	ppd-H1
ONICE	1980	6	Italy	Perga x Sam-Chio 36	W-1A	W	Winter	ppd-H1
OPAL	1998	2	United Kingdom	Puffin x Angora	W-1A	W	Winter	ppd-H1
ORCHIDEA		2	United Kingdom	Braun St. 301 x Vh St.5906	W-1A	W	Winter	Ppd-H1
OSIRIS	1921	6	Algeria	Selection from PI39590	W-1A	W	Winter	Ppd-H1
PANDA	1983	2	France	Katy x Gerbel	W-1A	W	Winter	ppd-H1

PASSPORT	1997	6	France	(Barberousse x 5.4) x Barberousse	W-5C	W	Winter	Ppd-H1
PASTORAL	1987	2	France	Igri x Mogador	W-1A	W	Winter	Ppd-H1
PATRICIA	1995	6	Austria	Romy x (Rachel x MR 13)	W-1A	W	Winter	Ppd-H1
PEARL	1997	2	United Kingdom	Puffin x Angora	W-1A	W	Winter	Ppd-H1
PERGA	1960	6	Germany	(Ragusa x Mahndorfen Victoria) x (Bolivia x Nacktgerste)	W-1A	W	Winter	ppd-H1
PILASTRO	1989	6	Italy	Arma x Sisfor L 38	W-1A	W	Winter	ppd-H1
PIRATE	1978	6	France	(LBP 259/711 x Ares 176) x Pella	W-1A	W	Winter	ppd-H1
PLAISANT	1979	6	France	Ager x Nymphe	W-5C	W	Winter	Ppd-H1
PLATINE	1996	2	France	Intro x Mariane	W-1A	W	Winter	Ppd-H1
PONENTE	2001	6	Italy	(Vetulkio x Arma) x Express	W-1A	W	Winter	Ppd-H1
PRINCESS	1989	6	France	(Gerbel x Barteng) x Barberousse	W-1A	W	Winter	Ppd-H1
PUFFIN	1989	2	United Kingdom	(Athos x Maris Otter) x Igri	W-1A	W	Winter	Ppd-H1
REBELLE	1988	6	France	(Barberousse x Monarque) x Pirate	W-1A	W	Winter	ppd-H1
RED	1990	2	Italy	Selection from isolating population not identified	S	W	Spring	Ppd-H1
ROBUR	1973	6	France	Ager x (Hatif de Grignon x Ares)	W-1A	W	Winter	ppd-H1
SAIGON	2002	2	United Kingdom	Opal x 93-5758	W-5C	W	Winter	Ppd-H1
SAMSON		6	France	Illia x Pirate	W-1A	W	Winter	Ppd-H1
SELVAGGIO	1982	6	Hungary	Montpellier x (Beta 40 x Algerian)	W-1A	W	Winter	ppd-H1
SENTA	1963	6	Germany	(Firlbecks 4zlg. x Ungarische) x Dea	W-1A	W	Winter	Ppd-H1
SERENO	1995	6	Italy	Multiple Crossbreeds	W-1A	W	Winter	Ppd-H1
SONJA	1974	2	Germany	Tria x Malta	W-1A	W	Winter	Ppd-H1
SONORA	1992	6	France	(Plaisant x Gerbel) x Jaidor	S	W	Spring	Ppd-H1
SPRITE	1992	2	United Kingdom	CWB 11/8 x Halcyon	W-1A	W	Winter	ppd-H1
TAMARIS	1992	6	France	Express x 507	W-1A	W	Winter	Ppd-H1
TAPIR	1980	6	Netherlands	DSGW 167 x Pella	W-1A	W	Winter	Ppd-H1
TARGET	1992	2	United Kingdom	Igri x (Ramage 2-row x Gerbel)	S	S	Spring	Ppd-H1
TIFFANY	1996	2	Germany	Labea x Marinka	W-1A	W	Winter	Ppd-H1
TIPPER	1981	2	United Kingdom	Dayton x Jotun x Alpha	W-1A	W	Winter	Ppd-H1
TORRENT	1987	2	United Kingdom	Fenella x TRI 685	W-1A	W	Winter	Ppd-H1
TRASIMENO	1992	2	Italy?	Osk4.41/2 x Igri	W-1A	W	Winter	Ppd-H1
TREBBIA	1990	6	Italy	Selection from Fior Synt 3	W-1A	W	Winter	ppd-H1
TRIA	1963	2	Germany	(LBP 348/342 x Firlbecks 4zlg.) x Carsten 1565	W-1A	W	Winter	Ppd-H1
ULTRA	1996	2	Italy	Line COIS x Slav Line	W-1A	W	Winter	ppd-H1
VANESSA	2000	2	Germany	(Br.652h x Br.1201a) x Astrid	W-1A	W	Winter	Ppd-H1
VERTICALE	2000	2	France	Target x Intro	W-1A	W	Winter	Ppd-H1
VERTIGE	1995	2	France	(Tompouce x Marinka) x Emeraude	W-1A	W	Winter	Ppd-H1

VETULIO	1983	6	Italy	Perga x Sekitorisai 1105	W-1A	W	Winter	Ppd-H1
VOGELSANGER GOLD	1965	6	Germany		W-1A	W	Winter	Ppd-H1
ZACINTO	2000	2	Italy	(IABO329 x Arda) x Arda	W-1A	W	Winter	ppd-H1
ZOE	1998	6	Germany		W-1A	W	Winter	ppd-H1

* VRN-H1 haplotypes defined in Cokram et al 2009 : W-1A (winter allele),W- 5C (winter allele). S = spring allele (predicted to correspond to spring haplotypes 3, 4A, 4B, 5A, or 5B). VRN-H2 scores: S = deletion of *ZCCT-Ha, -Hb, and -Hc* (diagnostic for spring allele); W = no deletion (diagnostic for winter allele)(Alessandro Tondelli, not published). **VRN-H2 scores: S = deletion of *ZCCT_Hc* candidate gene for VRNH2 (diagnostic for spring allele); W = no deletion (diagnostic for winter allele) (Alessandro Tondelli, not published). ***Predicted growth habit as determined by *VRN-H1* and *VRN-H2* multilocus genotype (Alessandro Tondelli, not published). ****Ppd-H1* allele, predicted by BK_12, BK_14, BK_15, BK_16, BOPA2_12_30871 and BOPA2_12_30872 SNP markers from Comadran et al. 2012: Ppd-H1= day-length strong sensitive allele (haplotype:CGGCGA), *ppd-H1*= day-length weak sensitive allele (aplotype: AAAGAG). In bold are the names of cultivars used in the preliminary glass-house trial for root phenotyping; cultivars highlighted in red are those phenotyped for root traits in the growth chamber experiment (Chapter 3).

2.3.3 STATISTICAL ANALYSES-PHENOTYPE

All statistical analyses were performed using the R software version 3.1.1 (The R development Core Team, 2008). Variance components for FD, LW including genotypes, replicates and locations as factors were calculated with a mixed linear model implemented by the "lmer" function from lme4 package version 1.1.7 (Bates et al., 2013), where genotypes, location, location by genotype interaction and replicates were considered as random factors. Broad-sense heritability for FD and LW was computed according to (Knapp et al., 1985): $h^2=\sigma^2g/(\sigma^2g+\sigma^2lg/n+\sigma^2e/n)$. Where σ^2g is the genetic variance, σ^2lg is the genotype-location interaction, σ^2e is the error variance, n is the number of locations. For all the other traits (LL, SL, T, NFRN, SD, PH), that were measured only in one environment, the formula is $h^2=\sigma^2g/(\sigma^2g+\sigma^2e)$.

Best Linear Unbiased Estimators (BLUEs) of FD, LW were calculated as the phenotypic values estimated for each genotype in a mixed linear model implemented by "lmer" function, where genotypes were set as fixed factor and location, location-genotype interaction and replicates as random factors. For BLUEs calculation of all the other traits only replicates were used as random factors. Genome wide association analyses (GWAS) and Pearson correlation analyses were calculated based on BLUEs.

2.3.3 STATISTICAL ANALYSIS - POPULATION STRUCTURE, LINKAGE DISEQUILIBRIUM AND GWAS ANALYSES

The population structure of the panel was investigated by principal coordinates analysis (PCoA) based on a correlation matrix using the PAleontological STastical (PAST) software (Hammer et al., 2001).

In order to identify the intra-chromosomal linkage disequilibrium (LD) among markers, squared allele frequency correlations (r^2) were calculated between pairs of loci using the TASSEL software (Bradbury et al., 2007), LD decay was evaluated by plotting significant ($p<0.001$) pair-wise r^2 values against genetic distances between each pair of loci and by fitting the locally weighted scatter plot smoothing (LOESS) curve on the graph using the R software (The R development Core Team, 2008). A critical r^2 values was estimated as the 95^{th} percentile of r^2 values between pairs of unlinked loci (pairs of loci on the same chromosome with >50 cM distance).

Genome wide analysis (GWAS) were performed with the GAPIT package version 1 (Lipka et al., 2012) implemented in the in R software (The R development Core Team, 2008). To identify significant marker trait associations a mixed linear model (MLM) described by the following formula was used: phenotype= M+Q+K+e in which M and e denote the genotypes at the marker and residuals, respectively. Q is a fixed factor due to population structure and K is a random factor due to co-ancestry of individuals. Here, the first 3 components of PCA and the kinship matrix (a matrix of similarity between genotypes based on the proportion of alleles mismatches at each SNP between pairs of genotypes) calculated in GAPIT with the Van Raden method (VanRaden, 2008), were used as Q and K, respectively. The p-values were adjusted based on a false discovery rate (FDR) (Benjamini and Hochberg, 1995) separately for each trait and a threshold value for significant association was set at 0.05. Manhattan plots displaying GWAS results were prepared with the qqman package (Turner, 2014) implemented in R software (The R development Core Team, 2008).

GWAS were also used to establish approximate position of those unmapped marker that were significantly associated to traits. As every SNP marker only has two alleles, we transformed SNP data in a numeric scale (A=1, C=2, G=3, T=4), that could be introduced in the model as the quantitative dependent variable, and association to other mapped markers indicated the approximated position on the POPSEQ map.

2.4 RESULTS

2.4.1 POPULATION STRUCTURE AND LINKAGE DISEQUILIBRIUM

To investigate population structure, we performed a principle component analysis (PCoA) with all markers filtered for missing data <0.05 and MAF> 0.1. The first two coordinates explained 17% and 10% of total variability, respectively. PCoA results indicated the existence of two major sub-populations, corresponding to two-rowed and six-rowed barley cultivars (Figure 2.7). The first two coordinates explained 17% and 10% of total variability, respectively.

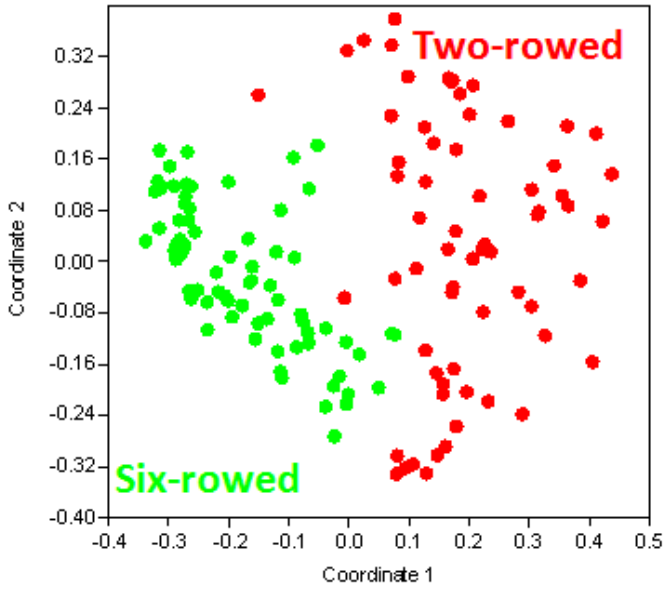

Figure 2.7. Principal coordinate analysis (PCoA) plot of the two first coordinates in 142 winter barley six-rowed and two-rowed cultivars. Coordinate 1 explains 17% of total variation, coordinate 2 explain 10 % of the total variation.

The mean of correlation coefficients between individuals of the two-rowed sub-group was of 0.39, while this mean was of 0.48 within the six-rowed individuals; the two-rowed winter barley genotypes thus showed a higher genetic diversity as compared to the six-rowed barley genotypes. BK_12, BK_14, BK_15, BK_16, BOPA2_12_30871 and BOPA2_12_30872, are designed on the Photoperiod Response gene 1 (*Ppd-H1*); these markers are in total linkage disequilibrium, thus in the examined population only 2 haplotypes are present (Table 2.1): this observation together with personal communication by Benjamin Kilian suggested that the two haplotypes correspond to the two functional alleles of *Ppd-H1*. The two functional haplotypes at *Ppd-H1* were non-randomly distributed between two- and six-rowed cultivars. Among the 40 cultivars with a photoperiod

insensitive *Ppd-H1* allele, only 5 varieties were characterized as six–rowed (Table 2.1). However, within the two-rowed cultivars both *Ppd-H1* alleles were equally distributed.

The r^2 scores between all intrachromosomal pairs of loci as a function of genetic distance is presented in Figure 2.8. We calculated the locally weighted scatter plot smoothing (LOESS) curve of r^2 to evaluate the average LD decaying along genetic distance. LOESS curve intercepts the r^2 critical value (the 95th percentile of r^2 values between unlinked loci) at a genetic distance of 4.5 cM, that can be considered as the maximum distance under which high r^2 values are most probably depending on physical linkage.

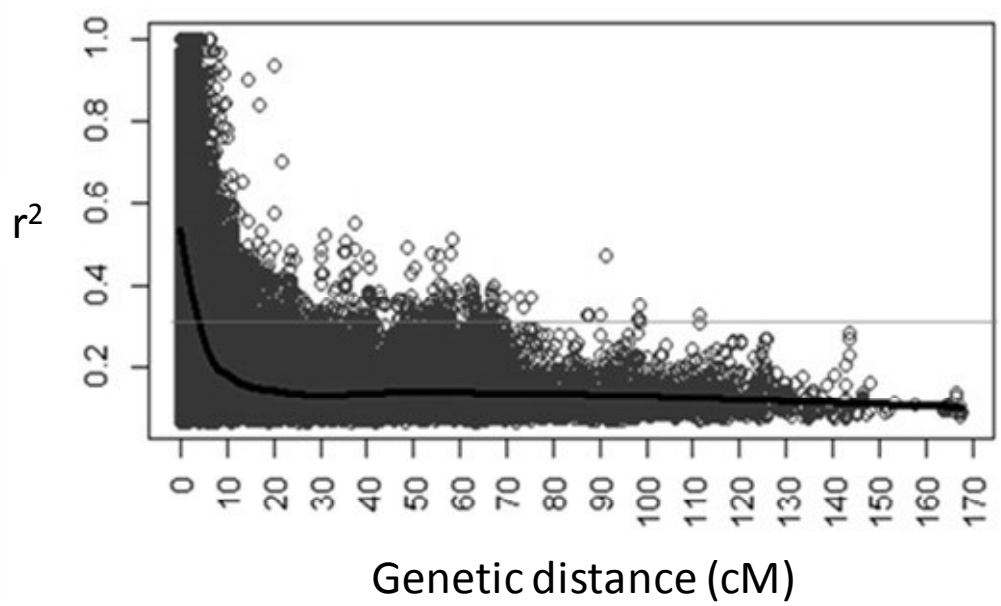

Figure 2.8. Intra-chromosomal LD decay of markers pairs over all chromosomes as a function of genetic distance. The fitted LOESS curve (black line) illustrates the LD decay, and the gray horizontal line represents the critical r^2 value.

2.4.2 PHENOTYPIC VARIATION AND GENOME-WIDE ASSOCIATION SCANS

Minimum, maximum, mean, standard deviation and heritability values for phenotypic traits are presented in Table 2.2.

Table 2.2. Mean, maxima, minima, standard deviations and heritability values of phenotypic traits are presented. FD IT: flowering date scored in Italy experiment; FD IR: flowering date scored in Iran experiment; das: days after sowing. LW IT leaf width scored in Italy experiment, LW IR: leaf width scored in Iran experiment; LL: leaf length; T: tillering, PH: plant height, SD: stem diameter, SL: spike length, NFRN: number of fertile rachis internodes, h^2: heritability in a broad sense.

	FD IT (das)	FD IR (das)	LW IT (mm)	LW IR (mm)	LL IR (mm)	T	PH (cm)	SD (mm)	SL (mm)	NFRN
mean	209	181	17.8	13	177	25.6	68.1	5.2	111.4	25.5
max.	230	175	24.5	19.3	68.3	68.3	106.3	6.3	155.4	41.3
min.	202	192	12.7	8.3	130	7.7	33.3	4	73.5	12.7
st. dev.	4.4	3.7	2.1	2	18.7	7.7	8.8	0.4	11.7	5.1
h^2 (%)	87		93		82	37	58	73	74	81

Table 2.3. Correlation coefficient between BLUEs values of traits.

	ROW-TYPE	FD	LW	LL	T	PH	SD	SL	NFRN
ROW-TYPE	1	-0.32**	0.22*	0.1	-0.67**	-0.02	0.48**	-0.6**	-0.85**
FD	-0.32**	1	0.32**	0.34**	0.14	0.32**	0.1	0.6**	0.4**
LW	0.22*	0.32**	1	0.83**	-0.21*	0.18*	0.65**	0.18*	-0.03
LL	0.1	0.34**	0.83**	1	-0.14	0.23*	0.55**	0.29**	0.07
T	-0.67**	0.14	-0.21*	-0.14	1	0.1	-0.29**	0.4**	0.6**
PH	-0.02	0.32**	0.18*	0.23*	0.1	1	0.29**	0.16	0.23*
SD	0.48**	0.1	0.65**	0.55**	-0.29**	0.29**	1	0.02	-0.21*
SL	-0.6**	0.6**	0.18*	0.29**	0.4**	0.16	0.02	1	0.68**
NFRN	-0.85**	0.4**	-0.03	0.07	0.6**	0.23*	-0.21*	0.68**	1

*: 0.005 < p-value < 0.05, ** p-value < 0.005. FD: flowering date, LW leaf width, LL: leaf length, T: tillering, PH: plant height, SD: stem diameter, SL: spike length, NFRN: number of fertile rachis nodes.

Row-type

Row-type is known to have strong pleiotropic effects on different traits (Kirby and Riggs, 1978), thus GWAS based on a population where row-type is the main factor of structuration is expected to find loci controlling row-type as associated with other traits. Genes determining row-type are well known, we run GWAS with using Q and K matrices to correct for population structure to determine which markers in our panel were associated to these genes. The results are displayed in Figure 2.9. Markers BOPA1_6208-987 and BOPA1_4098-758, mapped on chromosome 4H, at 26.3 and 25.9 cM on the POPSEQ reference map, were recovered as associated to row type with a Log10 p-value of 22.4 and 21.4 and 15.5, respectively (Table 2.4). Taking advantage of the IPK barley BLAST server (http://webblast.ipk-gatersleben.de/barley/), we anchored the POPSEQ genetic map to the barley physical map and found that this genomic region hosts the *INT-C* row-type gene, (position 25 cM). We can therefore consider markers BOPA1_6208-987 and BOPA1_4098-758 as diagnostic for *INT-C*. Markers BOPA1_2371-950 (2H, 80cM) and SCRI_RS_4930 (2H, 76.63 cM) were strongly associated with row type the trait with a –Log10 p-value of 15.6 and 6.8 (Table 2.4), respectively. As the *VRS1* gene sequence was mapped in position 79.39 on chromosome 2H (http://webblast.ipk-gatersleben.de/barley/), we considered the two markers as diagnostic for *VRS1*. For other unmapped markers associated to row-type, we ran a GWAS to establish their position on the map. BOPA1_2832-377, BOPA1_3687-271, BOPA1_952-1301, BOPA1_4616-503, BOPA1_12128-313, SCRI_RS_91810 comapped with BOPA1_6208-987 in chromosome 4H, position 26.35 (*INT-C*), while SCRI_RS_137263 and SCRI_RS_91810 comapped with BOPA1_2371-950 in chromosome 2H position 80cM (*VRS1*). We used a GWAS model that

strongly corrects for population structure: the first PCA coordinate is the one that discriminate between two-rowed and six-rowed cultivar (the two main sub-populations), with this model one would expect that loci related to row-type as being detected as responsible for population structure would not be associated to the trait because of model correction. Nevertheless the correction was not so strong to ignore these genes. When we ran GWAS excluding PCA (Q matrix), $-\text{Log}_{10}$ p-value of associations with *VRS1* and *INT-C* increased of ten units (result not shown).

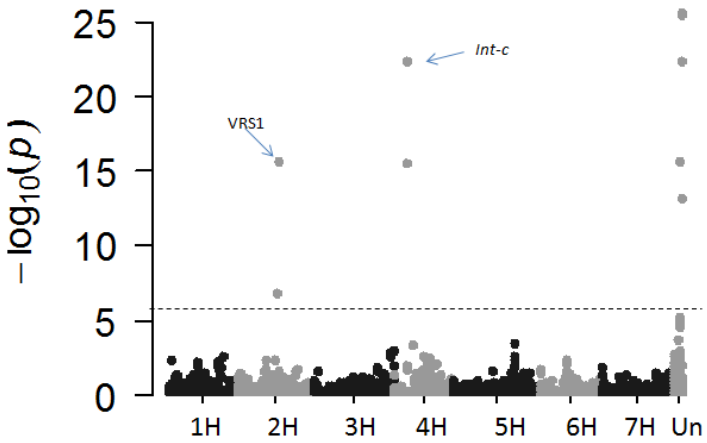

Figure 2.9. Manhattan plot displaying GWAS results for row-type. On x axis POPSEQ map position of markers along the seven barley chromosomes are plotted, "Un" indicate markers that are not mapped. On Y axis $-\text{Log}_{10}$ p-values of marker-trait association is plotted. The blue dashed line indicates the threshold for marker-trait association significance.

Flowering date, leaf length, leaf width and spike length

In Italy, plants flowered between 202 and 230 days after sowing (DAS) with a mean of 209 days (Table 2.4). In Iran, the number of days from sowing to flowering varied from a minimum of 175 to a maximum of 192 DAS with a mean of 181 DAS. Leaf length (LL) only scored in Iran, varied between 130 and 236 mm, with a mean of 177 mm. Leaf width (LW) was on average 17.8 mm in Italy with a minimum of 12.5 mm and a maximum of 24.7 mm. In Iran LW varied between 8.3 and 19.3 mm with an average of 13 mm. Thus there was a strong environmental effect on LW. Spike length (SL, measured only in Italy) ranged from a minimum of 73.5 mm and a maximum of 155.3 mm, with a mean of 111.4 mm High heritability values of 87%, 93%, 82% and 74% for FD, LL, LW and SL respectively, indicated that genetic components accounted for a major proportion of the total phenotypic variation for each trait.

In Table 2.3, Pearson correlation coefficients between the different traits are presented. A weak positive correlation was found between FD and LW with a Pearson correlation coefficient of 0.32; similarly, a weak positive correlation of 0.34 was detected between FD and LL, while a high correlation coefficient of 0.84 was revealed between LW and LL. SL was highly correlated with row-type, flowering date and NFRN (-0.6, 0.6, 0.68 respectively) and was moderately correlated with tillering (0.4).

In order to identify loci controlling variation for FD, LW, LL and SL, GWAS (with Q and K correction) were carried out using BLUEs calculated across the two environments.

Results (Figure 2.10, Table 2.4) show that the same locus on chromosome 2HS (markers BK_12, BK_14, BK_15, BK_16, BOPA2_12_30871 and BOPA2_12_30872 corresponding to the *Ppd-H1* gene (position 19.9 cM on the POPSEQ reference map, Mascher et al., 2013) controls variation for FD, LW, LL and SL. In particular, a 2 days delay in flowering date was estimated for the *ppd-H1* allele. In addition, *ppd-H1* was estimated to increase LL by 8.3 mm and LW by 1 mm. The mixed linear models including single marker effect (BK_12 or other markers associated to Ppd-H1, the model is Y=Marker+Q+K+e) explained 67%, 54%, 51% and 47 % of the total variability for FD, LL, LW and SL respectively, while the same mixed linear models without marker effect (considering only population structure and co-ancestry between genotypes, the model is Y=Q+K+e) explained 30%, 8%, 21% and 40% of FD, LL, LW and SL variability. Subtracting percentage of phenotypic variance explained by the model without the marker by the variance explained by the model with the marker, one can calculate approximately the phenotypic variance explained by the marker: following this procedure, *Ppd-H1* is estimated to explain 37%, 48%, 30% and 7% of variance for FD, LL, LW and SL, respectively. An additional marker associated to FD, LW and SL with a -Log10-p-value of 5.8, 4.3 and 5.4 respectively, explaining 30%, 23% and 6% of total variability, was SCRI_RS_233272. This marker was not mapped in POPSEQ, but our GWAS analyses linked it to *Ppd-H1*. Association scans pointed to additional markers associated to the different traits. For FD and SL significant association (–Log10-p.value of 5.4 and 4.9) was found with BOPA1_ConsensusGBS0008-1 (2H position 58.78 cM) and 3 other markers associated to FD (BOPA1_5046-619, BOPA1_217-677, BOPA1_1940-567) were linked to BOPA1_ConsensusGBS0008-1 by GWAS (Table2.4). The position of this marker corresponds to the location of the *HvCEN* gene (Comadran et al., 2012) based on anchoring to the POPSEQ map (58 cM, http://webblast.ipk-gatersleben.de/barley/) and consistent with the known effect of this gene

on flowering time (Comadran et al., 2012). SCRI_RS_171185, SCRI_RS_110647 and BOPA1_5379-595 (unmapped in POPSEQ) were also associated to FD, with a -Log10p-value of 3.8, 4 and 4.4 respectively: these markers were linked by GWAS to positions 13.5 cM, 38 cM and 52 cM on chromosome 2H (Table 2.4).

LW variability was associated to marker SCRI_RS_157866, at 110.2 cM on chromosome 4H, with the allele with lower frequency increasing LW by 0.7 mm on average. Allelic variation of SCRI_RS_153798 (unmapped) significantly influenced LW: this marker was mapped by GWAS at position 2H, 17.56 cM.

Table 2.4. Summary of significant marker-trait associations identified from GWAS.

	marker	Chr	Pos (cM)	-Log10(p)	MAF	R2 of model without SNP	R2 of model with SNP	Allele effect	Known loci in the region	Covariate used in GWAS
FD	*Ppd-H1*	2	19.9	7.7	0.27	30	67	2.1	*Ppd-H1*	
	SCRI_RS_233272	2*	19.9*	5.8	0.20	30	60	2.0		
	BOPA1_ConsensusGBS0008-1	2	58.78	4.8	0.20	30	57	1.7	*HvCEN*	
	BOPA1_5046-619	2*	58.78*	4.7	0.16	30	52	2.1		
	BOPA1_1940-567	2*	58.78*	4.2	0.13	30	50	2.0		
	BOPA1_217-677	2*	58.78*	4.2	0.13	30	50	2.0		
	BOPA1_5379-595	2*	52*	4.4	0.10	30	55	2.3		
	SCRI_RS_110647	2*	38*	4.0	0.16	30	47	1.9		
	SCRI_RS_171185	2*	13.5*	3.8	0.23	30	50	-2.5		
LL	*Ppd-H1*	2	19.9	4.8	0.27	8	54	8.1	*Ppd-H1*	
LL	SCRI_RS_1362	5	50	9.1	0.30	18	73	-10.4	*nld-1a*	FD
	SCRI_RS_127712	5	47.5	8.5	0.30	18	74	-10.2		
	SCRI_RS_189377	7	70.61	5.2	0.11	18	61	10.7		
LW	*Ppd-H1*	2	19.9	6.7	0.27	21	51	1.0	*Ppd-H1*	
	SCRI_RS_153798	2*	17.5*	4.4	0.25	21	34	0.7		
	SCRI_RS_233272	2*	19.9*	4.3	0.20	21	34	-0.8		
	SCRI_RS_157866	4	110.2	4.3	0.36	21	28	0.7		
SL	*Ppd-H1*	2	19.9	5.4	0.28	40	47	5.0	*Ppd-H1*	
	SCRI_RS_233272	2*	19.9*	5.4	0.21	40	46	5.1		
	BOPA1_ConsensusGBS0008-1	2	58.78	4.9	0.19	40	41	4.1	*HvCEN*	
ROW-TYPE	BOPA1_12128-313	4*	26.35*	25.7	0.49	93	97	n.a.	*Int-c*	
	BOPA1_4616-503	4*	26.35*	25.6	0.49	93	97	n.a.		
	BOPA1_6208-987	4	26.35	22.4	0.47	93	97	n.a.		
	BOPA1_2832-377	4*	26.35*	22.4	0.47	93	97	n.a.		
	BOPA1_3687-271	4*	26.35*	22.4	0.47	93	97	n.a.		
	BOPA1_4098-758	4	25.92	15.5	0.48	93	96	n.a.		
	BOPA1_952-1301	4*	26.35*	13.2	0.49	93	96	n.a.	*VRS1*	
	SCRI_RS_137263	2*	80.03*	15.7	0.44	93	96	n.a.		
	BOPA1_2371-950	2	80.03	15.6	0.44	93	96	n.a.		
	SCRI_RS_91810	2*	80.03*	15.6	0.44	93	96	n.a.		
	SCRI_RS_4930	2	76.63	6.8	0.44	93	95	n.a.		
PH	SCRI_RS_156276	5	44.51	5.7	0.11	31	47	7.6		
NFRN	BOPA1_4616-503	4*	26.35*	6.5	0.49	66	70	-4.0	*Int-c*	
	BOPA1_12128-313	4*	26.35*	6.5	0.49	66	70	-4.0		
	BOPA1_6208-987	4	26.35	5.3	0.46	66	71	3.7		
	BOPA1_2832-377	4*	26.35*	5.3	0.46	66	71	3.7		
	BOPA1_3687-271	4*	26.35*	5.3	0.46	66	71	3.7		
NFRN	BOPA1_4098-758	4	25.92	4.4	0.47	77	84	3.4	Int-c	Row-type
	BOPA1_952-1301	4*	25.92*	4.1	0.48	77	84	2.9		
	SCRI_RS_171786	7	67.92	4.1	0.43	77	80	-1.5	*HvCO1, HvCO12, HvCO13, HvCO15 ?*	
	SCRI_RS_192587	7	67.92	4.1	0.43	77	80	-1.5		
	SCRI_RS_207354	7	67.92	4.1	0.43	77	80	-1.5		
	SCRI_RS_127040	7	67.92	4	0.43	77	80	-1.5		
	SCRI_RS_132722	7	67.92	4	0.43	77	80	-1.5		
	SCRI_RS_158234	7	67.99	4	0.43	77	80	-1.5		
T	BOPA1_6208-987	4	26.35	5.2	0.47	47	64	5.6	*Int-c*	
	BOPA1_2832-377	4*	26.35*	5.2	0.47	47	64	5.6		
	BOPA1_3687-271	4*	26.35*	5.2	0.47	47	64	5.6		

FD: flowering date, LL: leaf length; LW: leaf width; SL: spike length; PH: plant height; NFRN: number of fertile rachis nodes, T: tillering; SD: stem diameter. Chr: chromosome; cM: centiMorgan; MAF: minimum allele frequency; R^2 of model with SNP: percentage of variance explained by the model including SNP ; R^2 of model without SNP: percentage of the model excluding the SNP; allele effect: phenotypic effect of minor allele (allele with the lower frequency) estimated by the model; *:map position inferred with GWAS. Markers associated to more than one trait are labeled with colors.

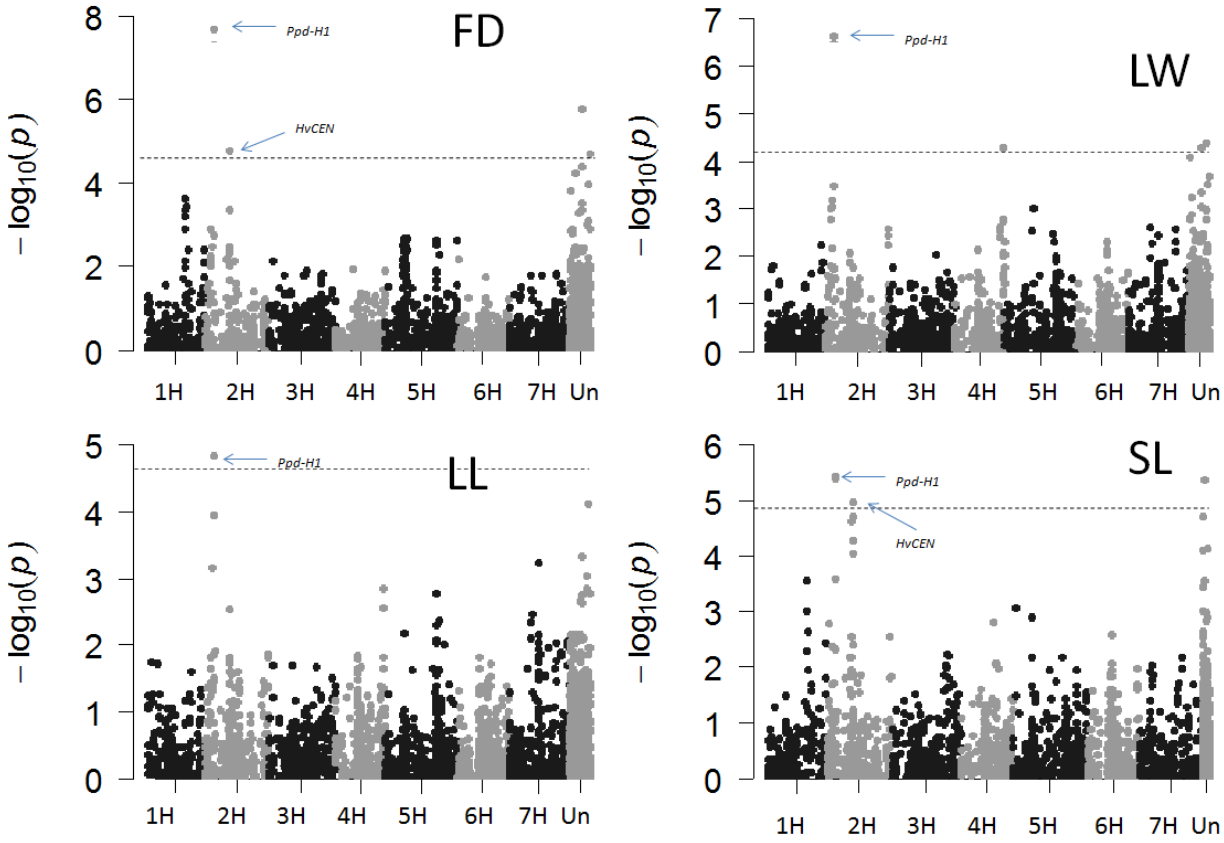

Figure 2.10. Manhattan plot displaying GWAS results for flowering date (FD), leaf length (LL), leaf width (LW) and spike length (SL). On x axis POPSEQ map positions of markers along the seven barley chromosomes are plotted, "Un" indicates markers that are not mapped in POPSEQ. On Y axis $-Log_{10}$ p-values of marker-trait association are plotted. The dashed line indicates the threshold for marker-trait association significance.

Together, these results show that allelic variation in the *Ppd-H1* genes significantly affects morphological traits such as LL, LW and SL, beside its known role in flowering time control. This suggests that genetic control on flowering date could have a pleiotropic effect on other morphological traits that may mask other genetic effects. For this reason we repeated GWAS for LW, LL and SL using flowering date as a cofactor (fixed effect) in further analyses.

For SL and LW no new significant association were found with this method, while new significant associations were uncovered between LL and SCRI_RS_1362 (5H, position 50 cM), SCRI_RS_127712 (5H, 47.5 cM) and SCRI_RS_189377 (7H, 70.61 cM) (Table 2.4 and Figure 2.11). Further analysis of the region on 5H showed a set of markers were not used in GWAS because of MAF < 10%: BOPA1_12045-83, BOPA1_ABC09365-1-3-378, BOPA1_5591-403, BOPA1_ABC11529-1-1-295, BOPA1_1910-1343 and BOPA1_ABC07010-1-2-150, mapped on 5H between 46.3 and

50.2 cM (Mascher et al., 2013). Interestingly, these markers were previously associated with the *narrow leaf dwarf 1a* (*nld-1a*) mutant (Druka et al. 2011). The *nld-1a* mutant exhibits narrow, erect, dark green leaves, with well developed midribs (Lundqvist and Franckowiak, 2002; Druka et al., 2011). The morphological characteristics and the position where the mutant is mapped point to a possible link between the *nld-1a* locus and the LL association peak on 5H (SCRI_RS_1362, SCRI_RS_127712).

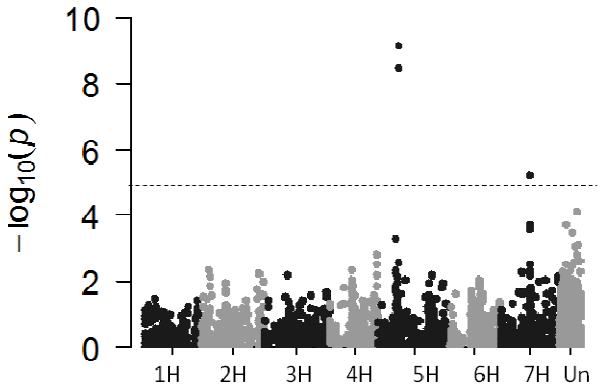

Figure 2.11. Manhattan plot displaying GWAS results leaf length (LL), using FD as covariate. On x axis POPSEQ map positions of markers along the seven barley chromosomes are plotted, "Un" indicates markers that are not mapped. On Y axis $-Log_{10}$ p values of marker-trait association is plotted. The dashed line indicates the threshold for marker-trait association significance.

Two genomic regions associated with FD, LW and SL in the present work may correspond to QTLs identified from a previous study on an advanced backcross population derived from a cross between a wild barley accession and a two-rowed spring cultivar (Gyenis et al., 2007). Using a linkage map including 112 SSR markers Gyenis et al., (2007), identified QTLs for heading date, flag leaf width and spike length on chromosomes 2H and, 4H. In order to compare the positions of these QTLs with those of our association peaks, we extracted relevant SSR primer sequences from the GrainGenes database (http://wheat.pw.usda.gov/cgi-bin/graingenes/browse.cgi?class=marker), aligned them primer sequences on the barley physical map using the IPK BLAST server (http://webblast.ipk-gatersleben.de/barley/,filtering for 100% of sequence identity) and anchored them to the POPSEQ genetic map. We applied this procedure to HVM36 an SSR marker on chromosome 2HL associated to flag leaf width, flowering date and spike length, and adjacent markers were GBM1035, UNB205 and GBM1006 (Gyenis et al., 2007): HVM36

mapped at 14.37 cM, while other markers described an interval between 14.37 and 40 cM on chromosome 2H, spanning the *Ppd-H1* locus.

Marker Bmag 0138.2, associated to a flag leaf width QTL in Gyenis et al 2007, was anchored to position 111.96 cM on chromosome 4H, and flanking markers Bmag0381.2 and HVM67 SSR were anchored to positions 74.46, 114.94cM in the POPSEQ map, respectively, suggesting this QTL may correspond to our LW locus associated with marker SCRI_RS_157866 at 110.2 cM on chromosome 4H.

Plant height

Plant height (PH) was measured only in Italy field experiment, it showed a moderate heritability (58%) in our germplasm panel with a mean of 68.1 cm, a maximum of 106.3 cm and a minimum of 33.3 cm (Table 2.4), and weakly but significant correlations with FD and stem diameter (SD) (Pearson correlation coefficient of about 0.3 (Table 2.3). In GWAS, marker SCRI_RS_156276, mapped on chromosome 5H position 44.5 cM, was significantly associated with the trait with a –Log10p-value of 5.7 (Figure 2. 12, Table 2. 4). An increase of 7.6 cm in plant height was estimated for genotypes carrying the minor allele (allele with lower frequency). The *ari-e* locus involved in controlling plant height was previously mapped on chromosome 5H within the region from 49.7 to 62 cM (Liu et al., 2014). This interval does not span SCRI_RS_156276 suggesting the association identified in our work may represent a distinct locus. Further analyses should clarify if this is really the case or not.

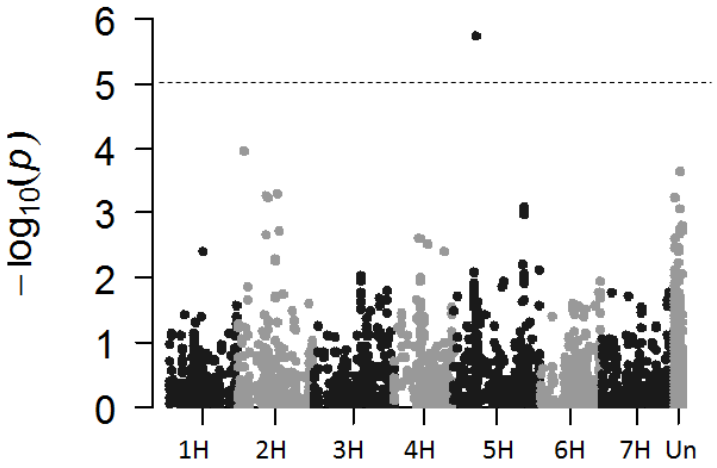

Figure 2.12. Manhattan plot displaying GWAS results for plant height (PH). On x axis POPSEQ map position of markers along the seven barley chromosomes are plotted, "Un" indicates markers that are not mapped.

On Y axis $-Log_{10}$ p values of marker-trait association are plotted. The dashed line indicates the threshold for marker-trait association significance.

Number of fertile rachis nodes (NFRN)

The number of fertile rachis nodes was measured only in the Italy experiment. NFRN is an indirect measure of number of seeds per spike: in six-rowed varieties (three spikelets per rachis node) the number of seeds per spike can be obtained multiplying NFRN by three, while in two-rowed varieties (one spikelet per rachis node) the number of seeds per spike is equal to NFRN. As seeds produced per rachis node are in constant ratio of 3:1 between six-rowed and two-rowed, NFRN was then the only measure that could be used to study spike fertility in a mixed panel of two-rowed and six-rowed varieties. The trait was highly heritable (h^2 = 81%), with a mean of 25 units and a standard deviation of 5. It was strongly correlated with row-type (Pearson correlation coefficient -0.85), in fact two-rowed genotypes had an average of 30 NFRN per spike, while 6-rowed had a mean of 22 NFRN per spike (the averages are significantly different ANOVA p-value: $2x10^{-12}$). Accordingly, markers associated with NFRN coincided with those associated with row-type (see previous paragraph): BOPA1_6208-987 (4H, 26.35 cM), BOPA1_4616-503, BOPA1_12128-313, BOPA1_2832-377 and BOPA1_3687-271 (Table 2.4 and Figure 2.13). Association between NFRN and genes controlling spike morphology is consistent with the well known tendency of two-rowed genotypes to develop more rachis nodes (Baldoni and Giardini, 2000), probably due to a pleiotropic effect of *VRS1* and *INT-C.*

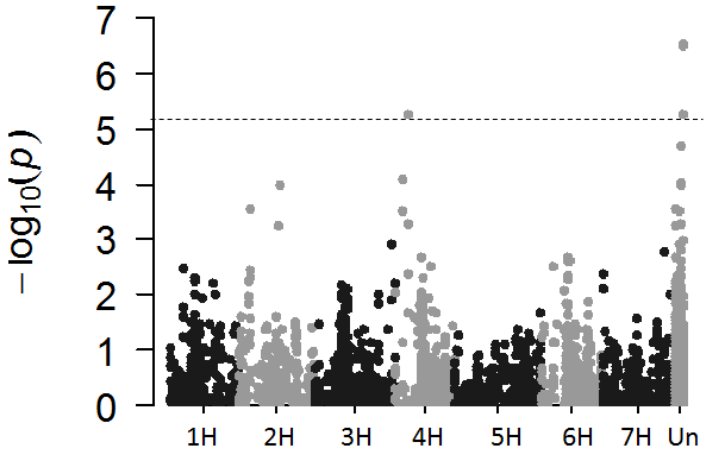

Figure 2.13. Manhattan plot displaying GWAS results for number of fertile rachis nodes per spike (NFRN). On x axis POPSEQ map position of markers along the seven barley chromosomes are plotted, "Un" indicates markers that are not mapped. On Y axis $-Log_{10}$ p values of marker-trait association is plotted. The dashed line indicates the threshold for marker-trait association significance.

Accordingly to the correlation between NFRN and row-type and statistic association between *INT-C* gene and NFRN we carried out a GWAS using row-type as covariate. With this method, rather than markers related to *INT-C* (BOPA1_4098-758, BOPA1_952-1301, 4HS, 25.92 cM), we found six markers (SCRI_RS_171786, SCRI_RS_192587, SCRI_RS_207354, SCRI_RS_127040, SCRI_RS_132722 and SCRI_RS_158234) associated to NFRN mapped at 67.9 cM on chromosome 7H (Figure 2.14 and Table 2.4)

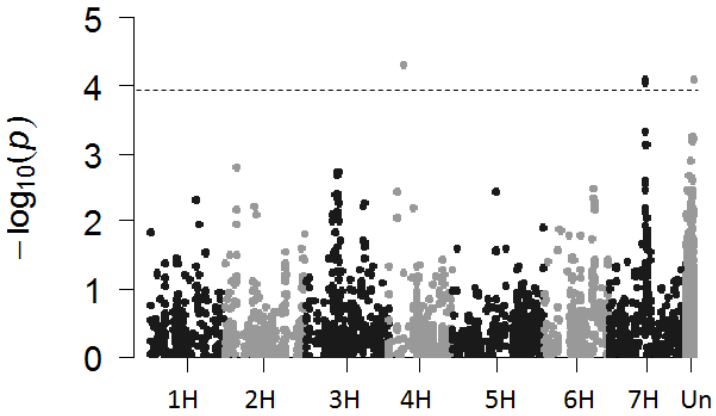

Figure 2.14. Manhattan plot displaying GWAS results for number of fertile rachis nodes per spike (NFRN), using row-type as covariate. On x axis POPSEQ map position of markers along the seven barley chromosomes are plotted, "Un" indicates markers that are not mapped. On Y axis $-\text{Log}_{10}$ p values of marker-trait association is plotted. The dashed line indicates the threshold for marker-trait association significance.

Stem diameter

Heritability for stem diameter (SD) was estimated to be 73%, with mean, maximum and minimum values of 5.1 mm, 6.2 mm and 4 mm, respectively. The trait was moderately correlated to row-type (Pearson correlation coefficient 0.48) and LL (Pearson correlation coefficient 0.55) and highly correlated with LW (Pearson correlation coefficient 0.65). Although no markers passed the significant threshold for this trait, two marker-trait associations may be recognized from the Manhattan plot in Figure 2.15, one with *Ppd-H1* markers.

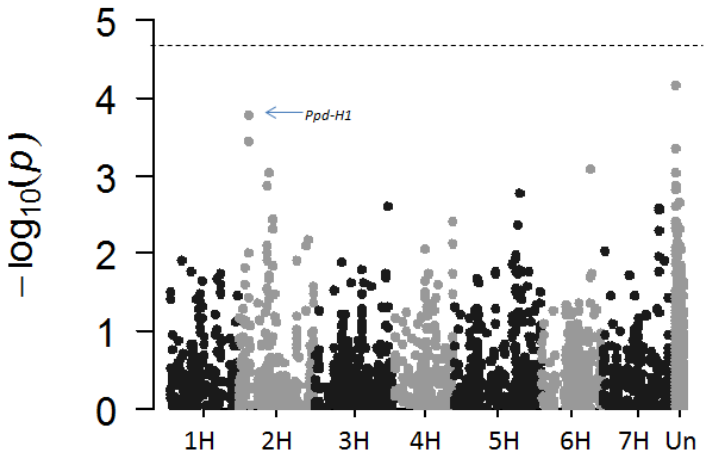

Figure 2.15. Manhattan plot displaying GWAS results for stem diameter (SD). On x axis POPSEQ map position of markers along the seven barley chromosomes are plotted, "Un" indicates markers that are not mapped. On Y axis $-Log_{10}$ p values of marker-trait association is plotted. The dashed line indicates the threshold for marker-trait association significance.

Tillering

Tillering was the trait with the lowest heritability (37%) (Table 2.2), probably due to the complex interplay of environmental and genetic factors influencing the trait, (see Chapter 3.3). Due to the pleiotropic effect of genes controlling spike morphology (Komatsuda et al., 2007; Ramsay et al., 2011), it is highly correlated with row-type (Pearson correlation coefficient -0.67) and NFRN (Pearson correlation coefficient 0.6). Accordingly, the only three significantly associated markers detected in GWAS were the same associated also to row-type: BOPA1_6208-987 (4H, 26.35 cM, corresponding to the region where the *Int.c* locus was mapped), BOPA1_2832-377 (mapped at 26.35 cM by GWAS), and BOPA1_3687-271 (mapped at 26.35 cM by GWAS) with –Log10P-value of 5.2 (Table 2.4, Figure 2.16). These results show that in our panel, genetic control of tiller number is dominated by genes underlying row-type.

For this reason we carried out a GWAS using row-type as covariate; with this model association with *INT-C* was not detected, indicating the effectiveness of model correction, nevertheless no markers passed the significant threshold for this trait, just one marker-trait associations may be recognized from the Manhattan plot (Figure 2.17), on chromosome 1H at position 100.8 cM (SCRI_RS_154528).

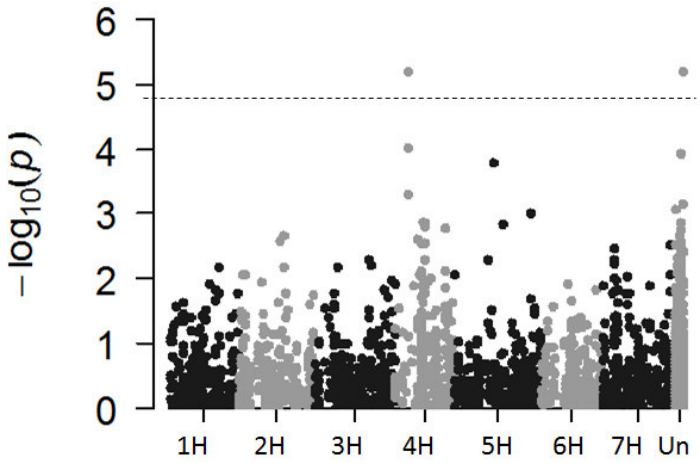

Figure 2.16. Manhattan plot displaying GWAS results for tillering. On x axis POPSEQ map position of markers along the seven barley chromosomes are plotted, "Un" indicates markers that are not mapped. On Y axis $-Log_{10}$ p-values of marker-trait association is plotted. The dashed line indicates the threshold for marker-trait association significance.

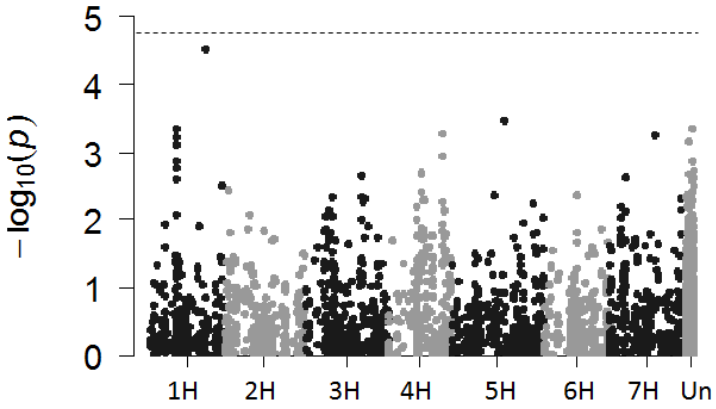

Figure 2.17. Manhattan plot displaying GWAS results for tillering, using row type as covariate. On x axis POPSEQ map position of markers along the seven barley chromosomes are plotted, "Un" indicates markers that are not mapped. On Y axis $-Log_{10}$ p-values of marker-trait association is plotted. The dashed line indicates the threshold for marker-trait association significance.

2 .4 DISCUSSION

Population structure

Most association studies in barley were carried out on panels of spring accessions or mixed panels of winter and spring accessions (Rostoks et al., 2006; Cockram et al., 2008; Stracke et al., 2009; Pasam et al., 2012; Tondelli et al., 2013). In this study we used an autumn sowed panel of winter cultivars where two-rowed and six-rowed types were equally represented, as reflected by analysis of population structure. This simple structure was already detected in other works (Rostoks et al., 2006; Cockram et al., 2010; Comadran et al., 2012; Pasam et al., 2012) and derives from modern breeding practices: contemporary European spring and winter varieties descend from a small number of successful European landraces selected around 100 years ago (Bothmer and Fischbeck, 2003). In our panel, the two-rowed barley sub-group showed a higher genetic diversity as compared to the six-rowed group. This was also observed by Comadran (Comadran et al., 2012) and may be due to the use of spring two-rowed varieties in breeding of winter two-rowed varieties (Bothmer and Fischbeck, 2003) potentially increasing genetic diversity. Based on genotyping of *Vrn-H1* and *Vrn-H2,* 7 (5 six-rowed and 2 two-rowed type cultivars) of the 142 genotypes showed a predicted spring growth habit, while three genotypes showed a facultative growth habit; however, their genetic backgrounds are clearly related to winter types; this was demonstrated by PCoA analyses of a comprehensive panel of spring and winter varieties in which they were positioned in the winter group (data not shown). *Vrn-H1* and *Vrn-H2* were not associated to any traits in our GWAS.

Pleiotropic effects of the *Ppd-H1* photoperiod response gene.

Ppdh-1 is the major determinant for photoperiod response in barley and may be a component of the circadian clock (Turner, 2005; Campoli et al., 2012b). The importance of *Ppd-H1* has always been related to spring varieties that have undergone a strong selection for reduced sensitivity to day length: the dominant allele (*Ppd-H1*) confers strong sensitivity to long days thereby accelerating flowering time, while the recessive allele (*ppd-H1*) confer reduced sensitivity to photoperiod thereby allowing the exploitation of longer growing seasons in temperate environments (Turner, 2005). In our panel only 4 six-rowed varieties carried the *ppd-H1* photoperiod insensitive allele, while in the two rowed group the two alleles were equally distributed. Barley with the responsive phenotype (*Ppd-H1*) is expected to predominate in regions

where the growing season is short with a dry summer; conversely, the reduced response associated with *ppd-H1* should predominate in regions with long growing seasons (Turner, 2005). In our panel the distribution of *Ppd-H1* alleles seems to follow this pattern: of the total number of genotypes which carried the *ppd-H1* allele, 63% are varieties from central and northern European countries, while 37% are Italian or French varieties; 64% of the varieties carrying the *Ppd-H1* photoperiod sensitive allele come from France and Italy, while the rest come from central and northern European countries. Nevertheless, the distribution of *Ppd-H1* alleles did not explain the diversity within two-rowed genotypes: in the PCoA analysis the two-rowed genotypes carrying *ppd-H1* did not cluster separately from those carrying the *Ppd-H1* allele (data not shown).

In other GWAS or Quantitative Trait Loci (QTL) mapping experiments (Hayes et al., 1993; Backes et al., 1995; Kjær et al., 1995; Qi et al., 1998; Gyenis et al., 2007; Pasam et al., 2012), based on spring or mixed spring-winter materials, QTLs for flowering time were mapped to the chromosomal position of the *Ppd-H1* locus. Jones et al. (2008) demonstrated that the functional mutation in *Ppd-H1* probably originated in wild barley, which is characterized by a winter growth habit, and was later adopted for spring cropping. Our results based on analysis of 6 markers diagnostic for *Ppd-H1* alleles show that the mutated allele is present in winter varieties and delays flowering time once the vernalization requirement is satisfied.

Genome wide association analyses showed that *Ppd-H1* also plays a major role in controlling LL, LW, and SL establishing a previously unknown link between the genetic control of flowering time and spike and leaf size. Interestingly, a previous study on an advanced backcross population derived from a cross between a wild barley accession and a two-rowed spring cultivar, identified QTLs for heading date, flag leaf width and spike length on 2HL (Gyenis et al., 2007) in a region spanning the *Ppd-H1* locus.

For LW, a marker at 110.2 cM on chromosome 4H was detected corresponding to a QTL for flag leaf width identified by Gyenis et al. (2007).

Together, these results show that in barley the genetic control of leaf size is partially dependent on genetic control flowering time.

Use of row-type and flowering date as covariate in GWAS

This work confirmed the known influence of row-type on traits like tillering and NFRN (Kirby and Riggs, 1978; Baldoni and Giardini, 2000). In our panel two-rowed cultivars exhibit an average of 30 tillers and 30 NFRN, while six-rowed varieties had an average of 22 tillers and 22 NFRN. In particular, the *vrs1-a* six-rowed allele is known to cause also a strong reduction in tillering while the *Int-c.a* six-rowed allele causes an increase in tillering, but its effect is weaker than *VRS1* (Ramsay et al., 2011). Kirby and Riggs (1978), analyzing one two-rowed cultivar, one six-rowed cultivar, the F1 progeny and F1 back-crosses to both parents, collected some evidence that differences between two-rowed or six-rowed morphology are not only due to the pleiotropic effects of row-type genes, but also because of patterns of development balanced by breeding practice for the particular row-type that are under independent genetic control Consistent with this idea, hybridization between different row-type cultivars produces a high frequency of poorly adapted genotypes. In our analyses markers linked to the *INT-C* locus are strongly associated with tillering variation, while *VRS1*-linked markers are not associated with tillering. The same happened for NFRN. Probably this is due to the correction by the model on markers linked to *VRS-1* (first coordinate values of PCA correlate with row-type variation).

Based on these results, we run GWAS for NFRN and tillering using row-type as covariate. A similar approach was applied in GWAS in human disease genetics (Pirinen et al., 2012; Winham et al., 2014). Although it was never applied to association mapping studies in plants, this approach has been successfully implemented in some QTL mapping analyses. In peach (Prunus persica), Pacheco et al. (2014) mapped QTLs for brown rot resistance using fruit maturity date as a covariate since this trait was correlated to the incidence of the disease. Zhou et al. (2012) showed that barley salinity tolerance is correlated to waterlogging tolerance and therefore used it as a covariate in a QTL mapping study of waterlogging tolerance . De Koeyer et al., (2004) found that covered/hulled caryopsis was correlated to grain quality and inserted it as a covariate in the model to map QTLs for grain quality in oat. With this model, we found six markers (5H, position 67.92-67.97 cM) that were significantly associated with NFRN. These same markers, were associated to the duration of the phase between awn primordia formation and tipping (awn arising from flag leaf) in a recently published GWA study (Alqudah et al., (2014). Awn primordium to tipping is the most decisive developmental phase for spikelet survival in barley (Alqudah and Schnurbusch, 2014). These markers are linked to BK_03 (97.91 cM) which is specific for *HvCO1*, a gene acting in the complex

system of photoperiod response (Campoli et al., 2012a). In our GWAS, similar to Alqudah et al. (2014), BK_03 (*HvCO1*) was much less associated to the traits than linked markers. These could be caused by the presence of other *CO* flowering date genes (*HvCO12, HvCO13, HvCO15, XvCCA-1, HvLHY*) that are present in this region (67.77-70.67) and may have effects on pre-anthesis development. Alqudah et al. (2014) concluded that variation around this gene may provide the genetic basis for observed pre-anthesis development variability. Anyway, it is interesting that the markers we found associated to spike fertility were the same associated to timing of spike development, and was already demonstrate that grain yield and grain yield potential are significantly influenced by reproductive, pre-anthesis phase duration (Slafer et al., 2001; Slafer, 2003). Furthermore, these results provide another support for the usefulness of GWAS models that employ phenotypic data as covariate.

Further GWAS should be focused on panels with uniform row-type to avoid confounding effects due to the segregation of row-type genes and additional loci involved in tillering and NFRN.

We detected an influence of flowering time on the variability of different morphological traits. In fact FD was correlated with LL, LW, SL and PH (Table 2.3). We thus run GWAS inserting FD BLUEs in the model as a covariate with the aim to account for pleiotropic effects of flowering date on other traits. In the present study, GWAS analyses using FD as a covariate detected three markers on 5H and 7H significantly associated to LL. Two markers mapped on chromosome 5H position 47.5-50 cM, within the region where the *nld-1a* mutant was introgressed by (Druka et al., 2011). Although further work is needed to validate the putative correspondence between our association peak and the *nld-1a* locus, this result provides preliminary support for the usefulness of this approach. One marker (SCRI_RS_189377) associated with LL was identified on chromosome 7H, at position 70.61 cM. This marker is located in the same region that hosts *HvCO12, HvCO13, HvCO15, XvCCA-1, HvLHY* (see the previous paragraph, Alqudah et al., 2014), nevertheless SCRI_RS_189377 does not correspond to any markers linked to these genes in the Alqudah et al. (2014) study.

Concluding remarks and outlook

In this chapter, effects of *Ppd-H1* on FD, LL and LW were supported by data from two different environments (Italy and Iran field trials). Data for other morphological traits are currently being collected from stocked material from the Iran experiment: when all data will be available, BLUEs across environment will be calculated and used for GWAS, to confirm previous findings.

In any case, results clearly show that different developmental and morphological traits are correlated and major genes with pleiotropic effect on multiple traits can mask effects of other genes. Pleiotropic effect of genes on different traits have been detected in previous works, (Bezant et al., (1996) carrying out a QTL mapping detected that the *semidwarf-1* gene other than its primary effect on plant height also had a major effect on ear emergence time; Tinker et al (1995) in a QTL mapping experiment detected one region near the end of chromosome 7 affecting lodging, yield, maturity, height, kernel weight, and test weight. Baum et al (2003) analyzed a population of RILs derived from a cross between *Hordeum vulgare* ssp. *spontaneum* and cultivar Arta under field drought stress conditions: the major QTL for plant height showed pleiotropic effects on traits such as days to heading, grain yield and shoot dry weight. The*Hordeum vulgare* spp. *spontaneum* allele increased plant height together with yield and total shoot dry weight and decreased days to heading under drought condition. Wang et al. (2010) carried out a QTL mapping experiment using a BC2 double haploid (DH) advanced backcross population derived from a cross between cultivar Scarlett and *Hordeum vulgare* spp. *spontaneum.* They detected *Ppd-H1*, *Vrn-H2* and *Vrn-H3* as QTLs for flowering date together with pleiotropic effects of these genes on plant height and yield components such as number of grains per spike. Pleiotropic effects of major genes on multiple traits were also detected in other species phylogenetically distant from barley. In peach, in a QTL mapping approach for fruit quality traits (fruit weight, external fruit skin overcolour, juice total soluble solids, juice titrable acidity and juice pH), most QTLs were located in the same region forming clusters of QTLs, this is likely due to a major pleiotropic effect of maturity date masking the identification of other QTLs for different traits (Eduardo et al., 2011).

Screening germplasm collections for major growth habit and row-type genes is thus a promising approach to assemble new association panels, preventing confounding effects and allowing additional loci to be detected. The use of traits that appear to influence other measures as covariate in GWAS models also seems to be a promising approach, even if the statistical power of this strategy is still to be evaluated.

3. EXPLORATION OF GENETIC VARIATION FOR ROOT EXTENSION IN WINTER BARLEY

3.1 INTRODUCTION

3.1.1 BARLEY ROOT ANATOMY

When a barley seed germinates, 5-7 seminal roots grow out from the coleorhiza (Hackett, 1969). These extend and branch, forming a fibrous, branched root mass. At 3-4 leaf stage adventitious roots start developing from basal nodes at the crown: at first many of these roots extend horizontally in the soil (Briggs, 1978). They are thicker, and less branched than seminal roots and if tillers become physically separated from the main culm, they can grow supported by adventitious roots only. Sometimes in drought or starvation stress the adventitious roots do not develop and seminal roots spread faster supporting the plant to maturity by themselves (Rich and Watt, 2013). In very deep soils roots may descend to 1.8-2.1m (Briggs, 1978) (Figure 3.1). The deepest roots are usually of seminal origin, these roots at the upper layers of the soil tend to be packed with adventitious roots. The maximal extent of the root system occurs at about the time of anthesis (Briggs, 1978).

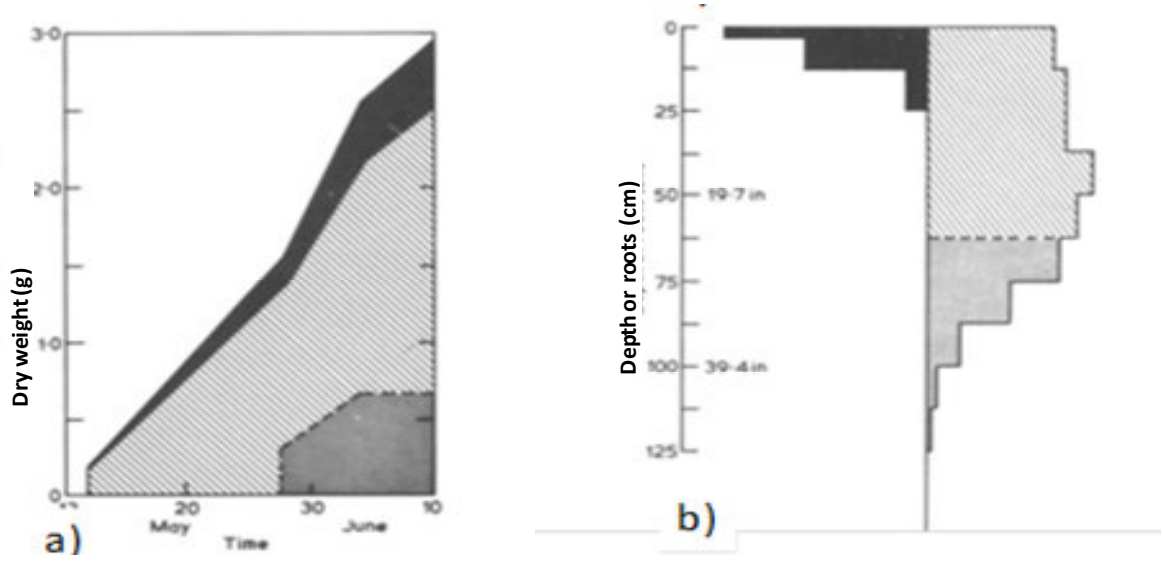

Figure 3.1. a) The increase in dry weight of the roots, until anthesis, in relation to time. b) the distribution of the root-mass at different depths, at anthesis. Black: crown roots; diagonal shading: seminal roots to 62.5cm ; stippled: seminal roots below 62.5cm (from Briggs, 1978)

Root development depends on the activity of the root apical meristem (RAM) and subsequent differentiation and expansion of other cells, so that the apex is continually being pushed forward

into the soil. The apex includes two different layers of cells. The outer layer, called “calyptrogen”, produces the calyptra, a slimy cup which protects the apex from the friction with the soil; it also contains cells rich in starch grains which may act as statoliths being responsible of gravitropism (Crespi, 2012). The inner layer consists of cells at the generative centre of the root which divide and subsequently extend to create the root cylinder, in which the cells are arranged in a series of concentric layers (Crespi, 2012).

Damaged root-tips will regenerate sometime during regeneration two distinct tips are formed and the root is forked. The cells behind the tip expand and vacuolate, and differentiate with increasing age (Crespi, 2012).

The epidermal layer of newly differentiated seminal root carries many root hairs. More internally there is an annulus of thin walled, loosely packed parenchymatic cells called cortex. Under the cortex there is a single layer of cells, the endodermis, the walls of which thicken with increasing age. Internal to the endodermis is the perycicle (Briggs, 1978). In the center of a root section, the stelar cylinder consists of parenchyma with alternating xylem and phloem elements. In young seminal roots there is a large central vessel (Briggs, 1978). Young adventitious roots have an essentially similar structure except for the several scattered large inner metaxylem vessels (Figure 3.2). When roots grow, a corky layer develops under the epidermis, parenchyma cell walls become thickened, a sclerenchyma develops in the outer cortex, and the walls of the cells of the stele become thickened: these changes confer more strength to the root (Figure 3.2).

The cortex parenchyma usually contains small air-spaces. Under conditions of poor aeration, in water culture, the roots become shorter and more numerous, and have greater diameters (Briggs, 1978). In these roots the cortex develops large air-passages separated by narrow strands of parenchyma. These enable the roots to receive more oxygen from the upper parts of the plant (Briggs, 1978).

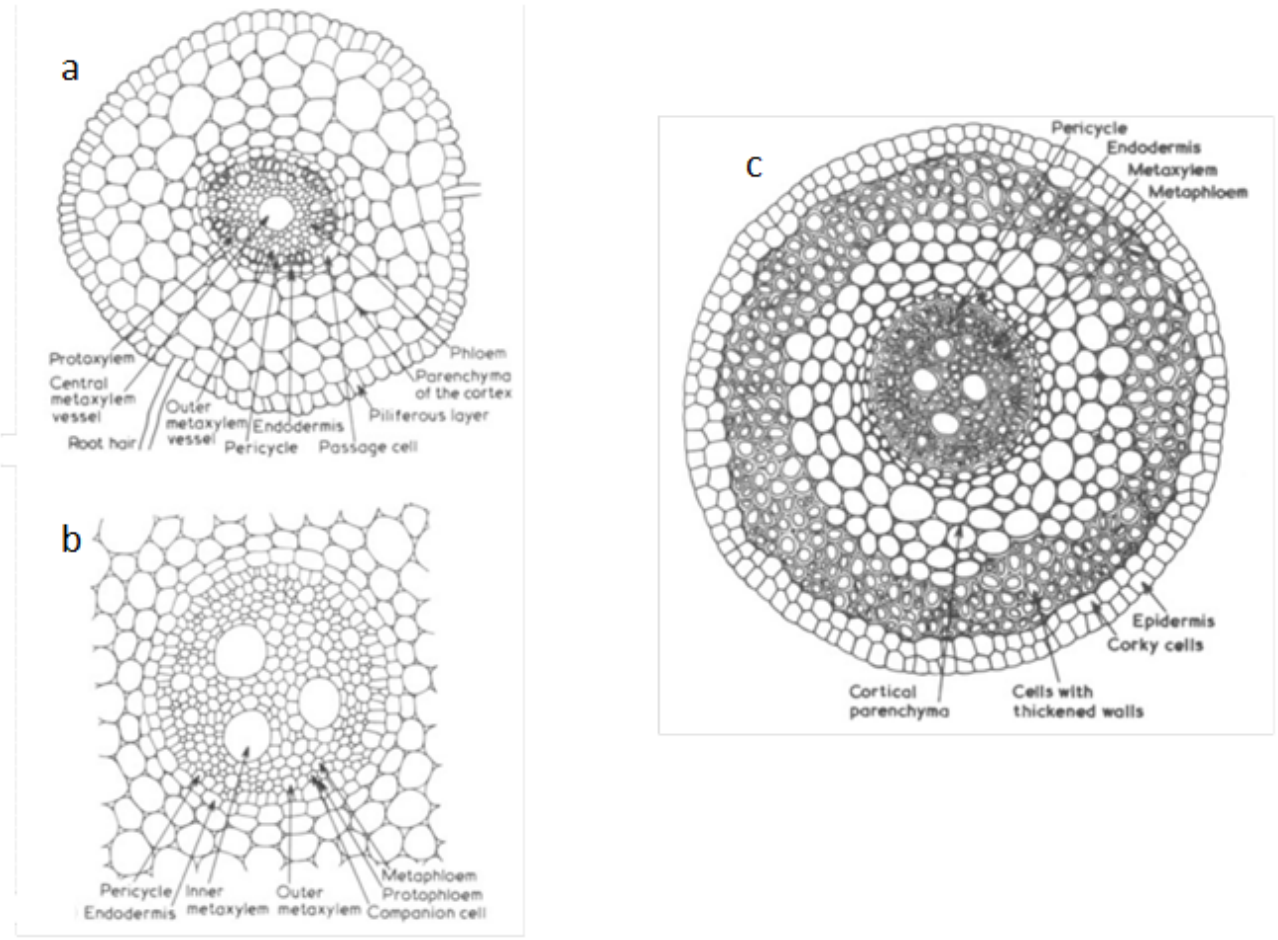

Figure 3.2. (a) Transverse sections of a young seminal root. (b) Transverse section of the stele of a young adventitious root. (c) Transverse section of a mature adventitious root. Image from Briggs, (1978).

Lateral roots (LR) develop from meristematic cells situated in the perycicle of an existing root (seminal or adventitious). These may divide and differentiate to give rise to lateral roots, which appear to erode, rather than force, their way to the exterior, through the cortex (Briggs, 1978). In cereals such as maize and rice, the endodermal cells also contribute to LR development and produce the epidermis and the root cap, whereas pericycle cells are the source of all remaining tissues (Hochholdinger, 2004) (Figure 3.3).

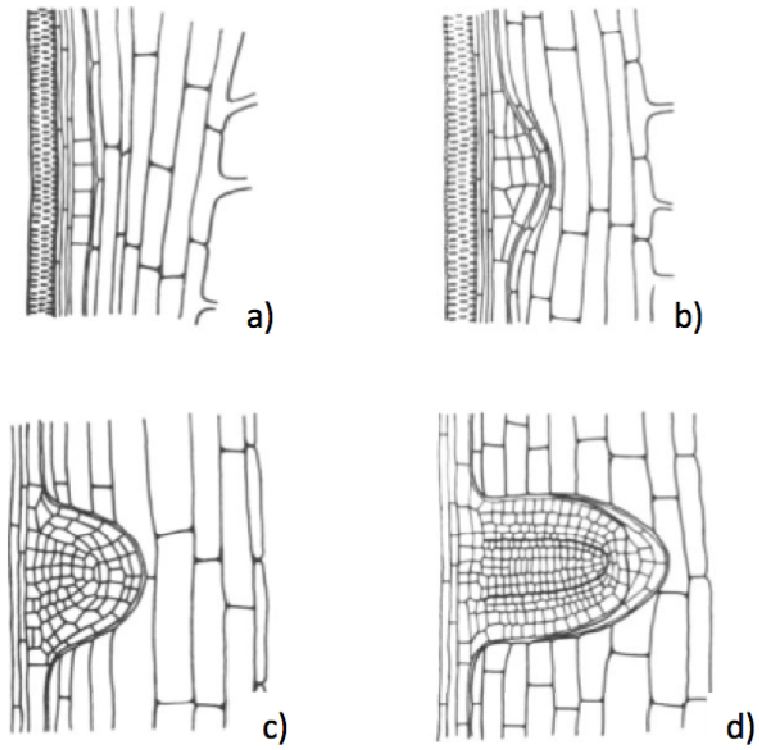

Figure 3.3. Stages in the development of a lateral root in barley seen in longitudinal section. (a) The establishment of a meristematic region. (b-d) Successive stages in the formation of the rootlet, within the cortex. Image from Briggs, (1978)

In contrast to LR, adventitious roots develop from basal stem nodes and consequently from different cell types. A conserved feature is that adventitious roots always develop from cells neighboring vascular tissues. In both maize and rice, cross sections in coleoptile nodes indicate that adventitious root primordia develop from cells close or adjacent to the vascular cylinder of the stem (Hetz et al., 1996; Inukai et al., 2005).

A root hair is an extension of a non-dividing epidermal cell known as a trichloblast (Schiefelbein, 2000). A root hair grows via the deposition of new membrane and cell wall precursors at the growing tip. Two main steps can be distinguished in root hair morphogenesis – the differentiation (specification) of trichoblasts and root hair development, which can be divided into three stages – root hair initiation, transition to tip growth and root hair elongation (Schiefelbein, 2000). They contribute to anchor plants in soil, uptake water and nutrients and are the sites of the interaction between plants and microorganisms (Schiefelbein, 2000). Brown et al. (2012) demonstrated that barley genotypes with no root hairs suffering extreme growth retardation in comparison with those with root hairs.

3.1.2 GENETIC AND HORMONAL CONTROL OF ROOT DEVELOPMENT AND ARCHITECTURE

A number of genes involved in root development and architecture have been identified in *Arabidopsis* (Tian et al.) although root system of dycotiledons is different from that of monocotyledon. In e.g. in *Arabidopsis* there is only one seminal roots that commonly grows to become a thick central taproot, which may or may not develop lateral roots. LRs reiterate the process and develop higher-order LRs. In rice some genes and signals have been identified.

In rice morphological differentiation of the embryo begins 4 days after pollination (DAP) (Itoh et al., 2005). Three organs are clearly defined at this stage: the coleoptile, the shoot apical meristem (SAM), and the RAM. Three are the rice mutants where seminal root development is altered: *radicleless 1* (*ral1*), *radicleless 2* (*ral2*), and *radicleless 3* (*ral3*) (Hong et al., 1995). In the *ral1* mutant, the basal structures of the embryo, including the mesocotyl and seminal root, are missing (Scarpella et al., 2003). Moreover, the mutant develops fewer adventitious roots than the wild type, demonstrating that seminal and adventitious roots are under separated but interconnected genetic controls. The diameter of *ral1* roots is reduced since the numbers of xylem and phloem vessels, and cortical cell layers are reduced, as is the diameter of the metaxylem cells (Scarpella et al., 2003). Furthermore, *ral1* plants are smaller and possess shorter leaves. The *ral1* mutant is defective in vascular pattern development both at embryonic and post embryonic stages and exhibits a reduced sensitivity to auxin, leading to the connection between embryo formation, seminal root formation and auxin response (Scarpella et al., 2003).

In rice, adventitious root primordia originate from ground meristem cells in the parenchyma adjacent to the peripheral cylinder of the vascular bundles in stems (Itoh et al., 2005); the establishment of adventitious root primordia is strictly under genetic control, while adventitious root outgrowth depends also on hormonal and environmental factors (Itoh et al., 2005)Rebouillat et al., 2009). *CROWN ROOTLESS1 (CRL1)* encodes a lateral organ boundary (LOB) family transcription factor, whose expression is regulated by auxin through an auxin response factor (ARF) (Inukai et al., 2005). The *crl1* mutant and the similar *crl2* mutant develop normal seminal roots but do not form crown root primordia further supporting the idea that seminal and adventitious roots are under different regulatory pathways and indicating that these genes are required for crown root primordium formation. In both mutants, several additional auxin-related

phenotypic traits are visible, including a decrease in LR number, auxin insensitivity in LR formation, and altered root gravitropism (Inukai et al., 2005).

LR in rice arise from anticlinal symmetrical divisions in the pericycle and endodermal cells located opposite to the protophloem and between two protoxylem poles (Kawata and Shimayama, 1965). The first LR primordia are visible 1.5 mm from the root tip. The *lateral root less 1* (*Lrt1*) mutant lacks lateral roots and also exhibits altered gravitropism and root-hair formation(Chhun et al., 2003). The mutation is dominant, suggesting that it is a gain of function. No significant differences exist between *Lrt1* and wild type regarding plant height, the number of crown roots, or seminal root length. *Lrt1* is also insensitive to indole-3-butyric acid, a natural auxin that was identified in monocots. *Lrt1* is similar in appearance to the *Solitary-root/ iaa14 (Slr1)* mutation described in *A. thaliana* (Fukaki et al., 2005); the *Slr1* mutant completely lacks lateral roots and is defective in root hair formation and the gravitropic response of the root, as well as being insensitive to auxins. The *Slr-1* mutation blocks early cell divisions in lateral roots (Fukaki et al., 2005). *SLR1* encodes *IAA14*, a member of the auxin – indole acetic acid (Aux/IAA) protein family. IAA14 represses auxin-induced gene expression and acts as a transcriptional repressor (Fukaki et al., 2005).

Many other mutants exhibiting altered LR development have been found in *Arabidopsis*, rice, and maize, and their characterization has helped to identify components of the polar auxin transport (PAT) and auxin signaling pathway required at each step of LR and adventitious root development (Komatsu et al., 2001; Rebouillat et al., 2009; Coudert et al., 2010; Petricka et al., 2012; Orman-Ligeza et al., 2013).

Cytokinines (CK) are a class of plant growth regulators known to promote cell division and shoot development. Their effect is opposite to auxin, acting as suppressors of adventitious root and LR formation in many species, including *Arabidopsis*, rice, alfalfa (*Medicago sativa*), and poplar (Werner, 2003; Gonzalez-Rizzo et al., 2006; Ramírez-Carvajal et al., 2009). In *Arabidobsis* adventitious roots arise from the vascular tissues (cambium and surrounding tissues) in derooted hypocotyls of older seedlings, in which secondary growth has initiated; or from the vascular tissues of stem cuttings (Bellini et al., 2014). In *Arabidopsis*, lines overexpressing CK oxidase/dehydrogenase–encoding genes have reduced endogenous CK levels and increased number of adventitious roots and LRs (Werner et al., 2003), and mutants altered in the expression of CK receptors have an increased frequency of LRs (Riefler et al., 2006). CKs modify the expression

of auxin polar transport genes (PIN genes), preventing the formation of the required auxin gradient in the LR founder cells and thereby inhibiting the initiation of LR primordia (Laplaze et al., 2007). Another study showed that zeatin riboside, one species of CK present in xylem sap, is the main suppressor of adventitious root formation in *Arabidopsis* hypocotyls (Kuroha and Satoh, 2007). CK receptors are required for the formation of auxin-transporting vascular tissues in hypocotyls, which is necessary for LR development but not for adventitious root development (Kuroha and Satoh, 2007). These results give a further demonstration that vascular development in adventitious roots and LRs are controlled by distinct mechanisms.

The role of ethylene in adventitious root and LR formation is complex, as ethylene biosynthesis is controlled by auxin and vice versa. In addition, ethylene regulates auxin transport and signaling (Stepanova and Alonso, 2009). Auxin and ethylene act either antagonistically or synergistically and have opposite effects on adventitious roots and LRs (Stepanova and Alonso, 2009; Muday et al., 2012).

Absisic acid (ABA) has been characterized as a negative regulator of adventitious roots and LRs, although few studies have reported a positive effect, suggesting that complex interactions might occur, possibly depending on the development phase (Bellini et al., 2014). In flooded rice plants, the balance between ethylene, GA, and ABA is altered upon submergence, and ABA negatively controlled adventitious root emergence, which was reduced to approximately 50% after ABA treatment (Steffens et al., 2006).

Although role of gibberellins (GAs) in the control of LR development is marginal, GA biosynthesis has been detected in the root tips of different plants, and GA signaling is required for primary roots growth of *Arabidopsis* and rice (Fu and Harberd, 2003; Kaneko et al., 2003). In contrast, GAs have a negative effect on adventitious root formation. Exogenously applied GA inhibits adventitious root formation in rice plants, whereas rice mutants deficient in GA biosynthesis develop more adventitious roots (Lo et al., 2008).

As most brassinosteroid (BR) biosynthesis and signaling mutants exhibit dwarf phenotypes, it is difficult to establish if effects on roots are due to a direct role of BR or to a pleiotropic effect due to dwarfing.BR, and auxin induce many auxin signaling genes involved in root growth and development. Like auxin, BRs promote PR??? growth at low concentrations but inhibit it at higher concentrations (Mussig et al., 2003). They also control LR development through a complex

interplay with auxin (Bao et al., 2004; Mouchel et al., 2004; Nemhauser et al., 2004). Rice mutants affected in BR biosynthesis, as *brd1* (*brassinosteroid-dependent 1*), show a significant reduction in BR content and abnormal root morphology phenotypes, which were restored by exogenously applied BR (Mori et al., 2002).

Strigolactones (SLs) have recently been described as negative regulators of adventitious root and LR development in different species, including *Arabidopsis*, tomato (*Solanum lycopersicum*), pea (*Pisum sativum*), and maize (Guan et al., 2012; Rasmussen et al., 2012a; Rasmussen et al., 2012b). They seem to act in interaction with ethylene, CKs, and auxin. Recent studies in *Arabidopsis* indicate that basipetal auxin transport and auxin accumulation in the rooting zone is probably negatively regulated by SLs (Rasmussen et al., 2012b).

3.1.3 ENVIRONMENTAL FACTORS INFLUENCING ROOT DEVELOPMENT

Root extension in cereals is an extremely plastic trait exhibiting high variation in relation to environmental conditions as overviewed in the following paragraphs.

Water availabilty

Under limited water conditions, tolerant plants tend to grow a deeper root system, prioritizing assimilates from shoot growth to root growth so roots can extend into still moist deeper zones (Gregory, 2006). In many species, a deeper root system is achieved by the ability to continue growth, even at extremely low water availability (Sharp et al., 2004). In barley under drought the adventitious roots do not develop while seminal roots grow deeper leading the plant to maturity by themselves (Briggs, 1978). Although roots can still grow at water contents that inhibit shoot growth, under extremely low water potentials (i.e. less than –1.5 MPa) root growth is inhibited (Salim et al., 1965). This was demonstrated in a pot experiment where water availability was stratified down the pot, and for wheat, oats, and barley root growth stopped when roots reached the dry (2.3% moisture content) soil layer (Salim et al., 1965). Continued elongation under water stress probably relates to the hydrotropic nature of roots which may allow them to bend towards areas of higher water potential (Takahashi, 1997; Eapen et al., 2005).

Nutrient availability

Root architecture depends on distribution of nutrients in the soil. A detailed analysis of root development in two barley cultivars (Maris Badger and Proctor) was carried out by measuring the number and length of seminal, secondary and adventitious roots under normal conditions compared to phosphorus and potassium starvation (Hackett 1969). Under nutrient starvation, both cultivars exhibited a reduction in the number and length of adventitious roots and length of primary roots. Proctor exhibited an increase in number and length of secondary axes under phosphorous starvation, while the opposite behaviour was observed in Maris Badger, indicating the presence of different response mechanism to nutrient starvation. Root elongation and branching can be triggered by local nutrient abundance (Robinson, 1994). Numerous studies examining root responses to nutrient heterogeneity have been published. Drew , (1975) demonstrated that barley plants grown for 21 days in pots stratified with different concentrations of phosphate, nitrate, or ammonium, seminal roots initiated many new first and second-order laterals in zones supplied with high nutrient concentration. Micro-computed tomography now allows non-destructive illustration of lateral root proliferation in nutrient patches (Rich and Watt, 2013). Root proliferation within patches of high nutrient availability can result from changes to branching or elongation (Fitter, 1994). The angle at which lateral branches emerge will affect the area over which the roots spread so narrower branching angles will create a denser patch, especially if the root also changes its branching pattern (Fitter, 1994).

Soil density

Soil density or hardness is another factor that strongly influences root development. Growing wheat plants in long cylindrical shaped pots filled with sand that was pressed at 1.0, 2.0, 3.5, and 5.5 MPa, Merotto and Mundstock (1999) found significant differences in root growth among the four soil treatments from as early as 16 d after emergence: roots in stronger soils showed strongly reduced length, surface area, and dry matter, but higher root diameter. This has also been shown in other cereals (e.g. maize, Goodamn et al., 1997; oat, Ehlers et al., 1983).

3.1.4 NATURAL VARIATION

Some differences in the root of different barley genotypes are result of environmental adaptation. For example in a direct comparison between barleys from the Indian sub-continent grown in field one site (Bose and Dixit, 1930) it was shown that barleys from areas with adequate soil moisture

tended to have comparatively shallow, 'mesophytic' (expanded orizontally, exploring the first soil layers), root systems, while barleys from dry regions produced deep, 'xerophytic' (expanded vertically, reaching the deeper soil layers to absorb water) rooting patterns(Figure 3.4).

Grando and Ceccarelli (1995) investigated seminal root characteristics and coleoptile length in three groups of barley germplasm: wild barley (*H. vulgare* ssp*. spontaneum*) accessions, landraces, and modem cultivars. Wild barley had an average of three seminal root axes, always less than modern varieties and landraces, intermediate to maximum seminal root length, and total root length similar to that of modern germplasm. Landraces did not differ from modern cultivars for number of seminal root axes, but they had the longest seminal root system. Modern cultivars had several short seminal roots. The results suggest that landraces have a more vigorous seminal root system than modern cultivars. Both landraces and *H. vulgare* ssp*. spontaneum* could thus be important genetic resources, which may contribute to specific adaptation of barley to moisture-stressed environments.

Naz et al. (2014) developed a population of 72 introgression lines (ILs) from an initial cross between the German spring cultivar Scarlett (*H. vulgare* ssp. *vulgare*) as recurrent parent and the wild barley accession ISR42-8 (*H. vulgare* ssp. *spontaneum*) from Israel. This population was grown together with parental lines in pots and subjected to control and drought treatments. The drought stress treatment was carried out 30 days after sowing by eliminating the water supply completely. Plants were kept under stress for 26 days till volumetric moisture content (VMC) reached the maximum drought stress threshold near to wilting point (VMC near to 0%) and root length and root dry weight were registered. Accession ISR42-8 exhibited a more vigorous root system than Scarlett, and this trait exhibited a good heritability in the population. Mean comparisons revealed superior performance of an introgression line for root length under drought stress conditions. This observation suggests the presence of drought inducible transgressive exotic alleles whose expression in the Scarlett background might be advantageous to that introgression line. QTL mapping identified 15 QTLs affecting root system extension, with one QTL located on chromosome 1H having the major effect: the isoline carrying the favorable allele exhibited root dry weight of 78.8% greater than population average.

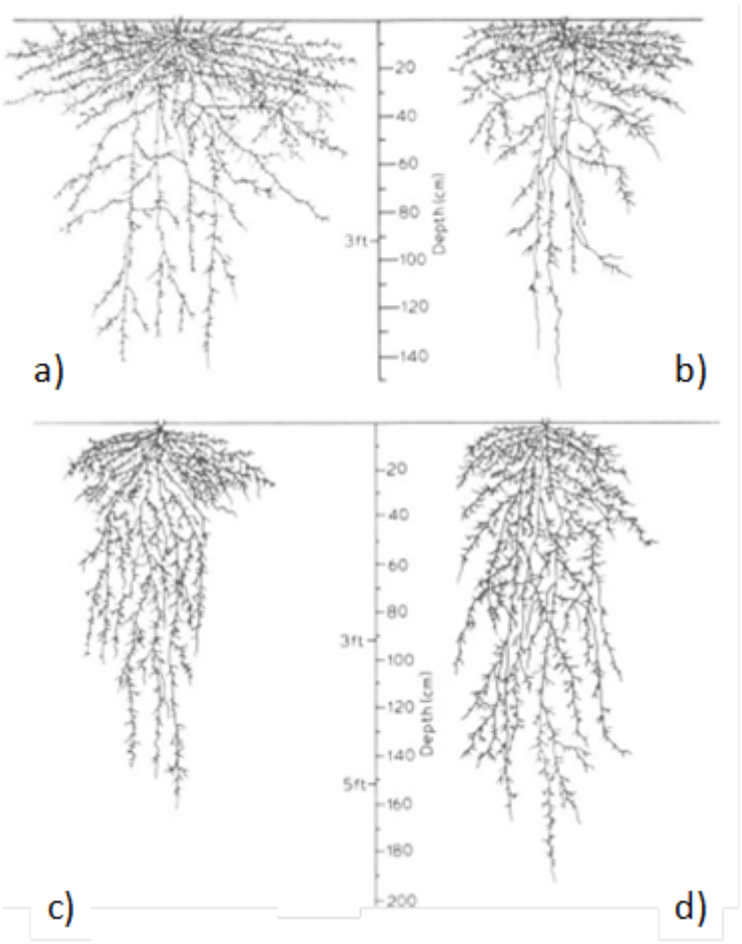

Figure 3.4. The extents of four types of rooting systems encountered in Indian barleys a, Mesophytic; b, semi-mesophytic; c, semi-xerophytic; d, xerophytic (Bose and Dixit, 1930).

3.1.5 BARLEY ROOT MUTANTS

Recently barley root mutants were identified from a mutagenized population of barley cv. 'Morex' produced by sodium-azide treatment (Talamè et al., 2008). This Targeting Induced Local Lesions IN Genomes (TILLING; McCallum et al., 2000) resource is named TILLMore (http://www.distagenomics.unibo.it/TILLMore/), and is available for both forward and reverse-genetics applications in barley. Screening for lines altered in root development was carried out on a subset of 1000 M 4 families from the TILLMore collection. The analysis was performed using a paper-roll approach as described by (Woll et al., 2005). The method is based on seedlings grown in rollers made of a rolled sandwich of filter paper (allowing to observe root development on the filter paper) and kept in a growth chamber under controlled conditions. Eight days old seedlings were collected and morphology of the seminal roots was visually compared to that of the wild type. A total of 72 lines with altered root development were detected, and can be divided in

different classes (short root, very short root, short and thick root, short and curly root, curly root, short root air, higly geotropic, root-to-leaf, hairless). Some of these mutants are currently under investigation at the University of Bologna (Italy).

Two barley genes responsible for the development of short root hairs (*rhs2* and *rhs3*) and one mutation leading to an irregular root hair pattern (*rhi2*) (from mutant collection of Department of Genetics, University of Silesia, Poland) were mapped on chromosomes 6H, 2H and 1H, respectively (Chmielewska et al., 2014). A comparative analysis of the physiologic parameters between some these mutants and their respective parental lines showed that altered root hair development had no effect on the performance of plants that were grown under controlled conditions (Chmielewska et al., 2014).

3.2 OBJECTIVES

Winter barley has agronomic interest in the Mediterranean area (Ullrich, 2010), where genetic improvement of drought tolerance is particularly important (Baum et al., 2003).

As development of the root system is connected to the ability of the plant to reach water (Rich and Watt, 2013), the goal of this chapter of my PhD project was to explore a collection of European winter barley cultivars for natural genetic variation in root extension with a view to carry out a GWAS for root traits.

3.3 MATERIALS AND METHODS

3.3.1 GENETIC MATERIALS

A preliminary greenhouse trial (see paragraph 3.4.2) was carried out on a panel of 100 European winter barley cultivars selected from the panel of 142 winter barley European cultivars described in chapter 2 (see paragraph 2.3.1, table 2.1.). Subsequent growth chamber experiments (see paragraph 3.4.3) included the whole panel (67 two-rowed and 75 six-rowed, released between 1921 and 2006). Each of the 100 cultivars (50 two-rowed and 50 six-rowed) used in the greenhouse trial was chosen based on its clustering in PCoA and on its average correlation coefficient with other accessions (calculated based on genotype) calculated with the PAST

software (Hammer et al., 2001): starting from a total 142 cultivars, those exhibiting low average correlation coefficient with other ones or clustering far from the two main sub-groups (two-rowed, six-rowed, Figure 2.7 in Chapter 2) were excluded to reach a final set of 100 lines.

2.4.2 GREENHOUSE TRIAL EXPERIMENTAL CONDITIONS

In order to establish suitable conditions to explore genetic variation for root traits, we initially carried out a greenhouse experiment on a set of 100 winter barley cultivars: single plants were grown in cylindrical pots (13 cm diameter x 60 cm height) filled with a mixture of field soil (clay soil) from CRA-GPG experimental field, Fiorenzuola d'Arda, Italy) and sand in proportion of 2:1 (in volume) respectively, and three plants (replicates) were considered for each genotype (total 300 plants). As we planned to evaluate different root and shoot traits, we decided to collect plants at the beginning of stem elongation. Results (data not shown) highlighted a low consistency among replicates, also due to difficulties in extracting roots from the hard soil resulting in breaking of roots and loss of material. This protocol was thus not judged reliable for further experiments. In the following experiments, efforts were directed to guarantee better consistency among replicates and more facility in root extraction.

2.4.3 GROWTH CHAMBER TRIAL EXPERIMENTAL CONDITIONS

The experimental design was a total randomized block with 3 blocks. Each block consisted of 142 pots: in each pot 3 plants of each of the 142 genotypes were grown. Thus each replicate was constituted by a pot of three plants, and 9 plants in total were examined for each genotype. The three plants of each replicate were considered as one unique sample, thus each score collected was the sum of the three plants. Due to space constraints in the growth chamber, blocks were sawn and collected one at time. Block/replicate *a* was sawn on April-29-2013 and collected on May 20/22, block/replicate *b* was sawn on June 24 and collected on July 12/15, block/replicate *c* was sawn on September 17 and collected on October 7/8. Growing conditions of the growth chamber were 16 h light at 22 °C and 8h dark at 18°C, relative air moisture was maintained at 65%. Pots were watered almost daily to maintain substrate moisture at field capacity.

Pots

Cylindrical pots (called rhizotrons) with diameter of 10 cm and 50 cm height were produced by cutting PVC tubes as indicated in Shashidhar, (2012). The bottom of each rhizotron was built by inserting at one end of the tube a small cylindrical florist pot (10 cm diameter and 10 cm height); this was filled with a small amount of expanded clay to drain water.

Substrate

Many substrates were tested with the cultivar Aldebaran in 5 replicates, with the aim to find a substrate that would ensure reproducibility and ease of root extraction:

- S1: mix of siliceous sand and CRA-GPG field soil in proportion of 2:1 (the inverse of the greenhouse experiment), supplemented with 0.3 g/L NH_4NO_3 0.15 g/L K_2HPO_4.
- S2: mix of perlite, CRA-GPG field soil and sand in proportion of 6:2:1 supplemented with 0.3 g/L NH_4NO_3 and 0.15 g/L K_2HPO_4.
- S3: siliceous sand supplemented with 1g/L of the controlled release fertilizer Basacote® Plus 3M (COMPO).
- S4: siliceous sand supplemented with 2.5 g/L of the controlled release fertilizer Basacote® Plus 3M (COMPO).

Siliceous sand composition is listened in Table 3.1. Basacote® Plus 3M fertilizer (COMPO, Table 3.2) is a coated fertilizer that ensures a continuous and constant release of nutrients. All the components of different substrates were mixed uniformly by a cement mixer.

Table 3.1. Composition of sand used in growth room experiments. VAGA S.r.l, Sostegno - SP 199 27010 Costa de' Nobili, Pavia, Italy.

Chemical analysis			
SiO_2	83.3%	MgO	1.5%
FeO_2	2.1%	Na_2O	2%
$Al2O_3$	6.6%	K_2O	2.1%
CaO	1.2%		
Mineralogical analysis			
Quartz	61.8%		
Granitoid rocks	16.5%		
Feldspars	12.7%		
Other minerals (traces)	9%		
Granulometry	0.1-4 mm		

Table 3.2. Composition of Basacote® Plus 3M fertilizer (COMPO GmbH & Co. KG Gildenstraße 38 48157 Münster, Germany)

NO_3-	7.40%
NH_4+	8.80%
P_2O_5 soluble in water	8%, 6% soluble in CH_3COONH_5
K_2O	12%
MgO	2%, 1.4% soluble in water
SO_3-	5%, 4% soluble in water
B	0.02%
Cu	0.05%
Fe total	0.4%, 0.15% Fe-EDTA
Mn	0.06%
Mo	0.02%
Zn	0.02%

In comparison to S3 and S4, for plants grown in S1 and S2 root extension exhibited higher variation among replicates (data not shown). The high variation in S1 and S2 might be due to higher soil density inside the pots; this was visibly detectable with a simple trial: after filling pots in S1 and S2 the volume of the substrate was continuously compressed by beating the pots on the floor,

instead volume of sand remained constant. It was demonstrated that cereal root development is influenced by the hardness of soil (Merotto and Mundstock, 1999)

Moreover plants grown in S3 exhibited a more extended root system than in S4, probably due to low concentration of fertilizer that stimulated root growth. S3 was then selected as substrate for further analyses.

Plant collection, root extraction and analysis

Initially 5 seeds were planted in each pot; after germination seedlings were reduced to 3/pot. Plants were collected at the 4 leaf stage (Zadocks stage 14, Zadocks et al., 1974). Pots were submerged in a plastic tank filled with tap water to disperse the substrate. After removal of the pot, plants with intact root systems were carefully sieved using a metal net previously positioned at the bottom of the tank. Whole plants were conserved at 4°C in ethanol 50 % until the time of analysis. Roots were separated from shoots and scanned with an EPSON expression 10000 XL scanner: roots were put in a glass tray filled with water that was put on the scanner. Scans were taken at a resolution of 400 dpi , (Figure 3.5). Shoots were dried in anoven at 60°C for 36 h.

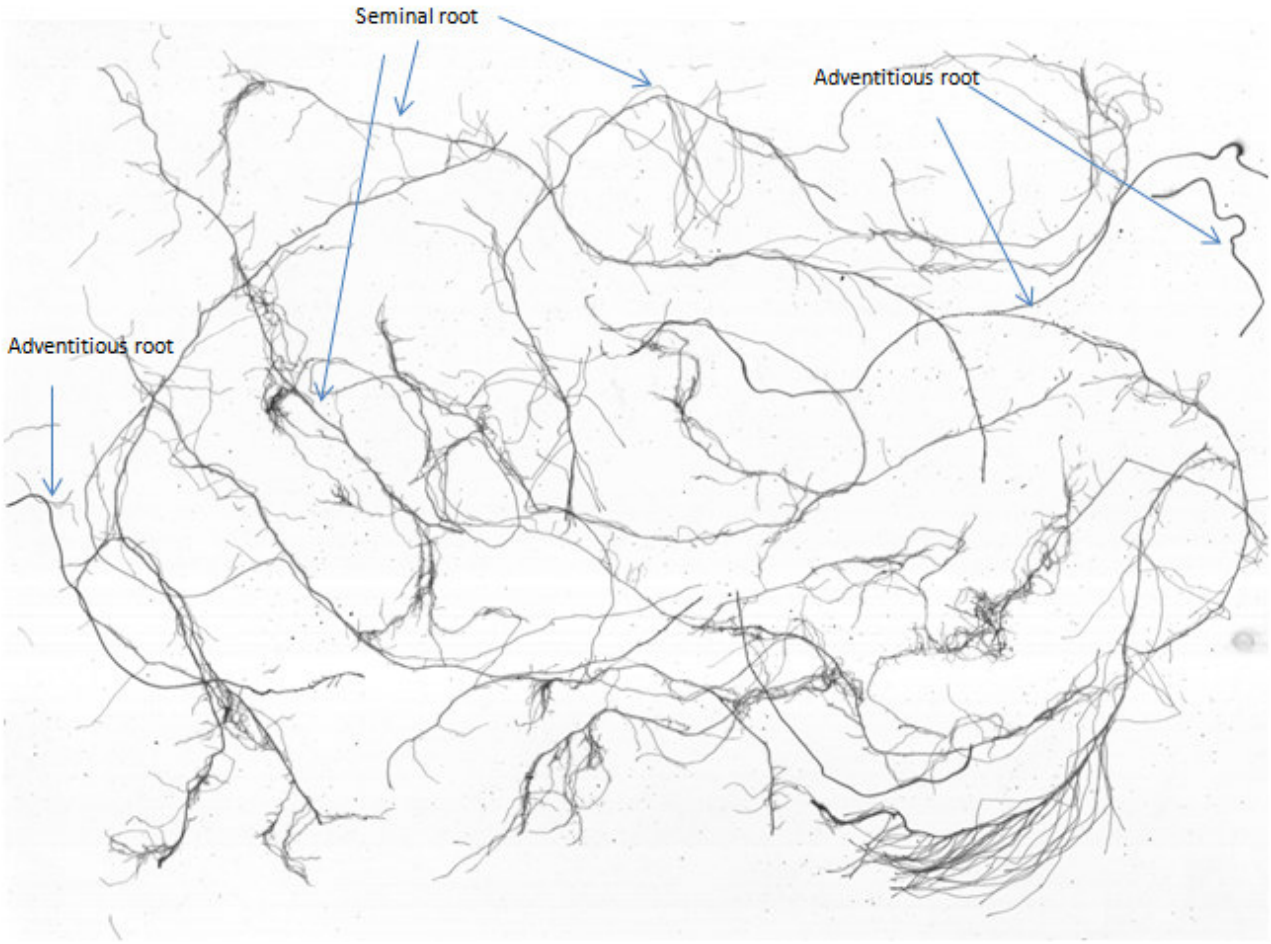

Figure 3.5. Example of root scan from a single barley plant at the 4 leaf stage, seminal roots (longest and branched) can be distinguished from adventitious roots (shorter, thicker and less branched). Seminal roots are the majority of harvested roots.

The obtained images were analized by winRHIZO (www.regentinstruments.com/assets/winrhizo_about.html) a software designed to analyze images and calculate the total root extension as a sum of lengths of primary and secondary roots. Total root extension of the three plants per pot was valuated per se and also divided by shoot dry weight of the three plants. ANOVAs were carried out on data collected with R software (The R development Core Team, 2008) considering genotypes and blocks as fixed factors. Heritability calculation were carried out with R software (The R development Core Team, 2008) as in previous chapter (paragraph 2.3.3) with the formula $h^2=\sigma^2g/(\sigma^2g+\sigma^2e)$ were σ^2g is the variance due to genotypes and σ^2e is the residual variance.

3.5 RESULTS AND DISCUSSION

Preliminary experiments were conducted first in the greenhouse and then in the growth room to identify a suitable developmental stage and protocol for analysis of the root system using rhizotrons (see materials and methods). Results from these trials (data not shown) led us to focus on the 4 leaf stage and substrate S3 (see materials and methods). To conduct an initial survey, we carried out a groth room experiment to analyse the root system of 31 genotypes with three replicates. Nine plants per genotype for a total of 279 plants were scanned and images were analyzed with winRHIZO software: results are summarized in Table 3.3.

Table 3.3. Mean, maxima, minima, standard deviations and heritability values of phenotypic traits are presented. Root extension is the sum of the length of primary and secondary roots of each replicate (three plants).

	Root extension (cm)	**Shoot dry weight (g)**	**Root extension/shoot dry weight (cm/g)**
Max	5156	0.56	17064.7
Min	1676	0.18	6298.
Average	3325	0.32	10611.5
St. dev.	765	0.07	2103.1
Heritabilty	75%	33%	25%

Root extension per se exhibited good heritability (75%), with a mean of 3325 cm, variation among blocks was also significant (ANOVA p-values was of 3.4×10^{-13} for blocks and 2×10^{-16} for genotypes). Looking at Figure 3.6 we can see that average root extension was increasing from block *a* to block *c*. Blocks have been sown and collected in three independent experiments: although the same settings were maintained for all three experiments the amount of irrigation water was not measured and may have varied leading to these differences among the blocks. Anyway whatever was the cause of variation between blocks, this was not a source of error: in Figure 3.6 we can see that for each genotype the root extension measured in block *a* < root extension in block *b*< root extension in block *c* (Figure 3.6 b), and the variance due to genotypes is higher than variance of error (Figure 3.6 b). This indicates that despite the variation among blocks there were homogeneous growth conditions across pots, and this may be due to the substrate S3 that we used. Thus finally we registered a good hereditability of 75%.

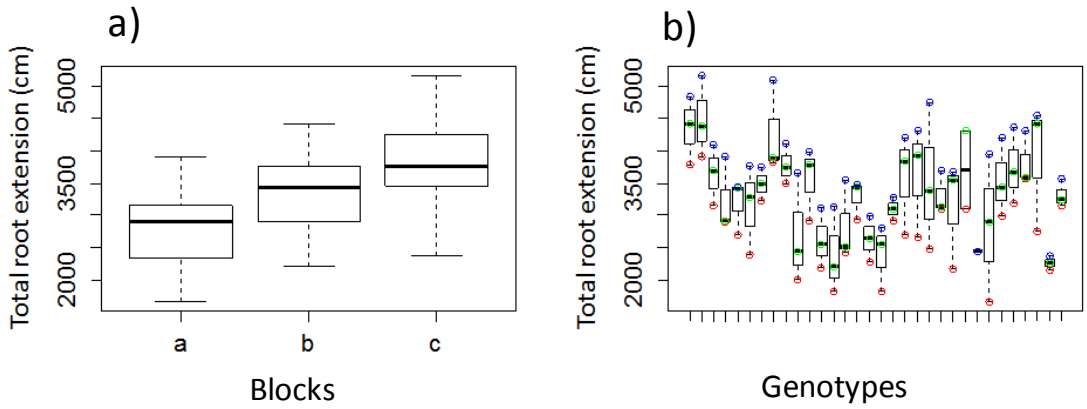

Figure 3.6. a) Box-plot of total root extension plotted on blocks. b) Box-plot of total root extension plotted on genotypes; data from blocks *a, b, c* are labeled with red, green, blue respectively.

In addition to evaluating root development per se, we were also interested in measuring the relative growth of shoot and root. Pearson correlation between shoot dry weight and root total extension was of 0.61 with a P-value of $4.6x10^{-11}$ (Figure 3.7). Shoot dry weight exhibited low heritability (25%), with a mean of 0.32 g (Table 3.3).

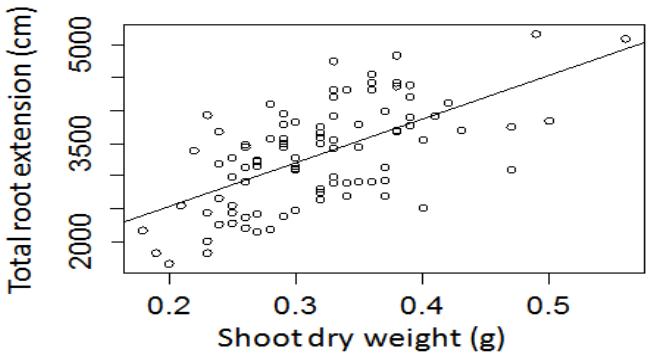

Figure 3.7. Correlation plot between total root extension and shoot dry weight.

We divided total root extension by shoot dry weight in order to get a general quantitative measure of the relative growth of shoot and root: for this trait the effect of blocks and genotypes were much less statistically significant compared to root extension per se (ANOVA p-values: 0.008 and 0.014 for blocks and genotypes respectively, Figure 3.8) and heritability was low, 22% (Table 3.3).

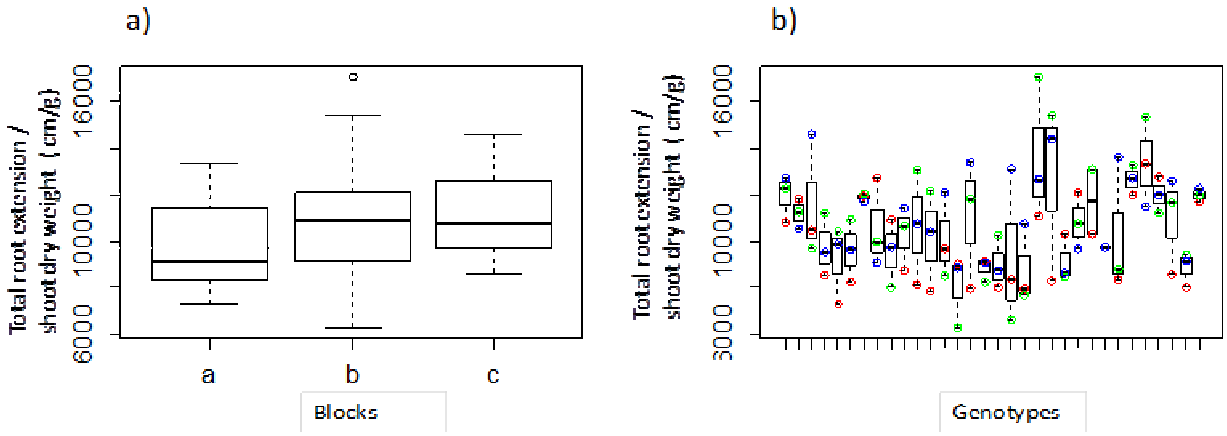

Figure 3.8. a) Box-plot total root extension divided by shoot dry weight plotted on blocks. b) Box-plot of total root extension divided by shoot dry weight plotted on genotypes; data from blocks *a, b, c* are labeled with red, green, blue respectively.

From analyses of the 31 genotypes subset we could conclude that:

- for total root extension there was an unexpected significant variability among blocks that likely indicates an uncontrolled factor of variation, possibly water input;
- nevertheless, variance explained by genotypes was much higher than error indicating that substrate S3 provides a good reproducibility of results;
- total root extension exhibited good heritability (75%);
- normalization of total root extension on shoot dry weight seems problematic (heritability 22%), probably due to the low heritability of shoot dry weight in these conditions;
- finally, these results should be considered preliminary and more work is needed to standardize the system to reduce variation among blocks and evaluate the usefulness of the data for detecting QTLs for root development at this early stages. Indeed, differences among genotypes could be also due to factors related the seed quality, e.g the seedling vigour.

An alternative approach would be to collect material at later stages, possibly at anthesis, when the genetic potential for root and shoot development is fully expressed and genotypes could be compared for their distribution of resources between root and shoot, maybe through a simple measure of root and shoot dry weight.

Anyway, despite some shortcomings, we developed a easy to manage and reproducible protocol to phenotype root extension in barley. More variability may be uncovered by exploring wild barleys (*Hordeum vulgare* spp. *spontaneum*) or landraces.

4. MORPHOLOGICAL CHARACTERIZATION OF *mnd6.6*, A BARLEY HIGH TILLERING MUTANT

4.1 INTRODUCTION

Previous chapters were dedicated to the evaluation and dissection of natural genetic variation for morphological traits in a winter barley germplasm panel. Results from GWAS on shoot traits (Chapter 2) clearly show that different developmental and morphological characters are correlated and major genes with pleiotropic effects on multiple traits can mask effects of other genes. In addition to genetic factors, some phenotypes are strongly influenced by environmental factors. This was particularly true for tillering, whose variability was lowly genetically heritable and was associated to major row-type loci (Paragraph 2.4.2). Indeed, tillering is known to be affected by environmental conditions such as plant density/light quality, and nutrient availability (Evers, 2006; Umehara et al., 2008; Whipple et al., 2011; Alam et al., 2014) and such factors likely complicated genetic dissection of this trait in our field experiment on the winter barley panel. Conversely, in the past decade genetic studies of tillering have been accelerated by the analysis of high- and low-tillering Mendelian mutants, especially in rice (Hussien et al., 2014). In barley, a number of tillering mutants are known and few of the corresponding genes have been identified (see Introduction Chapter 3). In particular, previous studies have focused on characterization of reduced-tillering mutants such as *uniculm2* (*cul2*), *low number of tillers1* (*lnt1*), *absent lower laterals* (*als*), *uzu* (Lundqvist and Franckowiak, 1996; Chono, 2003; Babb and Muehlbauer, 2003; Pozzi et al., 2003; Bilgic et al., 2007; Dabbert et al., 2009; Okagaki et al., 2013) and indicated that multiple pathways are involved in tiller bud formation and outgrowth. Despite this progress, understanding of the ontogenetic basis of tillering phenotypes is still limited in barley, especially in the case of mutants exhibiting increased tiller numbers.Compared to wild-type, barley *many-noded dwarf* (*mnd*) mutants *mnd.f*, *mnd.h*,*mnd5.g* (unmapped, Druka et al., 2011), *mnd.4e*, *mnd6.6* (position 96.6 cM on POPSEQ allelic,chromosome 5HL,Mascher et al 2014), *mnd3.d* (3H; Druka et al., 2011) and *mnd1.a* (4HL , Druka et al., 2011) are characterized by higher number of leaves produced per culm, increased tillering and a reduced height-

For example, field-grown *mnd1.a* plants exhibit about 1/2 normal height with numerous tillers. Each tiller has 12 to 20 small leaves and a spike of 1/2 normal size or less. Additional tillers with 4 to 7 leaves may develop from the uppermost culm nodes. When grown in the greenhouse, plants are taller than normal sibs and each tiller may have 15 to 20 nodes. The rate of leaf primordium initiation is normal, but their expansion into leaves is much more rapid (Lundqvist and Franckowiak, 1996).

Mutants at the *mnd6.6* locus have on average twice as many leaves than wild-type plants as a result of a faster leaf emergence.. Despite the larger number of internodes (8-9 in the mutant versus 4-5 in the wild-type), mutant plant height was reduced by about one third under field conditions, while in green-house grown plants height was equal between mutant and wild type (Mascher et al., 2014). The *mnd6.6* mutant was associated to the complete deletion of the *HvMND* gene, cloned by Mascher et al., (2014) using a mapping-by-sequencing approach In the same study, the *mnd4.e* mutant was shown to harbour a non-synonymous mutation of the same gene (Druka et al., 2011; Mascher et al., 2014).

HvMND encodes a member of the CYP78A family of cytochrome P450 enzymes. Four other *CYP78A* genes were found in the whole genome shotgun assembly of barley (Mascher et al., 2014). *CYP78A* genes are expressed in various plant tissues with different genes of the family being most abundant in different tissues. Among the four barley *CYP78A* genes, *HvMND* was the most ubiquitous, being expressed in embyo, seedling roots, seedling shoots, young developing inflorescence, developing inflorescence, early stages of developing grains, although only weak expression was detected in developing grains 15 days after anthesis (Mascher et al., 2014). In vitro studies indicated that CYP78A enzymes catalyze the hydroxylation of fatty acids (Imaishi et al., 2000; Kai et al., 2009). Plants synthesize many fatty acid derivatives, several of which act as signaling molecules such as jasmonic acid (Weber, 2002) . Nevertheless the reactions catalyzed by CYP78A genes and the regulatory pathways governing their activity are largely unknown (Mizutani and Ohta, 2010).

The rice *pla1* mutant phenotype is very similar to *mnd* mutant and the *PLA1* gene shares 54% amino acid sequence identity with *HvMND* (Mascher et al., 2014). Nevertheless, *PLA1* is not the orthologue of *HvMND*: the orthologue of *HvMND* in rice, Os09g09g3594, is located in a syntenic

region on rice chromosome 9 (Mayer et al., 2011) and shows 75% identity with HvMND ot the protein level. PLA1 does not have a clear orthologue in barley (Mascher et al., 2014).

In rice *plastochron1* mutants accelerated emergence of vegetative leaves leads to twice as many leaves compared with wild-type siblings (Itoh et al., 1998). The large number of leaves of *pla1* plants was a consequence of rapid leaf initiation because the duration of the vegetative phase was almost equal in *pla1* and wild-type plants. The SAM of *pla1* plants was enlarged due to an enhanced divisions but leaf size and plant height were reduced to about half of that of the wild type.

The *pla1* mutation also caused alterations in panicle development in the reproductive phase. In the strongest allele *pla1-1* many primordia of primary rachis branches (inflorescence branches) were converted into vegetative shoots that in turn produced panicles. In the weak allele *pla1-2*, proximal primary branch primordia developed into vegetative shoots with abnormally elongated bracts; and the remaining primordia formed a small panicle in which rachis internodes and branches were truncated at extremities. (Miyoshi et al., 2004).

In situ hybridization analysis showed that *PLA1* is expressed in leaf founder cells, but not in the SAM.

In the first youngest leaf primordium, expression was detected at the leaf margin and the abaxial side of the proximal region that later differentiated into the sheath (Miyoshi et al., 2004). In the second youngest leaf primordia *PLA1* mRNA was localized at the leaf margin and the abaxial side of the basal leaf region, *PLA1* expression was restricted to the lamina joint just above the blade-sheath boundary. *PLA1* expression was also detected in early reproductive phase (Miyoshi et al., 2004). In rice, after transition to reproductive growth, the young inflorescence meristem produces several primary rachis branches with bracts at the base in a spiral phyllotaxis (Itoh et al., 2005). Later spikelets are formed by other small branch meristems, while bracts growth ceases (Itoh et al., 2005). In young inflorescence apices, *PLA1* expression was detected in developing bract leaves and their primordia before their emergence but not in the rachis and primary rachis branch meristems. In addition *PLA1* expression was detected in rachis internodes.

Members of the *CYP78A* family may act in the same physiological pathway as *Arabidopsis ALTERED MERISTEM PROGRAM 1* (*AMP1*) and homologous rice gene *PLASTOCHRON3*. *AMP1* and *PLA3* encode a glutamate carboxypeptidases: *Arabidopsis* mutants show pleiotropic phenotypes such as a shortened plastochron, aberrant meristem programs, and early flowering (Helliwell et al., 2001) and rice mutants exhibit shorter plastochron (Komatsu et al., 2001) . Phylogenetic analyses have shown that CYP78A enzymes have evolved in *Triticeae* differently respect to rice and maize and suggested that *HvMND* may have taken over the functions of a lost ortholog of rice *PLA1* and Arabidopsis *CYP78A7*; this supports the hypothesis that several CYP78A enzymes act in the same physiological pathway and may catalyze similar biochemical reactions (Mizutani and Ohta, 2010).

While the cited studies established a link between plastochron (intervening period between sequential leaf primordium formation) duration and tiller development, the ontogenetic events leading to increased tillering in these mutants are still unclear, especially in barley.

4.2 OBJECTIVE

Objective of the present chapter was to carry out a detailed morphological characterization of the *mnd6.6* mutant in order to gain insight into the developmental progression leading to the high-tillering phenotype in barley. I carried out the experiments presented in this chapter at the Max Planck Institute for Plant Breeding Research (MPIZ, Cologne, Germany), in the framework of a collaboration between our laboratory and the group of Dr. Maria von Korff.

4.3 MATERIAL AND METHODS

4.3.1 GENETIC MATERIAL

The *mnd6.6* mutant derives from ethylene imine mutagenesis of the Bonus genotype: it was isolated by U. Lundqvist and then introgressed into the Bowman two-rowed cultivar in a window of 11 cM (Druka et al., 2011). For our experiments we compared this *mnd6.6* introgression (GSHO 2235) line with the Bowman background (PI 483237) (genetic stocks from MPIZ germplasm collection).

Initial phenotyping analyses were carried out on mutant and wild-type plants grown outdoors in large pots, scoring for number of culm and plant height. A more detailed morphological dissection was carried out on plants grown in a controlled growth chamber.

4.3.2 GARDEN EXPERIMENT

Twenty-four wild type and *mnd6.6* plants were germinated in mid February 2014 in small pots (5x8x10 cm, one seed per pot) in the greenhouse. About 1-2 weeks after germination, seedlings were transferred to an outdoors garden (MPIZ, Cologne, Germany). After six weeks (end of March 2014), plants were transplanted to individual 12 L pots filled with organic soil. Tiller number was counted at anthesis (7-11 June 2014, Zadocks stage 68, Zadocks et al., 1974)). Growing plants and tillering scoring at anthesis was carried out by MPIPZ staff. At harvesting stage (4 August 2014) tiller number was registered again on 13 plant per genotype, along with plant height and number of elongated internodes of the three tallest culms .

4.3.3 GROWTH CHAMBER EXPERIMENT

Plants were grown individually in pots (5 x 8 x 10 cm) filled with organic soil. After sowing, pots were kept for 3 days at 4°C (to ensure uniform germination), and then transferred to a growth chamber with 16 h of light at 20°C and 8 h of dark at 18°C.

Starting from 5 days after emergence (DAE), 5 plants per genotype were dissected every 3-4 days (until 30 DAE) and every 7 days until anthesis.

The traits registered were:

- main shoot apex Waddington stage (WS) (Waddington et al., 1983).
- number of leaves per each vegetative axis,
- number of axillary buds per each vegetative axis,
- number of tillers (this term include also “tillers” developed from nodes that were elevated above the crown level) arising from each vegetative axis, independently by their stage. We distinguished between primary (arising from main stem), secondary (arising from primary tillers) and tertiary (arising from secondary tillers).
- number of elongated internodes on main culm and tillers (for tillers it was measured only in the last two dissections),

The Waddington scale is a quantitative scale of development from seedling emergence (0) to pollination (10) based on the morphogenesis of the spike initial, then the floret and finally the

pistil (Waddington et al., 1983). This scale allows to quantify developmental progress of the shoot apex without involving any attribute of growth or size of the plant or its organs (Table 1).

Table 1. The Waddington scale (Waddington et al.,1983)

Stage	Description	Stage	Description
1	Transition apex (vegetative stage)	6	Stylar canal remaining as a narrow opening
1.5	Early double ridge stage (trasition to reproductive stage)	6.5	Styles promoninent
2	Double ridge stage (spiklet primordia are visible)	7	Styles elongating
2.25	Triple mound present (the 3 spikelet primordia are visible)	7.5	Stigmatic branches just differentiating
2.5	Glume primordium present	8	Stigmatic branches elongating
3	Lemma floret primordium present	8.5	Hairs non ovary wall just differentiating
3.5	Stamen primordium present	8.75	Stigmatic branches and hairs on ovary wall elongating
4	Pistil primordium present	9	
4.5	Carpel primordium present	9.25	Styles and stigmatic branches erect
5	Carpel extending rounf three sides of ovule	9.5	Styles and stigmatic branches spreading
5.5	Stylar canal closing	10	Pollination

As we scored plants also after pollination, we arbitrarily added 2 stages: the start of caryopsis filling (stage 11) and anthesis (stage 12).

Dissection consisted in separating tillers from the main stem and removing leaves one by one counting axillary buds. The main shoot apex was examined under a Leica stereo-microscope and photographs were taken by a JVC digital camera mounted on the stereoscope. Since plants had to be destructed to carry out these analyses, data from different developmental time-points came from different individuals.

4.3.4 DATA ANALYSES

Collected data were analyzed with R software (The R development Core Team, 2008). To verify if the development of mutant and wild-type were significantly different we developed linear models or step-wise linear models (where the genotypes were the fixed factors, the WS was the covariate, and traits were the dependent variables) performing analyses of covariance (ANCOVA); when we detected a significant interaction between genotypes and WS (different slopes) or a significant difference between genotypes (different intercepts) we considered the two regressions as significantly different.

4.4 RESULTS

4.4.1 OVERALL PHENOTYPES OF *mnd6.6* MATURE PLANTS

Figure 4.1 depicts Bowman and *mnd6.6* plants from our garden experiment at anthesis stage.

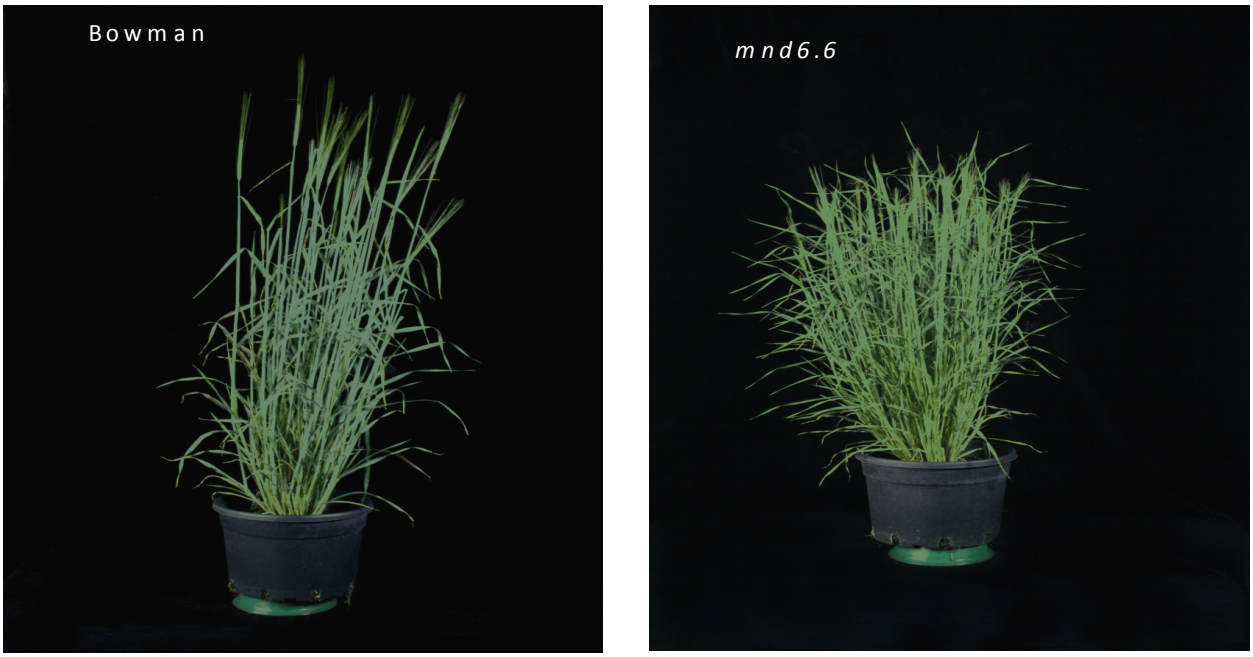

Figure 4.1. Bowman and *mnd6.6* plants at anthesis. (Image courtesy of MPIZ)

At this stage, number of productive and unproductive tiller (including also developed "tillers" from nodes that were elevated above the crown level, below) differed significantly in the two genotypes (ANOVA p-value: 9.15×10^{-7}): the mutant exhibited an average of 68 tillers(standard deviation=12), while Bowman had an average of 40 tillers(standard deviation= 7). At harvesting time, Bowman plants exhibited on average 102 tillers, significantly fewer (ANOVA p-value: 3.23×10^{-13}) than *mnd6.6* plants with an average of 308 tillers. In both genotypes there was an increase in tillering between anthesis and harvesting stage, and this difference was consistently higher in *mnd6.6* as tillering increased on average 4.8 fold, while in Bowman it increased 2.5 fold (ANOVA p-value: 2×10^{-6}).

Bowman plants were significantly taller (ANOVA p.value: 2×10^{-16}) than *mnd6.6*, with an average of 103 and 72 cm respectively.

When the tallest culms where examined, Bowman plants exhibited 6 elongated internodes, compared to 7 elongated internodes in *mnd6.6*.

Moreover in mnd6.6 was observed but not quantified a consistent number of tillers arising from nodes elevated above the crown level,

4.4.2 DEVELOPMENTAL ANALYSIS OF THE HIGH-TILLERING PHENOYPE OF THE *mnd6.6* MUTANT

In order to examine in detail the developmental progression that leads to the *mnd6.6* high-tillering phenotype, mutant and wild-type Bowman plants were grown under controlled conditions in a growth room and apical and axillary development were scored at different time points. A total of 67 plants per genotype were dissected, spanning almost the whole plant cycle (from the one leaf stage until anthesis, approximately 58 days).

Apex developmental rate

No significant difference in apex developmental rate (ANCOVA p-value: 0.21 for difference between genotypes and ANCOVA p-value: 0.15 for interaction genotypes-WS) was registered between the *mnd6.6* mutant and the wild type (Figure 4.2). The double ridge stage (WS 2) - marking the transition to the reproductive phase- was reached by *mnd6.6*, and Bowman at 12 DAE: at this stage the shoot apex stops producing leaves and becomes an inflorescence meristem where spikelet primordia can be seen. Both genotypes reached pollination stage (WS 10) at around 51 DAE. At 58 DAE both lines exerted anthers (anthesis). These results show that the *mnd6.6* mutation does not affect the developmental rate of the shoot apex and the length of the vegetative phase.

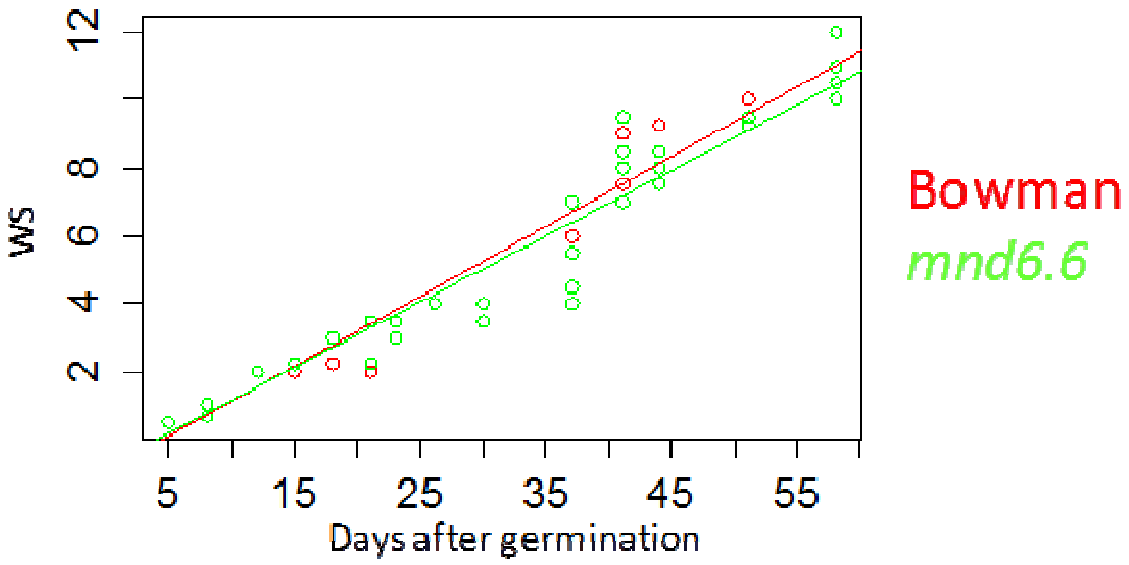

Figure 4.2 Shoot apex Waddington stage (WS) plotted against the days after germination.

Total number of tillers

Differences in tiller number became evident from Waddington stage (WS) 3.5-4 (Figure 4.3), when the mutant exhibited more tillers than wild type (ANCOVA p-value of the difference between genotypes =1.64×10^{-7}, WS-genotype interaction p-value= 1.94×10^{-8}). The highest tiller number registered in *mnd6* was 22, plants dissected between WS 8 and anthesis (WS 12) had an average of 16 tillers. In Bowman the maximum number of tillers (18) was registered from an individual at WS 8, and the average tiller number for this genotype from WS 8 till anthesis was 11. After stage 8 the slope became negative, this is due to the fact that, last plant to be dissected were the less vigorous that were discarded to be dissected in the previous stages. In better condition we would expect in Bowman a plateau starting from WS 8.

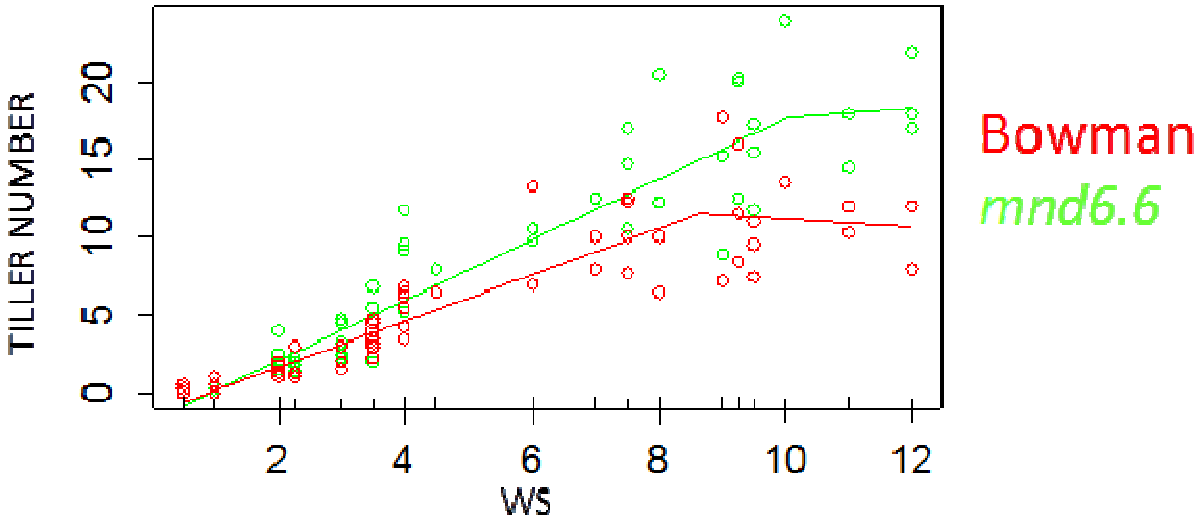

Figure 4.3. Number of tillers plotted on main shoot apex Waddington stage (WS).

Number of vegetative apices

In addition to counting tillers, we also recorded the total number of axillary buds per plant analyzed. Considering that each tiller derives from outgrowth of an axillary bud , the intensity of axillary development can be better described by a score (the number of shoot apices, NSA),which includes both axillary buds and shoot apices of growing tillers. Thus, NSA is the sum of number of tillers and axillary buds. Figure 4.4 shows that NSA is higher in *mnd6.6* compared to wild type (ANCOVA p-value of the difference between genotypes: $1x10^{-12}$, p-value of WS-genotype interaction: $1.49x10^{-8}$) starting from early stages. The maximum NSA (48) was reached by a *mnd6.6* individual at WS 8, while the average of mnd6.6 NSA was 35 from Waddington stage (WS 8) until anthesis.

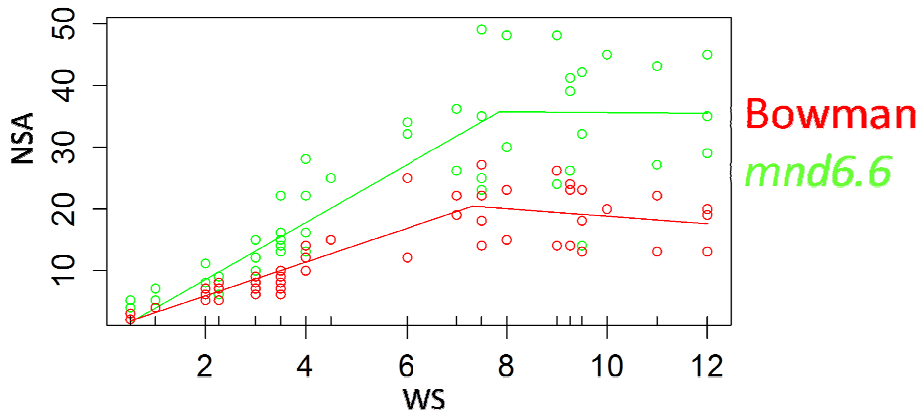

Figure 4.4. Total number of shoot apices (NSA) plotted on main shoot apex Waddington stage (WS).

After WS 8 a plateau was reached. In Bowman the highest NSA was 23 at WS 8, with an average of 19 NSA. From WS 8 the slope became negative; the reasons of the negative slopes as already explained before was probably due to the low vigor of the last plants analyzed: in better conditions we would expect an horizontal plateau starting from WS 8.

We further recorded the distribution of NSA (axillary buds + tillers) and tillers between primary (arising from main stem), secondary (arising from primary tillers) and tertiary (arising from secondary tillers). Results of this analysis show that the higher number of tillers and NSA in *mnd6.6* is due mostly to secondary and tertiary order branches (Figure 4.5). Obviously number of tillers and number of NSA are strictly connected. In fact, for a given stage n, the number tillers determines the number of axillary buds, and at stage n+1 the number of tillers depends on number of axillary buds present at stage n.

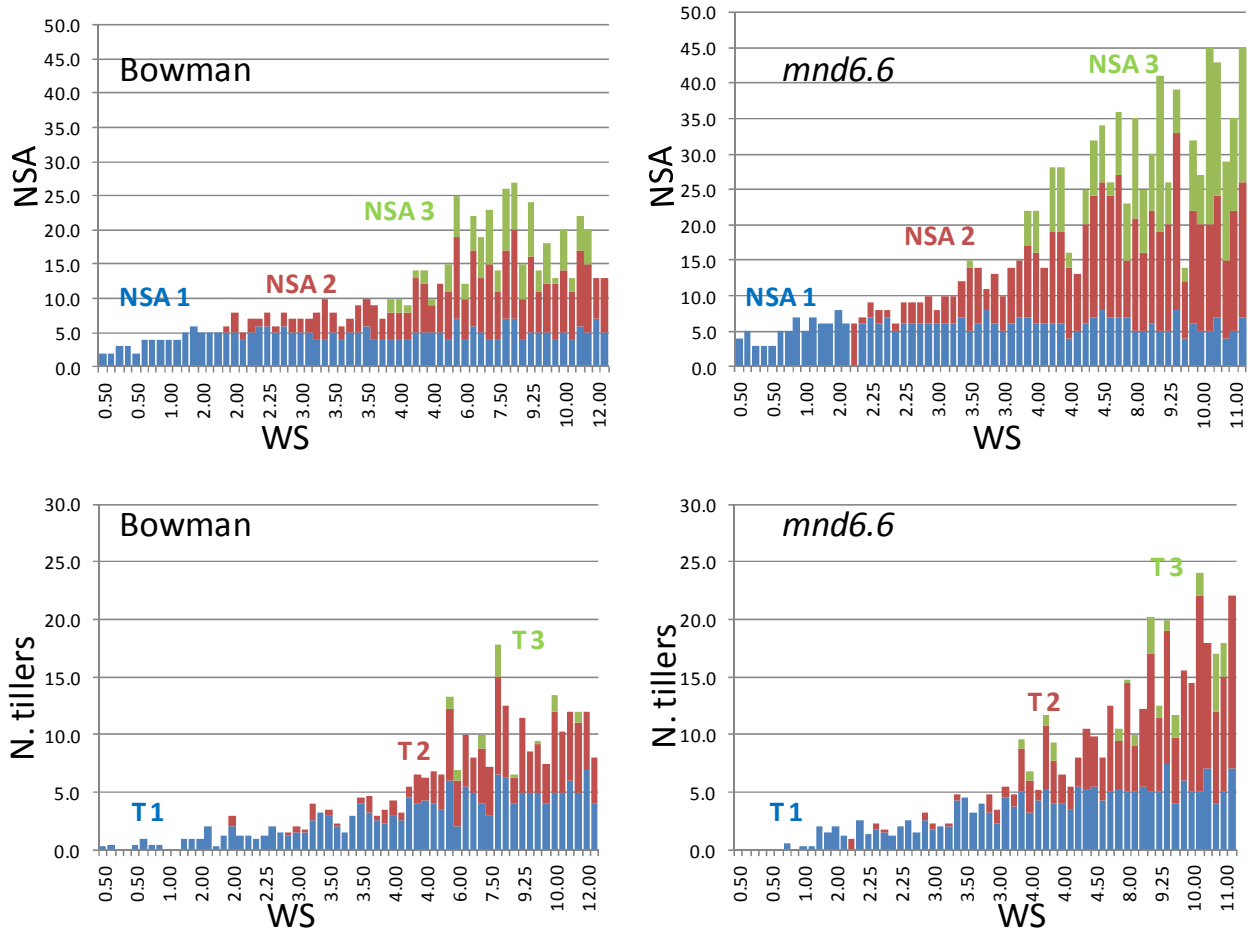

Figure 4.5. Number of tillers and vegetative apices plotted vs. WS. The amount in primary, secondary and tertiary tillers and vegetative apices is reported (explanation in the text). NSA1: number of primary shoot apices, NSA2: number of secondary shoot apices, NSA3: tertiary vegetative axes, T1: primary tillers, T2: secondary tillers, T3: tertiary tillers.

Number of leaves

Lateral buds giving rise to tillers and branches derive from secondary meristems formed in leaf axils and lateral bud development is tightly linked to leaf development (Oikawa and Kyozuka, 2009) For this reason, in parallel to quantification of axillary development, we also registered the number of leaves seen on each plant (Figure 4.6). Results show that *mnd6.6* mutant plants produce many more leaves than the wild type (ANCOVA p-value of genotypes-WS interaction: $2x10^{-16}$), consistent with the higher number of vegetative axes. In latest stages, 71 leaves were produced on average by *mnd6.6* plants, in contrast to 39 leaves in Bowman. To check how many leaves were produced per vegetative axis we counted the number of leaves produced from main stems.

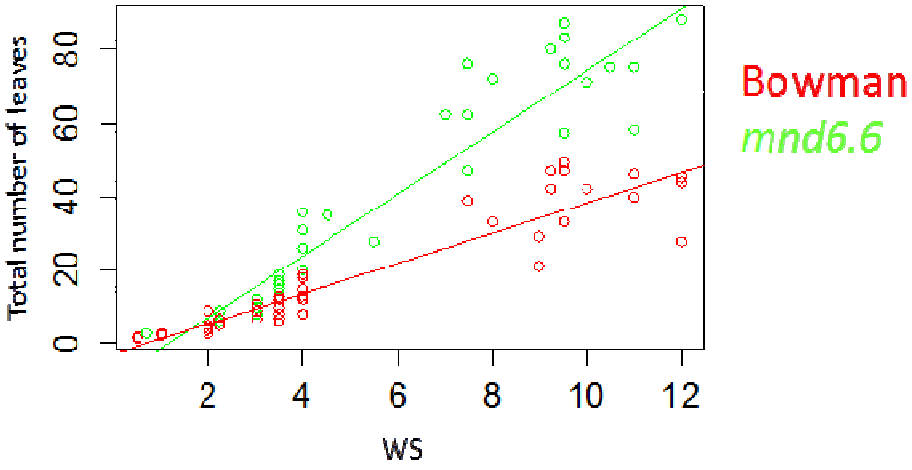

Figure 4.6. Total number of leaves plotted on main shoot apex Waddington stage (WS).

In Figure 4.7 the number of leaves per main stem is plotted against WS: both genotypes reached their maximum number of leaves at WS 7. Bowman had a maximum of 8-9 leaves , while *mnd6.6* maximum number was of 11-12.

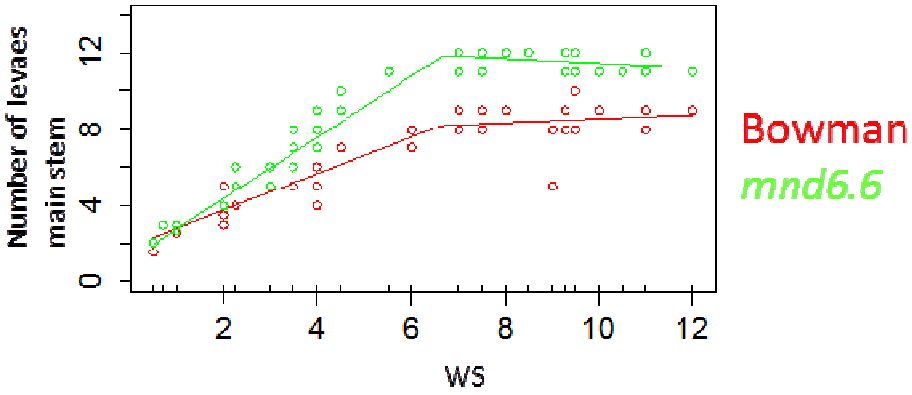

Figure 4.7. Number of on main stem leaves plotted on main shoot apex Waddington stage (WS).

This trend was also detected in tillers. We counted the number of leaves produced by the two main tillers in ten plants (per line) at latest stages: Bowman produced an average of 6 leaves from the first two tillers, while *mnd6.6* produced an average of 9 leaves (Figure 4.8).

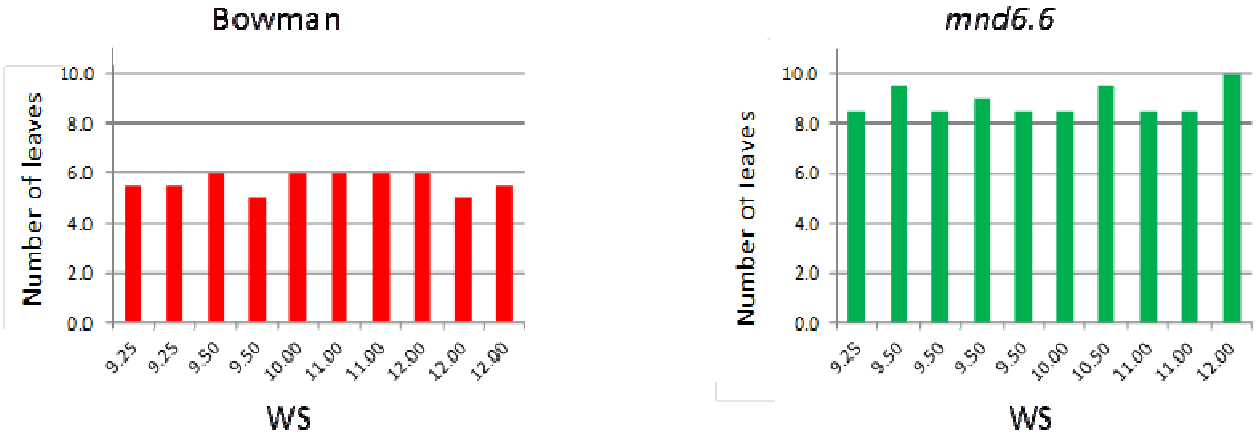

Figure 4.8 Individual average number of leaves produced by the two main tillers at latest stages, each column represent one individual, for wich individual WS is reported.

Together, these results indicate that the higher total number of leaves in *mnd6.6* plants is due to both a higher number of vegetative axes and a higher number of leaves produced from each vegetative axis. As the mutation does not affect the duration of the vegetative phase, we conclude that *mnd6.6* plants have a shorter phyllochron (intervening period between the sequential emergence of leaves) compared to Bowman. Approximate phyllochron could be calculated as inverse of the slope of the ascendant regression lines of main stem number of leaves regressed on DAE: 6.6 and 4.2 days were the calculated phyllocron of Bowman and *mnd6.6,* respectively.

Tillering in relation to leaf production

In principle, increased tillering in *mnd6.6* mutants could be explained by two alternative mechanisms: 1) *mnd6.6* and Bowman make the same number of buds per stem, but the proportion of buds which develops tillers is higher in the mutant; 2) the proportion of buds which develop tillers is equal among wild-type and mutant, but the mutant produces more buds per vegetative axis. The higher number of leaves present in *mnd6.6* culms suggests that the higher number of tillers is linked to the increased number of axils, consistent with the second hypothesis.

To check if this is really the case, we estimated the ratio of axillary buds that grow into tillers by dividing the total number of tillers by the total NSA and we plotted these scores against WS (Figure 4.9). If the first hypothesis were true, we would expect this ratio to be higher in *mnd6.6*.

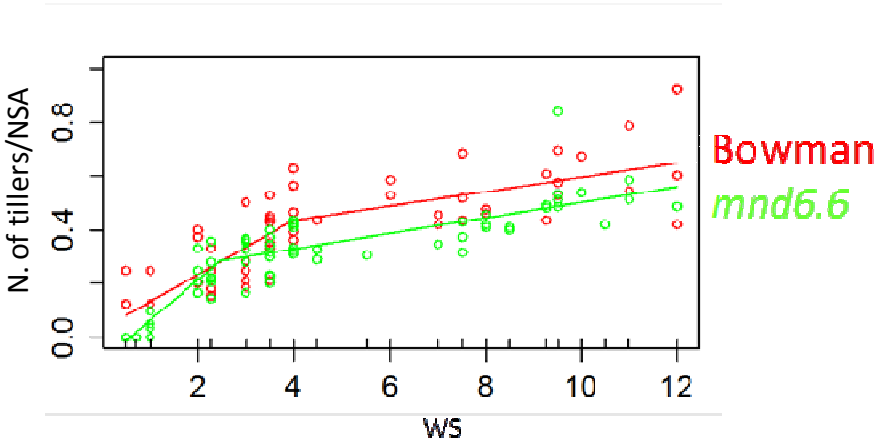

Figure 4.9 Proportion of total number of tillers on total number of vegetative apices.

Contrary to this hypothesis, the ratio is actually higher in Bowman (ANCOVA p-value=0.0008) (Figure 4.9).

Next, we divided the total NSA by the total number of leaves and plotted it against WS. As can be seen in Figure 4.10, the proportions NSA on the number of leaves during all plant development (except the early stages, where genotype-WS interaction is significant p-value:0.03) are almost same in Bowman and *mnd6.6* (the ANCOVA p-value of difference between genotypes of 0.16).

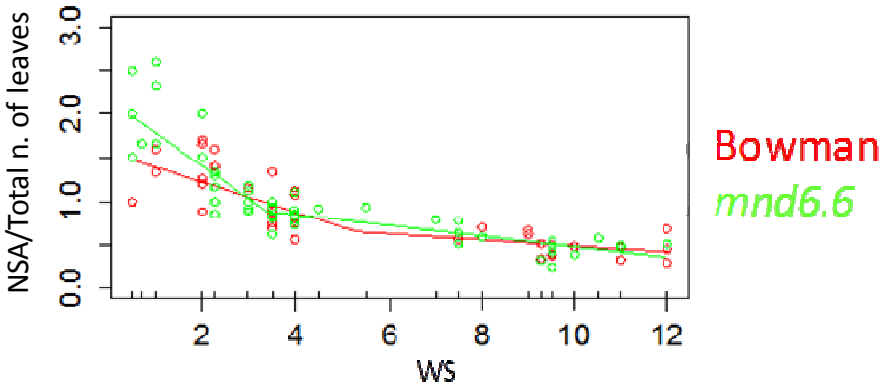

Figure 4.10 Proportion of Total number of vegetative apices on total number of leaves, plotted on Waddington stage.

Finally, we divided the number of tillers by the number of leaves (ie axils) and plotted this ratio against WS. Results show that this proportion is slightly higher in Bowman (ANCOVA p-value for difference between genotypes equal to 1.5×10^{-8}) along all the plant cycle (Figure 4.11), confirming that the higher number of tillers in *mnd6.6* is correlated to the higher number of leaf axils.

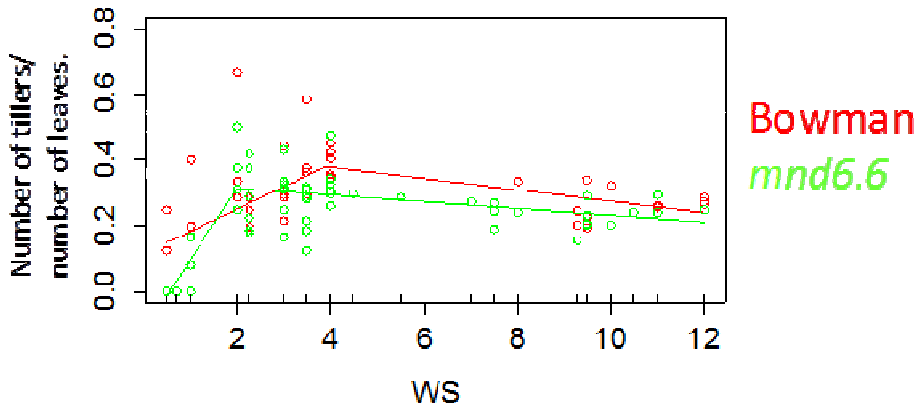

Figure 4.11. Proportion of total number of tillers on total number of leaves, plotted against Waddington stage.

In summary, the higher number of tillers in *mnd6.6* is not due to increased tiller outgrowth, but rather is associated to a higher number of axillary buds deriving from the increased number of leaf axils present in the mutant. This effect is reinforced by the iterative pattern of tiller formation: once a new axis of growth is established, it produces more leaves and more buds and so on. This is reflected in the increased number of secondary and tertiary tillers observed in *mnd6.6* plants. Thus, the high-tillering phenotype of *mnd6.6* plants is at least in part a consequence of shorter phyllochron duration.

Stem elongation

In the garden experiment, we observed significant differences in plant height between *mnd6.6* and Bowman. In order to better characterize this aspect of the mutant phenotype, we measured the number of elongated internodes of main stem and regressed it on WS, finding a consistent difference (ANCOVA p-value for genotype-WS interaction: $3x10^{-10}$) between the two genotypes (Figure 4.12). Stem elongation began in both lines between WS 3 and WS 4: based on regression slope we estimated for *mnd6.6* a 0.9 increase in number of elongated internodes per Waddington stage, while in Bowman the increase was of 0.6. At later stages the average number of elongated internodes in ten plants was of 7.6 in *mnd6.6* and 5.5 in Bowman. At anthesis, average plant

height of *mnd6.6* (42 cm) was inferior then that of Bowman plants (52 cm) consistent with results from the garden experiment.

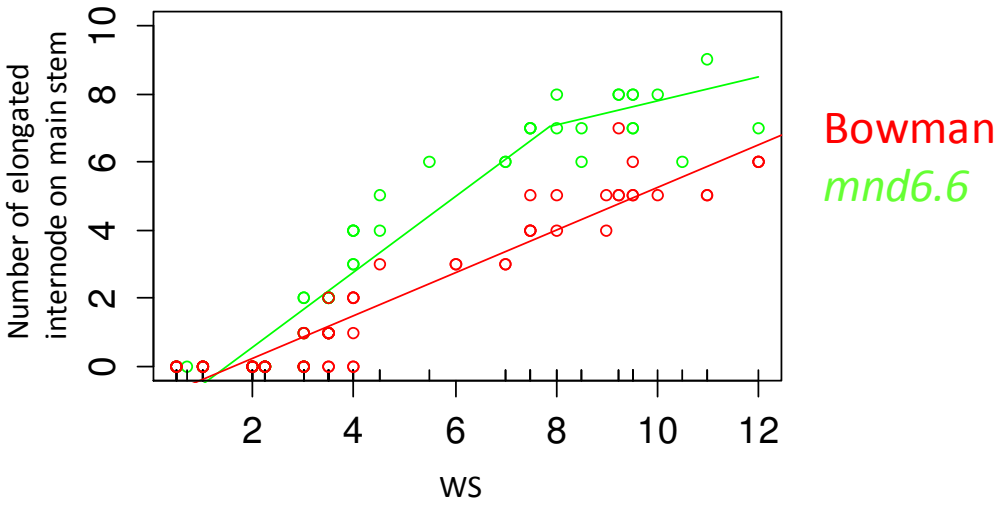

Figure 4.12. Number of elongated internodes on main stem plotted against Waddington stage.

Tiller outgrowth from nodes above the crown

In later WS stages, *mnd6.6* plants developed "tillers" also from nodes that were elevated above the crown level. To quantify this phenotype, we scored the NSA ("tiller"+axillary bud) and number of "tillers", arising from these "aerial nodes" (nodes inserted at the top of internodes elongated more than 1 cm). We took this measurement only at the last time-point, so only 5 plant per genotype were scored, nevertheless results were quite clear: in *mnd6.6* over an average total of 10 shoot apices (SA) per plant inserted at aerial nodes, an average 6 of the 10 shoot apices were tiller. In bowman only in two plants, two and one tiller from aerial nodes were detected (Figure 4.13).

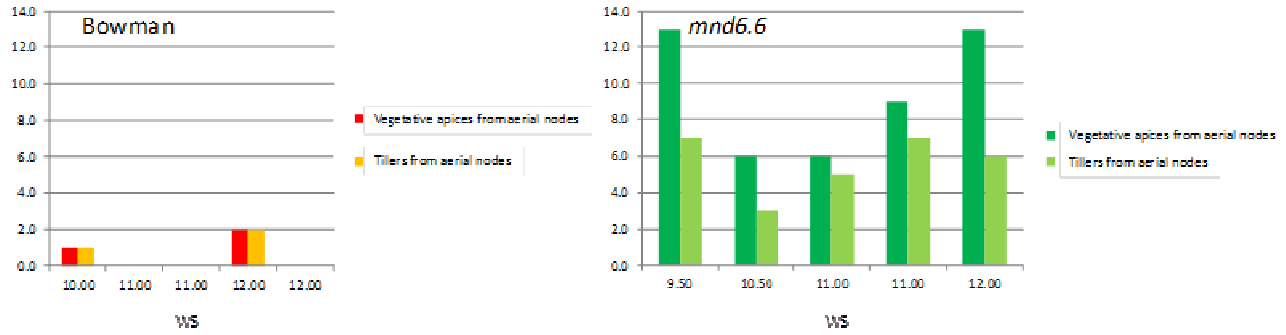

Figure 4.13. Number of vegetative apices and "tillers" developed from aerial nodes, on five Bowman and five *mnd6.6* plants. Waddington stage of the plants is reported.

"Secondary" spikes

During dissection, from WA 3.5-4 we started to detect the presence of an inflorescence branch or "secondary" spike primordium, arising from the first node of the rachis in place of spikelets (Figure 4.14). This phenotype appeared in 50% of *mn6.6* plants, also in tillers, and in some cases two "secondary spikes" appeared from first and second rachis node. These "secondary" spike primordia developed fertile spikes that often were carried on a very short internode with a small leaf or a bract at the base (Figure 4.15).

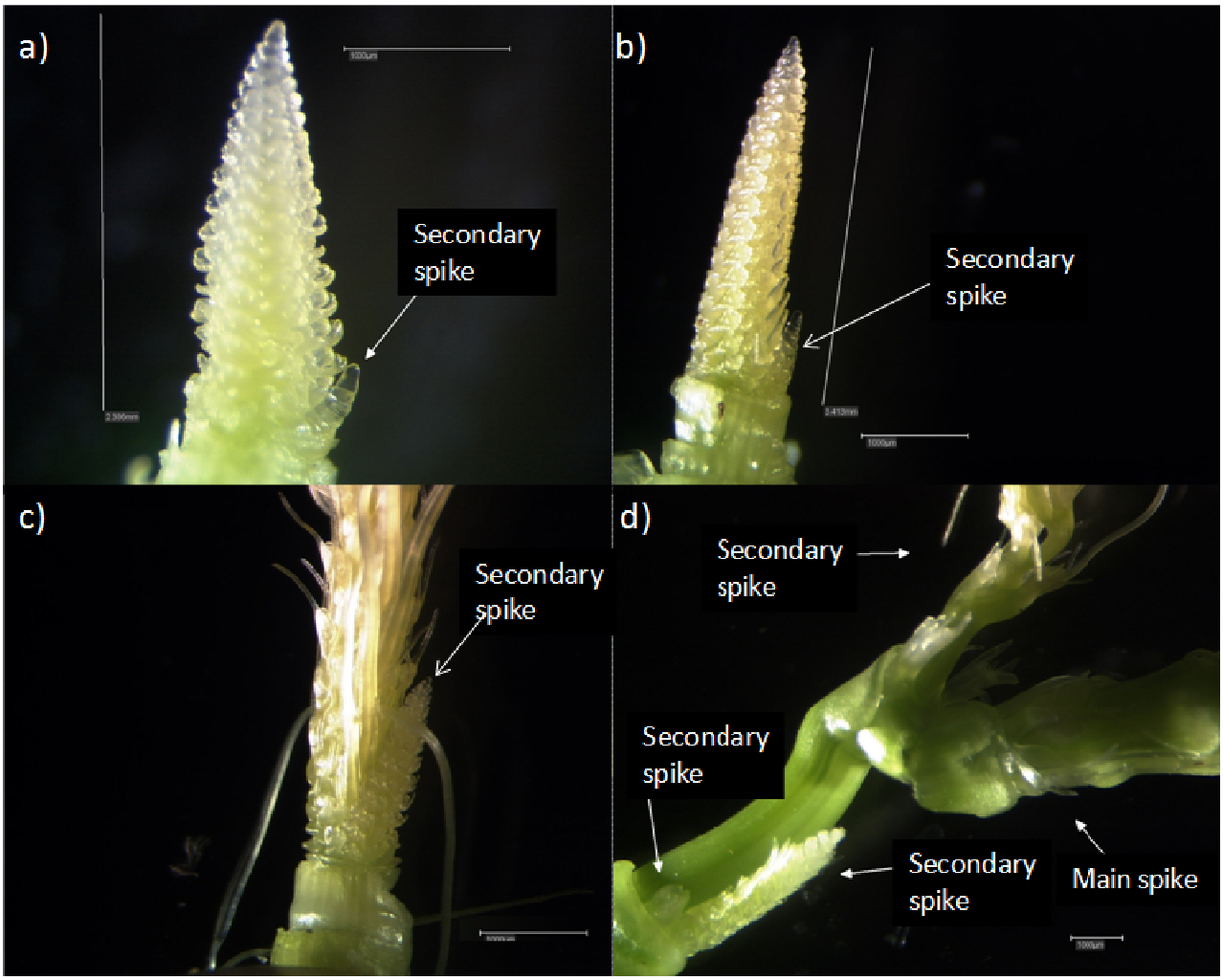

Figure 4.14. Formation of "secondary spikes" from first nodes of spike primordia.a) the main spike is at WS 4, while "secondary" spike is at WS 0.5. b) main spike at WS 5, "secondary" spike at WS 3. c) main spike at WS 7.5, "secondary" spike at WS 4. d) main spike at WS 9.5 with three "secondary" spikes at WS 7, 5 and 1.

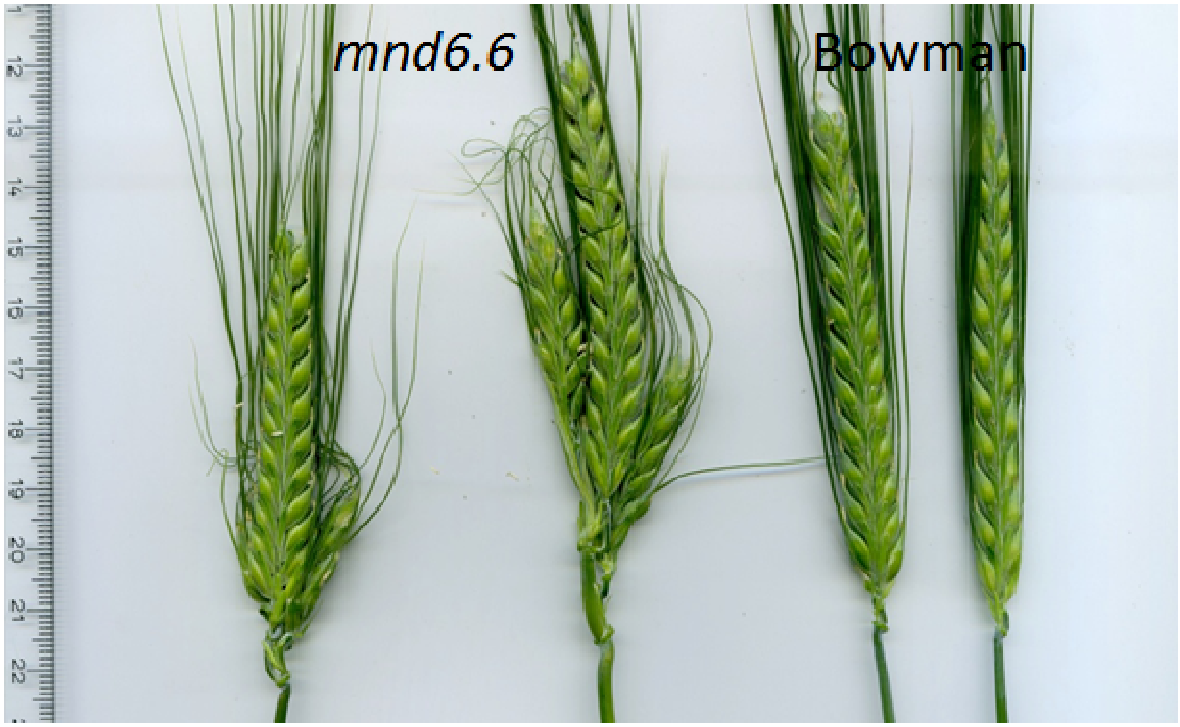

Figure 4.15. Branched inflorescences with "secondary" spikes in *mnd6.6*, compared with Bowman.

4.4 DISCUSSION

Results from the garden and growth chamber experiments were consistent, although obviously plants grown outdoors in big pots over a longer period were much more developed than plants grown in the growth chamber in small pots under long photoperiod. Dissection of *mnd6.6* and Bowman development from the first leaf stage through to maturity showed a marked increase in the number of axillary buds in the mutant giving rise to elevated tiller numbers. This overproduction of axillary buds was associated with increased numbers of leaves produced on culms as a result of shorter phyllochron.We measured phyllochron (intervening period between the sequential leaf emergence) but not plastochron (intervening period between sequential leaf primordium formation). Nevertheless we guess that the two measurements should be proportional, also because maximum main stem leaf number was reached at the same time by *mnd6.6* and Bowman. Thus, our results confirm the similarity between barley *mnd6.6* and *pla1* in rice, as both mutants exhibit accelerated leaf production, and a consequent increase in leaf and tiller numbers, with unaltered vegetative period duration.

In this work we demonstrated that augmented tillering in *mnd6.6* is due to an increased number of axillary buds, but the proportion of axillary bud on leaf axils is not altered in mutants, and the higher number of buds is proportional to higher number of leaves. Together with *mnd6.6* increased leaf number, also an increased number of elongated internodes was detected. It seems that reduced phyllochron correlates with a general de-repression of vegetative growth that also lead to the frequent develop of axillary buds (and then tillers) from aerial nodes. This mechanism may apply to other mutants that exhibit increased numbers of leaves and tillers, such as barley *mnd-1* and *gra.a*.

Similarities between *pla-1* and *mnd6.6* extend also to reproductive organs. In *pla-1* mutants, primordia of primary rachis branches (inflorescence branches) were converted into vegetative shoots that in turn produced panicles; in *mnd6.6*, branching at basal rachis nodes.

Together, these results indicate that *HvMND* plays a role in repressing axillary development.

The relation between number of leaves have been already found in barley natural variation, (Kirby et al., 1985) dissected the develop of 13 winter barley cultivar and 9 wheat spring and winter cultivars grown in field in normal agronomic condition, they found that both in barley and wheat the main shoot leaf number at which tillering ceased was correlated with total number of leaves on the main shoot. They postulated that rate of tillering could vary with rate of leaf production and that genetic variation in rate of leaf production could be used to predict and select for different tillering patterns. Instead in sorghum, a significant negative correlation was found between tillering and leaf size, but no correlation was found between tillering and phyllochron (Alam et al., 2014). Miyamoto et al., (2004) in a population of recombinant inbred line found that three phyllochron QTLs coincided to the two major QTLs for tillering number.

The relation between phyllocron and tillering has agronomic implications. For example, early plant vigour (fast leaf area development) is an important adaptation of barley and durum wheat to terminal drought in Mediterranean environments (van Oosterom and Acevedo, 1992; López-Castañeda and Richards, 1994) because it limits water losses by evaporation from soil surface and encourage growth, when evaporative demand is low. Early plant vigour could be achieved by shortening phyllochron, but this may have pleiotropic effects and result in increased tillering whose benefits would have to be evaluated.

5. CONCLUSIONS

Root and shoot architecture traits are key factors in plant performance, competition with weeds, adaptation and stress responses thus having an important impact on yield and yield stability. In formulating cereal ideotypes, breeders proposed hypothetical optimal morphological parameters that were modelled in relation to different environmental conditions.

Understanding and manipulation of morphological traits is key in view of breeding improved crops for future agriculture.

The objective of this project was to explore genetic variation for a number of root and shoot architecture traits in barley to identify and characterize genomic regions or genes controlling these traits and understand how different traits are influencing each other.

To this end, two approaches were undertaken: the first exploits natural variation in a panel of modern and old European barley cultivars through an association mapping approach (Chapters 2 and 3); the second was to characterize the ontogenetic basis of increased tillering in the *mnd6* high tillering barley mutant (Chapter 4).

To study root architecture we performed greenhouse and growth-chamber experiments using field soil and sand as substrate, respectively. The first aim was to measure differences in relative growth of shoots and roots, and then get more detailed data on root architecture, e.g. maximum length, branching, total extension of secondary roots, with a view to dissecting genetic variation for these traits through association mapping. Root extension was measured by scanning of the root system and image analyses. Root extension per se exhibited a good heritability, indicating the reproducibility of results, but this was not true for shoot dry weight that exhibited a low heritability. Consequently also dry root extension normalized on shoot dry weight exhibited a low heritability. Results showed some limitations inherent to our approach: due to the limited development of the analyzed plants that were collected in early stages, we could not detect significant genetic variation in the relative growth of roots with respect to shoots. Possibly genetic variability for root/shoot development could be more evident when measured at the stage of maximum root and shoot development (anthesis); while this would exclude precise phenotyping through image analyses, because of the difficulties of extricating and scanning the whole root system, simple measures could be taken e.g. dry weight and maximum length that may be associated to phenotypic variation. In any case, the protocol developed for root phenotyping in

the growth-room experiment gave reproducible results and may be used for further experiments on more genetically diverse germplasm (e.g. *Hordeum vulgare* spp. *spontaneum*, landraces). The substrate used (sand supplemented with control release fertilizer) ensures both homogeneous growing conditions (due to the constant density of sand and uniform fertilizing) and easiness of root extraction.

Analysis of shoot architecture traits based on field phenotyping data showed good heritability for most traits except for tillering. A major QTL determining flowering date, leaf length, leaf width and spike length was associated with *Ppd-H1*, a gene involved in photoperiod response. Minor associations to flowering date and spike length were detected for three markers linked to the *HvCEN* gene, also related to flowering date independently from photoperiod. An additional minor association for leaf width was found with one marker mapping at 110 cM on chromosome 4H. These results highlight that the two genes related to flowering date (especially *Ppd-H1*) had strong pleiotropic effects on morphological traits that could have masked other minor effects. Based on correlation of leaf size with flowering date, we tested a GWAS model where flowering date was used as covariate, finding two new significant associations for leaf length: a minor association on chromosome 7H (position 70.6 cM), and a more significant association on chromosome 5H (47.5-50 cM), in a region hosting a mutant locus causing reduced leaf dimensions. This result provides preliminary support for the usefulness of this approach.

Plant height variation was associated to a marker mapped on 5H, 44.5 cM.

Row-type defined the population structure in our winter barley panel. As already described in the literature, row-type was correlated to several plant architecture traits. In fact tillering and the number of fertile rachis nodes (NFRN) were found to be associated to the *INT-C* gene (one of the two main genes responsible for row type). We then tried to correct for row-type pleiotropic effects using this trait as covariate in GWAS. With this model we detected an association of NFRN to a group of markers lying on chromosome 7H (position 67.9 cM): these markers were also recovered by Alqudah et al., (2014) as associated to the duration of the phase between awn primordia formation and tipping (awn arising from flag leaf), supporting the validity of our covariate analysis.

Tillering is a plastic trait, regulated by a complex network of genetic and environment factors, and in previous works on natural variation, the amount of phenotypic variation explained by genetic

variance was small (Hayes et al., 1993; Baum et al., 2003). Also in our experiment tillering was the trait, which exhibited the lowest heritability. In our GWAS tillering was associated only to the *INT-C* gene, consistent with established knowledge that two-rowed varieties produce more tillers than six-rowed.

To circumvent the limited power of the GWAS approach for this trait and understand more about the mechanisms subtending tiller formation, we dissected the morphological development of the high tillering *mnd6.6* mutant, comparing it to that of the wild-type (Chapter 4). Results show that the mutant is not altered in timing of apical meristem development and differentiation to spike, but has a shorter phyllochron that leads to an increment in the number of leaves per vegetative axis. This in turn results in a higher number of axillary buds and a higher number of tillers. It seem that there is a general de-repression of vegetative growth that also lead to the outgrowth of axillary buds and tillers from aerial nodes.

Overall, results from this PhD project allow us to draw some conclusions regarding both a strictly scientific and a breeding perspective. Firstly, few QTLs were detected that explain the phenotypic variation for our morphological traits, with some major genes having strong pleiotropic effects that mask minor genetic effects. The use of traits that appear to influence other measures as covariates in GWAS models also seems to be a promising approach, even if the statistical power of this strategy is still to be evaluated. Germplasm collections with uniform growth habit and row-type are an attractive alternative to prevent confounding effects and allow additional loci to be detected. A second aspect concerns the phenotyping approach: in Chapter 2 we measured for example the largest leaves of each plant based on the reasoning that in this way we could measure the genetic potential of each genotype and leaf size traits showed good heritability, but this strategy might have some consequences. For a given culm, the largest leaf was the one below the flag leaf, the second last to be formed: our results indicate that the timing of elongation of this leaf depend on timing of flowering (as demonstrated by correlation between flowering date and leaf dimension and the QTLs for leaf width and length corresponding to *Ppd-H1*), our hypothesis is that leaf elongation ceases with flowering. The first leaves at the base of the plant reach their maximum dimension long before flowering date (in field they are already dried at flowering date) and the two traits would not correlate. Thus phenotyping for dimension of first leaves formed at early stages may prevent detection of pleiotropic effect of flowering date related genes allowing the detection of new QTLs. Moreover based on the correlation we found between phyllochron and

tillering, phenotyping for early plant vigour would also elucidate more about the complex genetic control of tillering.

Much was speculated about the narrow genetic base of modern cultivars (Fischbeck, 2003; Rostoks et al., 2006). While significant genetic variation was identified for various traits within the gene pool of our winter barley collection variability of morphological traits as leaf dimension was subordinated to the length of vegetative period. Indeed, flowering date is one of the major factors on which breeding practice has worked to adapt barley to different environments. Beyond modern European varieties, barley breeding for new ideotypes should explore wider genetic resources as was done by IRRI (International Rice Research Institute) for breeding of the rice New Plant Type (Peng et al., 2008). Ongoing international projects are in fact dedicated to the exploration of genetic variability from *Hordeum* spp. *spontaneum* or landraces using genomic approaches to identify new potentially useful alleles. In any case, the existence of correlations between different phenotypes calls for careful evaluation of sources of traits to avoid undesired effects on other traits.

REFERENCES

Abdallah JM, Goffinet B, Cierco-Ayrolles C, Pérez-Enciso M (2003) Linkage disequilibrium fine mapping of quantitative trait loci: a simulation study. Genet Sel Evol GSE **35**: 513–532

Abdurakhmonov IY, Abdukarimov A (2008) Application of Association Mapping to Understanding the Genetic Diversity of Plant Germplasm Resources. Int J Plant Genomics **2008**: 1–18

Agusti J, Greb T (2013a) Going with the wind--adaptive dynamics of plant secondary meristems. Mech Dev **130**: 34–44

Agusti J, Greb T (2013b) Going with the wind--adaptive dynamics of plant secondary meristems. Mech Dev **130**: 34–44

Alam MM, Hammer GL, van Oosterom EJ, Cruickshank AW, Hunt CH, Jordan DR (2014) A physiological framework to explain genetic and environmental regulation of tillering in sorghum. New Phytol **203**: 155–167

Alqudah AM, Schnurbusch T (2014) Awn primordium to tipping is the most decisive developmental phase for spikelet survival in barley. Funct Plant Biol **41**: 424

Alqudah AM, Sharma R, Pasam RK, Graner A, Kilian B, Schnurbusch T (2014) Genetic Dissection of Photoperiod Response Based on GWAS of Pre-Anthesis Phase Duration in Spring Barley. PLoS ONE **9**: e113120

Ando T, Yamamoto T, Shimizu T, Ma XF, Shomura A, Takeuchi Y, Lin SY, Yano M (2008) Genetic dissection and pyramiding of quantitative traits for panicle architecture by using chromosomal segment substitution lines in rice. Theor Appl Genet **116**: 881–890

Atsmon D, Jacobs E (1977) A Newly Bred “Gigas” Form of Bread Wheat (Triticum aestivum: Morphological Features and Thermo-photoperiodic Responses1. Crop Sci **17**: 31

Autran D, Jonak C, Belcram K, Beemster GTS, Kronenberger J, Grandjean O, Inzé D, Traas J (2002) Cell numbers and leaf development in Arabidopsis: a functional analysis of the STRUWWELPETER gene. EMBO J **21**: 6036–6049

Babb S, Muehlbauer GJ (2003) Genetic and morphological characterization of the barley uniculm2 (cul2) mutant. TAG Theor Appl Genet Theor Angew Genet **106**: 846–857

Backes G, Graner A, Foroughi-Wehr B, Fischbeck G, Wenzel G, Jahoor A (1995) Localization of quantitative trait loci (QTL) for agronomic important characters by the use of a RFLP map in barley (Hordeum vulgare L.). Theor Appl Genet **90**: 294–302

Balding DJ (2006) A tutorial on statistical methods for population association studies. Nat Rev Genet **7**: 781–791

Baldoni R, Giardini L (2000) Coltivazioni erbacee. Cereali e proteaginose. Pàtron

Bao, Shen, Brady, Muday, Asami, Yang (2004) Brassinosteroids interact with auxin to promote lateral root development in Arabidopsis. Plant Physiol **134**: 1624– 1631

Barber J (2009) Photosynthetic energy conversion: natural and artificial. Chem Soc Rev **38**: 185–196

Barraclough PB, Kuhlmann H, Weir AH (1989) The Effects of Prolonged Drought and Nitrogen Fertilizer on Root and Shoot Growth and Water Uptake by Winter Wheat. J Agron Crop Sci **163**: 352–360

Bates D, Maechler M, Bolker B, Walker S (2013) lme4: Linear mixed-effects models using Eigen and S4.

Baum M, Grando S, Backes G, Jahoor A, Sabbagh A, Ceccarelli S (2003) QTLs for agronomic traits in the Mediterranean environment identified in recombinant inbred lines of the cross "Arta" × H. spontaneum 41-1. Theor Appl Genet **107**: 1215–1225

Bellini C, Pacurar DI, Perrone I (2014) Adventitious roots and lateral roots: similarities and differences. Annu Rev Plant Biol **65**: 639–666

Benjamini Y, Hochberg Y (1995) Controlling the False Discovery Rate: A Practical and Powerful Approach to Multiple Testing. J R Stat Soc Ser B Methodol **57**: 289–300

Bezant J, Laurie D, Pratchett N, Chojecki J, Kearsey M (1996) Marker regression mapping of QTL controlling flowering time and plant height in a spring barley (Hordeum vulgare L.) cross. Heredity **77**: 64–73

Bilgic, Cho, Heinenen, Muehlbauer (2007) Genetics of the reduced tillering barley mutants Uniculm2 (Cul2), Uniculm4 (Cul4) And A Tillering Suppressor (Suc2). Plant Anim. Genomes XV Conf.

B

Blum A (1988) Plant breeding for stress environments. CRC Press, Boca Raton, Fla

Booker J, Auldridge M, Wills S, McCarty D, Klee H, Leyser O (2004) MAX3/CCD7 Is a Carotenoid Cleavage Dioxygenase Required for the Synthesis of a Novel Plant Signaling Molecule. Curr Biol **14**: 1232–1238

Borém A, Mather DE, Rasmusson DC, Fulcher RG, Hayes PM (1999) Mapping Quantitative Trait Loci for Starch Granule Traits in Barley. J Cereal Sci **29**: 153–160

Borner A, Korzun V (1996) Genetical studies of two barley mutants differing intheir GA response. Barley Genet Newsl **25**: 27–29

Borràs-Gelonch G, Slafer GA, Casas AM, van Eeuwijk F, Romagosa I (2010) Genetic control of pre-heading phases and other traits related to development in a double-haploid barley (Hordeum vulgare L.) population. Field Crops Res **119**: 36–47

Bose RD, Dixit PD (1930) IndianJ. agric. Sci., I, 90-108. Indian J Agron Sci 90–108

Bossinger G, Rhode W, Lundqvist U, Salamini F (1992) Genetics of Barley Development: Mutant Phenotypes and Molecular Aspects. Barley Genet. Biochem. Mol. Biol. Biotechnol. P. R. Shewry (ed) C.A.B International Wallingford, Oxon OX108DE, UK, pp 231–263

Bothmer R von, Fischbeck G, eds (2003) Diversity in barley: (Hordeum vulgare), 1st ed. Elsevier, Amsterdam; Boston

Bradbury PJ, Zhang Z, Kroon DE, Casstevens TM, Ramdoss Y, Buckler ES (2007) TASSEL: software for association mapping of complex traits in diverse samples. Bioinformatics **23**: 2633–2635

Braulio J, Cloutier S (2012) Association Mapping in Plant Genomes. Genet. Divers. Plants

Breseghello F, Sorrells ME (2006) Association mapping of kernel size and milling quality in wheat (Triticum aestivum L.) cultivars. Genetics **172**: 1165–1177

Breuer C, Ishida T, Sugimoto K (2010) Developmental control of endocycles and cell growth in plants. Curr Opin Plant Biol **13**: 654–660

Briggs DE (1978) The morphology of barley; the vegetative phase. Barley. Springer Netherlands, pp 1–38

Brown LK, George TS, Thompson JA, Wright G, Lyon J, Dupuy L, Hubbard SF, White PJ (2012) What are the implications of variation in root hair length on tolerance to phosphorus deficiency in combination with water stress in barley (Hordeum vulgare)? Ann Bot **110**: 319–328

Caldwell KS, Russell J, Langridge P, Powell W (2006) Extreme population-dependent linkage disequilibrium detected in an inbreeding plant species, Hordeum vulgare. Genetics **172**: 557–567

Campoli C, Drosse B, Searle I, Coupland G, von Korff M (2012a) Functional characterisation of HvCO1, the barley (Hordeum vulgare) flowering time ortholog of CONSTANS. Plant J **69**: 868–880

Campoli C, Pankin A, Drosse B, Casao CM, Davis SJ, von Korff M (2013) HvLUX1 is a candidate gene underlying the early maturity 10 locus in barley: phylogeny, diversity, and interactions with the circadian clock and photoperiodic pathways. New Phytol **199**: 1045–1059

Campoli C, Shtaya M, Davis SJ, von Korff M (2012b) Expression conservation within the circadian clock of a monocot: natural variation at barley Ppd-H1 affects circadian expression of flowering time genes, but not clock orthologs. BMC Plant Biol **12**: 97

Chandler PM, Marion-Poll A, Ellis M, Gubler F (2002) Mutants at the Slender1 Locus of Barley cv Himalaya. Molecular and Physiological Characterization. Plant Physiol **129**: 181–190

Chaudhury AM, Letham S, Craig S, Dennis ES (1993) amp1 - a mutant with high cytokinin levels and altered embryonic pattern, faster vegetative growth, constitutive photomorphogenesis and precocious flowering. Plant J **4**: 907–916

Chen WY, Liu ZM, Deng GB, Pan ZF, Liang JJ, Zeng XQ, Tashi NM, Long H, Yu MQ (2014) Genetic relationship between lodging and lodging components in barley (Hordeum vulgare) based on unconditional and conditional quantitative trait locus analyses. Genet Mol Res **13**: 1909–1925

Chen X, Min D, Yasir TA, Hu Y-G (2012) Genetic Diversity, Population Structure and Linkage Disequilibrium in Elite Chinese Winter Wheat Investigated with SSR Markers. PLoS ONE **7**: e44510

Chhun T, Taketa S, Tsurumi S, Ichii M (2003) Interaction between two auxin-resistant mutants and their effects on lateral root formation in rice (Oryza sativa L.). J Exp Bot **54**: 2701–2708

Chmielewska B, Janiak A, Karcz J, Guzy-Wrobelska J, Forster BP, Nawrot M, Rusek A, Smyda P, Kedziorski P, Maluszynski M, et al (2014) Morphological, genetic and molecular characteristics of barley root hair mutants. J Appl Genet **55**: 433–447

Chono M (2003) A Semidwarf Phenotype of Barley uzu Results from a Nucleotide Substitution in the Gene Encoding a Putative Brassinosteroid Receptor. PLANT Physiol **133**: 1209–1219

Clark L, Fisher K (1988) Vegetative morphology of grasses. Grass Syst. Evol., Smithsonian Institution Press. Barkworth ME, Washington DC, USA, pp 37–45

Close TJ (2004) A New Resource for Cereal Genomics: 22K Barley GeneChip Comes of Age. PLANT Physiol **134**: 960–968

Close TJ, Bhat PR, Lonardi S, Wu Y, Rostoks N, Ramsay L, Druka A, Stein N, Svensson JT, Wanamaker S, et al (2009) Development and implementation of high-throughput SNP genotyping in barley. BMC Genomics **10**: 582

Cockram J, Chiapparino E, Taylor SA, Stamati K, Donini P, Laurie DA, O'Sullivan DM (2007) Haplotype analysis of vernalization loci in European barley germplasm reveals novel VRN-H1 alleles and a predominant winter VRN-H1/VRN-H2 multi-locus haplotype. Theor Appl Genet **115**: 993–1001

Cockram J, White J, Leigh FJ, Lea VJ, Chiapparino E, Laurie DA, Mackay IJ, Powell W, O'Sullivan DM (2008) Association mapping of partitioning loci in barley. BMC Genet **9**: 16

Cockram J, White J, Zuluaga DL, Smith D, Comadran J, Macaulay M, Luo Z, Kearsey MJ, Werner P, Harrap D, et al (2010) Genome-wide association mapping to candidate polymorphism resolution in the unsequenced barley genome. Proc Natl Acad Sci **107**: 21611–21616

Comadran J, Kilian B, Russell J, Ramsay L, Stein N, Ganal M, Shaw P, Bayer M, Thomas W, Marshall D, et al (2012) Natural variation in a homolog of Antirrhinum CENTRORADIALIS contributed to spring growth habit and environmental adaptation in cultivated barley. Nat Genet **44**: 1388–1392

Cosgrove DJ (2005) Growth of the plant cell wall. Nat Rev Mol Cell Biol **6**: 850–861

Coudert Y, Périn C, Courtois B, Khong NG, Gantet P (2010) Genetic control of root development in rice, the model cereal. Trends Plant Sci **15**: 219–226

Crespi M, ed (2012) Root genomics and soil interactions. John Wiley & Sons, Hoboken, N.J

Dabbert T, Okagaki RJ, Cho S, Boddu J, Muehlbauer GJ (2009) The genetics of barley low-tillering mutants: absent lower laterals (als). Theor Appl Genet **118**: 1351–1360

Danyluk J, Kane NA, Breton G, Limin AE, Fowler DB, Sarhan F (2003) TaVRT-1, a Putative Transcription Factor Associated with Vegetative to Reproductive Transition in Cereals. Plant Physiol **132**: 1849–1860

Distelfeld A, Li C, Dubcovsky J (2009) Regulation of flowering in temperate cereals. Curr Opin Plant Biol **12**: 178–184

Doebley JF, Gaut BS, Smith BD (2006) The Molecular Genetics of Crop Domestication. Cell **127**: 1309–1321

Doebley J, Stec A, Hubbard L (1997) The evolution of apical dominance in maize. Nature **386**: 485–488

Doley M. (1983) Aliometric relationships in spring barley. Univ. of Minnesota, St. Paul

Donald CM (1968) The breeding of crop ideotypes. Euphytica **17**: 385–403

Döring H-P, Lin J, Uhrig H, Salamini F (1999) Clonal analysis of the development of the barley (Hordeum vulgare L.) leaf using periclinal chlorophyll chimeras. Planta **207**: 335–342

Doust AN, Kellogg EA (2006) Effect of genotype and environment on branching in weedy green millet (Setaria viridis) and domesticated foxtail millet (Setaria italica) (Poaceae). Mol Ecol **15**: 1335–1349

Drew MC (1975) COMPARISON OF THE EFFECTS OF A LOCALISED SUPPLY OF PHOSPHATE, NITRATE, AMMONIUM AND POTASSIUM ON THE GROWTH OF THE SEMINAL ROOT SYSTEM, AND THE SHOOT, IN BARLEY. New Phytol **75**: 479–490

Druka A, Franckowiak J, Lundqvist U, Bonar N, Alexander J, Houston K, Radovic S, Shahinnia F, Vendramin V, Morgante M, et al (2011) Genetic Dissection of Barley Morphology and Development. Plant Physiol **155**: 617–627

Dubcovsky J, Chen C, Yan L (2005) Molecular characterization of the allelic variation at the VRN-H2 vernalization locus in barley. Mol Breed **15**: 395–407

Duggan B, Richards RA, van Herwaarden A., Fettel NA (2005) Agronomic evaluation of a tiller inhibition gene (tin) in wheat. I. Effect on yield, yield components, and grain protein. Aust J Agric Res **56**: 169–178

Dunn GJ, Briggs KG (1989) Variation in culm anatomy among barley cultivars differing in lodging resistance. Can J Bot **67**: 1838–1843

Durack PJ, Wijffels SE, Matear RJ (2012) Ocean salinities reveal strong global water cycle intensification during 1950 to 2000. Science **336**: 455–458

Eapen D, Barroso ML, Ponce G, Campos ME, Cassab GI (2005) Hydrotropism: root growth responses to water. Trends Plant Sci **10**: 44–50

Eduardo I, Pacheco I, Chietera G, Bassi D, Pozzi C, Vecchietti A, Rossini L (2011) QTL analysis of fruit quality traits in two peach intraspecific populations and importance of maturity date pleiotropic effect. Tree Genet Genomes **7**: 323–335

Ehlers W, Kopke U, Hesse F, Bohm W (1983) Penetration resistance and root growth of oats in tilled and untilled loess soil. Soil Tillage Res **3**: 261–275

Ellis RP, Forster BP, Gordon DC, Handley LL, Keith RP, Lawrence P, Meyer R, Powell W, Robinson D, Scrimgeour CM, et al (2002) Phenotype/genotype associations for yield and salt tolerance in a barley mapping population segregating for two dwarfing genes. J Exp Bot **53**: 1163–1176

Evers JB (2006) Cessation of Tillering in Spring Wheat in Relation to Light Interception and Red: Far-red Ratio. Ann Bot **97**: 649–658

Fan J, Gunderson KL, Bibikova M, Yeakley JM, Chen J, Wickham Garcia E, Lebruska LL, Laurent M, Shen R, Barker D (2006) Illumina Universal Bead Arrays. Methods Enzymol **410**: 57–73

Farooq M, Kobayashi N, Ito O, Wahid A, Serraj R (2010) Broader leaves result in better performance of indica rice under drought stress. J Plant Physiol **167**: 1066–1075

Faure S, Turner AS, Gruszka D, Christodoulou V, Davis SJ, von Korff M, Laurie DA (2012) Mutation at the circadian clock gene EARLY MATURITY 8 adapts domesticated barley (Hordeum vulgare) to short growing seasons. Proc Natl Acad Sci **109**: 8328–8333

Fischbeck G (2002) Contribution of barley t o agriculture: a brief overview. Barley Sci., Food Products Press, Binghamton. Food Products Press, Binghamton, NY., New York, pp 1–14

Fischbeck G (2003) Diversity in barley: (Hordeum vulgare), 1st ed. Elsevier, Amsterdam; Boston

Fischer RA (2007) Understanding the physiological basis of yield potential in wheat. J Agric Sci **145**: 99

Fischer RA (2008) The importance of grain or kernel number in wheat: A reply to Sinclair and Jamieson. Field Crops Res **105**: 15–21

Fischer RA (1985) Number of kernels in wheat crops and the influence of solar radiation and temperature. J Agric Sci **105**: 447–461

Flint-Garcia SA, Thornsberry JM, Buckler ES (2003) Structure of linkage disequilibrium in plants. Annu Rev Plant Biol **54**: 357–374

Foley JA, Ramankutty N, Brauman KA, Cassidy ES, Gerber JS, Johnston M, Mueller ND, O/'Connell C, Ray DK, West PC, et al (2011) Solutions for a cultivated planet. Nature **478**: 337–342

Ford KE, Gregory PJ, Gooding MJ, Pepler S (2006) Genotype and fungicide effects on late-season root growth of winter wheat. Plant Soil **284**: 33–44

Forster BP, Franckowiak JD, Lundqvist U, Lyon J, Pitkethly I, Thomas WTB (2007) The Barley Phytomer. Ann Bot **100**: 725–733

Franckowiak JD (2000) Notes on plant height in six-rowed barley and FHB resistance. Barley Genet VIII Proc Eighth Int Barley Genet Symp **2**: 107–109

Fukaki H, Nakao Y, Okushima Y, Theologis A, Tasaka M (2005) Tissue-specific expression of stabilized SOLITARY-ROOT/IAA14 alters lateral root development in Arabidopsis. Plant J Cell Mol Biol **44**: 382–395

Fu X, Harberd NP (2003) Auxin promotes Arabidopsis root growth by modulating gibberellin response. Nature **421**: 740–743

Garris AJ (2004) Genetic Structure and Diversity in Oryza sativa L. Genetics **169**: 1631–1638

Garris AJ, McCouch SR, Kresovich S (2003) Population structure and its effect on haplotype diversity and linkage disequilibrium surrounding the xa5 locus of rice (Oryza sativa L.). Genetics **165**: 759–769

Geller GN, Smith WK (1982) Influence of leaf size, orientation, and arrangement on temperature and transpiration in three high-elevation, large-leafed herbs. Oecologia **53**: 227–234

Gladun I, Karpov E (1993a) Production and partitioning of as- similates between the panicle and vegetative organs of rice after flowering. Russ J Plant Physiol **40**: 728–773

Gladun I, Karpov E (1993b) Distribution of assimilates from the flag leaf of rice during the reproductive period of development. Russ J Plant Physiol **40**: 215–219

Goldstein DB, Weale ME (2001) Population genomics: linkage disequilibrium holds the key. Curr Biol CB **11**: R576–579

Gomez-Roldan V, Fermas S, Brewer PB, Puech-Pagès V, Dun EA, Pillot J-P, Letisse F, Matusova R, Danoun S, Portais J-C, et al (2008) Strigolactone inhibition of shoot branching. Nature **455**: 189–194

Gonzalez N, Vanhaeren H, Inzé D (2012) Leaf size control: complex coordination of cell division and expansion. Trends Plant Sci **17**: 332–340

Gonzalez-Rizzo S, Crespi M, Frugier F (2006) The Medicago truncatula CRE1 Cytokinin Receptor Regulates Lateral Root Development and Early Symbiotic Interaction with Sinorhizobium meliloti. PLANT CELL ONLINE **18**: 2680–2693

Grando S, Ceccarelli S (1995) Seminal root morphology and coleoptile length in wild (Hordeum vulgare ssp. spontaneum) and cultivated (Hordeum vulgare ssp. vulgare) barley. Euphytica **86**: 73–80

Gregory PJ (2006) Plant roots: growth, activity, and interaction with soils. Blackwell Pub, Oxford; Ames, Iowa

Gregory PJ, McGowan M, Biscoe PV, Hunter B (1978) Water relations of winter wheat: 1. Growth of the root system. J Agric Sci **91**: 91–102

Guan JC, Koch KE, Suzuki M, Wu S, Latshaw S, Petruff T, Goulet C, Klee HJ, McCarty DR (2012) Diverse roles of strigolactone signaling in maize architecture and the uncoupling of a branching-specific subnetwork. Plant Physiol **160**: 1303–1317

Gupta PK, Rustgi S, Kulwal PL (2005) Linkage disequilibrium and association studies in higher plants: Present status and future prospects. Plant Mol Biol **57**: 461–485

Gyenis L, Yun SJ, Smith KP, Steffenson BJ, Bossolini E, Sanguineti MC, Muehlbauer GJ (2007) Genetic architecture of quantitative trait loci associated with morphological and agronomic trait differences in a wild by cultivated barley cross. Genome Natl Res Counc Can Génome Cons Natl Rech Can **50**: 714–723

Hackett C (1969) A study of the root system of barley. II Relationship between root dimension and nitrient uptake. New Phytol **68**: 1023–1030

Hammer Ø, Ryan P, Harper D (2001) PAST: Paleontological Statistics software package for education and data analysis. Palaeontol Electron **4**: 9

Ha S, Vankova R, Yamaguchi-Shinozaki K, Shinozaki K, Tran L-SP (2012) Cytokinins: metabolism and function in plant adaptation to environmental stresses. Trends Plant Sci **17**: 172–179

Hayes PM, Liu BH, Knapp SJ, Chen F, Jones B, Blake T, Franckowiak J, Rasmusson D, Sorrells M, Ullrich SE, et al (1993) Quantitative trait locus effects and environmental interaction in a sample of North American barley germ plasm. Theor Appl Genet **87**: 392–401

Helliwell CA, Chin-Atkins AN, Wilson IW, Chapple R, Dennis ES, Chaudhury A (2001) The Arabidopsis AMP1 Gene Encodes a Putative Glutamate Carboxypeptidase. Plant Cell **13**: 2115–2126

Hemming MN, Peacock WJ, Dennis ES, Trevaskis B (2008) Low-temperature and daylength cues are integrated to regulate FLOWERING LOCUS T in barley. Plant Physiol **147**: 355–366

Hetz W, Hochholdinger F, Schwall M, Feix G (1996) Isolation and characterization of rtcs, a maize mutant deficient in the formation of nodal roots. Plant J **10**: 845–857

Higuchi M, Pischke MS, Mahonen AP, Miyawaki K, Hashimoto Y, Seki M, Kobayashi M, Shinozaki K, Kato T, Tabata S, et al (2004) In planta functions of the Arabidopsis cytokinin receptor family. Proc Natl Acad Sci **101**: 8821–8826

Hill WG, Robertson A (1968) Linkage disequilibrium in finite populations. Theor Appl Genet **38**: 226–231

Hochholdinger F (2004) Genetic Dissection of Root Formation in Maize (Zea mays) Reveals Root-type Specific Developmental Programmes. Ann Bot **93**: 359–368

Hong S-K, Aoki T, Kitano H, Satoh H, Nagato Y (1995) Phenotypic diversity of 188 rice embryo mutants. Dev Genet **16**: 298–310

Hong Z (2003) A Rice Brassinosteroid-Deficient Mutant, ebisu dwarf (d2), Is Caused by a Loss of Function of a New Member of Cytochrome P450. PLANT CELL ONLINE **15**: 2900–2910

Horton P (2000) Prospects for crop improvement through the genetic manipulation of photosynthesis: morphological and biochemical aspects of light capture. J Exp Bot **51**: 475–485

Hoskins PH, Poehlman JM (1971) Pleiotropic Effects of Uzu and Spike-Density Genes in a Barley Cross. J Hered **62**: 153–156

Huang BE, George AW, Forrest KL, Kilian A, Hayden MJ, Morell MK, Cavanagh CR (2012) A multiparent advanced generation inter-cross population for genetic analysis in wheat. Plant Biotechnol J **10**: 826–839

Hubisz MJ, Falush D, Stephens M, Pritchard JK (2009) Inferring weak population structure with the assistance of sample group information. Mol Ecol Resour **9**: 1322–1332

Hussien A, Tavakol E, Horner DS, Muñoz-Amatriaín M, Muehlbauer GJ, Rossini L (2014) Genetics of Tillering in Rice and Barley. Plant Genome **7**: 0

Ikeda-Kawakatsu K, Yasuno N, Oikawa T, Iida S, Nagato Y, Maekawa M, Kyozuka J (2009) Expression Level of ABERRANT PANICLE ORGANIZATION1 Determines Rice Inflorescence Form through Control of Cell Proliferation in the Meristem. Plant Physiol **150**: 736–747

Imaishi H, Matsuo S, Swai E, Ohkawa H (2000) CYP78A1 preferentially expressed in developing inflorescences of Zea mays encoded a cytochrome P450-dependent lauric acid 12-monooxygenase. Biosci Biotechnol Biochem **64**: 1696–1701

Inukai Y, Sakamoto T, Ueguchi-Tanaka M, Shibata Y, Gomi K, Umemura I, Hasegawa Y, Ashikari M, Kitano H, Matsuoka M (2005) Crown rootless1, which is essential for crown root formation in rice, is a target of an AUXIN RESPONSE FACTOR in auxin signaling. Plant Cell **17**: 1387–1396

Islam TMT, Sedgley RH (1981) Evidence for a “uniculm effect” in spring wheat (Triticum aestivum L.) in a mediterranean environment. Euphytica **30**: 277–282

Itoh J, Hasegawa A, Kitano H, Nagato Y (1998) A recessive heterochronic mutation, plastochron1, shortens the plastochron and elongates the vegetative phase in rice. Plant Cell **10**: 1511–1522

Itoh J-I, Nonomura K, Yamaki S, Inukai Y, Yamagishi H, Kitano H, Nagato Y (2005) Rice Plant Development: from Zygote to Spikelet. Plant Cell Physiol **46**: 23–47

Ivandic V, Malyshev S, Korzun V, Graner A, Börner A (1999) Comparative mapping of a gibberellic acid-insensitive dwarfing gene (Dwf2) on chromosome 4HS in barley. Theor Appl Genet **98**: 728–731

Jander G, Norris SR, Rounsley SD, Bush DF, Levin IM, Last RL (2002) Arabidopsis Map-Based Cloning in the Post-Genome Era. Plant Physiol **129**: 440–450

Jia Q, Zhang J, Westcott S, Zhang X-Q, Bellgard M, Lance R, Li C (2009) GA-20 oxidase as a candidate for the semidwarf gene sdw1/denso in barley. Funct Integr Genomics **9**: 255–262

Jones H, Leigh FJ, Mackay I, Bower MA, Smith LMJ, Charles MP, Jones G, Jones MK, Brown TA, Powell W (2008) Population-Based Resequencing Reveals That the Flowering Time Adaptation of Cultivated Barley Originated East of the Fertile Crescent. Mol Biol Evol **25**: 2211–2219

Jung M, Ching A, Bhattramakki D, Dolan M, Tingey S, Morgante M, Rafalski A (2004) Linkage disequilibrium and sequence diversity in a 500-kbp region around the adh1 locus in elite maize germplasm. TAG Theor Appl Genet Theor Angew Genet **109**: 681–689

Kai K, Hashidzume H, Yoshimura K, Suzuki H, Sakurai N, Shibata D, Ohta D (2009) Metabolomics for the characterization of cytochromes P450-dependent fatty acid hydroxylation reactions in Arabidopsis. Plant Biotechnol **26**: 175–182

Kaneko M, Itoh H, Inukai Y, Sakamoto T, Ueguchi-Tanaka M, Ashikari M, Matsuoka M (2003) Where do gibberellin biosynthesis and gibberellin signaling occur in rice plants? Plant J Cell Mol Biol **35**: 104–115

Karsai I, Szucs P, Mészáros K, Filichkina T, Hayes PM, Skinner JS, Láng L, Bedo Z (2005) The Vrn-H2 locus is a major determinant of flowering time in a facultative x winter growth habit barley (Hordeum vulgare L.) mapping population. TAG Theor Appl Genet Theor Angew Genet **110**: 1458–1466

Kawahara H, Chonan N, Wada K (1968) Interrelation of the growth among leaves, panicles and internodes, and a histological observation on the meristem of culm. Proc Crop Sci Soc Jpn 372–383

Kawata, Shimayama (1965) On the lateral root primordia formation in the crown roots of rice plants. Proc Crop Sci Soc Jpn 423–431

Kebrom TH, Burson BL, Finlayson SA (2006) Phytochrome B Represses Teosinte Branched1 Expression and Induces Sorghum Axillary Bud Outgrowth in Response to Light Signals. Plant Physiol **140**: 1109–1117

Kebrom TH, Spielmeyer W, Finnegan EJ (2013) Grasses provide new insights into regulation of shoot branching. Trends Plant Sci **18**: 41–48

Khush GS (2001) Green revolution: the way forward. Nat Rev Genet **2**: 815–822

Kirby E, Aplleyard M (1987) Cereal Development Guide., Second Edition. Arable Unit, Soneleigh, Warwickshare

Kirby EJM (1988) Analysis of leaf, stem and ear growth in wheat from terminal spikelet stage to anthesis. Field Crops Res **18**: 127–140

Kirby EJM, Appleyard M, Fellowes G (1985) Leaf emergence and tillering in barley and wheat. Agronmomie EDP Sci **5**: 193–200

Kirby EJM, Riggs TJ (1978a) Developmental consequences of two-row and six-row ear type in spring barley: 2. Shoot apex, leaf and tiller development. J Agric Sci **91**: 207–216

Kirby EJM, Riggs TJ (1978b) Developmental consequences of two-row and six-row ear type in spring barley: 2. Shoot apex, leaf and tiller development. J Agric Sci **91**: 207–216

Kjær B, Jensen J, Giese H (1995) Quantitative trait loci for heading date and straw characters in barley. Genome **38**: 1098–1104

Knapp SJ, Stroup WW, Ross WM (1985) Exact Confidence Intervals for Heritability on a Progeny Mean Basis. Crop Sci **25**: 192–194

De Koeyer DL, Tinker NA, Wight CP, Deyl J, Burrows VD, O'Donoughue LS, Lybaert A, Molnar SJ, Armstrong KC, Fedak G, et al (2004) A molecular linkage map with associated QTLs from a hulless × covered spring oat population. Theor Appl Genet **108**: 1285–1298

Komatsuda T, Maxim P, Senthil N, Mano Y (2004) High-density AFLP map of nonbrittle rachis 1 (btr1) and 2 (btr2) genes in barley (Hordeum vulgare L.). Theor Appl Genet **109**: 986–995

Komatsuda T, Pourkheirandish M, He C, Azhaguvel P, Kanamori H, Perovic D, Stein N, Graner A, Wicker T, Tagiri A, et al (2007) Six-rowed barley originated from a mutation in a homeodomain-leucine zipper I-class homeobox gene. Proc Natl Acad Sci **104**: 1424–1429

Komatsu K, Maekawa M, Ujiie S, Satake Y, Furutani I, Okamoto H, Shimamoto K, Kyozuka J (2003) LAX and SPA: Major regulators of shoot branching in rice. Proc Natl Acad Sci **100**: 11765–11770

Komatsu M, Maekawa M, Shimamoto K, Kyozuka J (2001) The LAX1 and FRIZZY PANICLE 2 Genes Determine the Inflorescence Architecture of Rice by Controlling Rachis-Branch and Spikelet Development. Dev Biol **231**: 364–373

Koppolu R, Anwar N, Sakuma S, Tagiri A, Lundqvist U, Pourkheirandish M, Rutten T, Seiler C, Himmelbach A, Ariyadasa R, et al (2013) Six-rowed spike4 (Vrs4) controls spikelet determinacy and row-type in barley. Proc Natl Acad Sci **110**: 13198–13203

Korner C, Pelaez M-RS, John P (1989) Why Are Bonsai Plants Small? A Consideration of Cell Size. Funct Plant Biol **16**: 443–448

Krouk G, Ruffel S, Gutiérrez RA, Gojon A, Crawford NM, Coruzzi GM, Lacombe B (2011) A framework integrating plant growth with hormones and nutrients. Trends Plant Sci **16**: 178–182

Kuroha T, Satoh S (2007) Involvement of cytokinins in adventitious and lateral root formation. Plant Root **1**: 27–33

Kwon CS (2005) WUSCHEL is a primary target for transcriptional regulation by SPLAYED in dynamic control of stem cell fate in Arabidopsis. Genes Dev **19**: 992–1003

Lander ES, Botstein D (1989) Mapping mendelian factors underlying quantitative traits using RFLP linkage maps. Genetics **121**: 185–199

Laplaze L, Benkova E, Casimiro I, Maes L, Vanneste S, Swarup R, Weijers D, Calvo V, Parizot B, Herrera-Rodriguez MB, et al (2007) Cytokinins Act Directly on Lateral Root Founder Cells to Inhibit Root Initiation. Plant Cell Online **19**: 3889–3900

Laurie DA, Pratchett N, Snape JW, Bezant JH (1995) RFLP mapping of five major genes and eight quantitative trait loci controlling flowering time in a winter x spring barley (Hordeum vulgare L.) cross. Genome Natl Res Counc Can Génome Cons Natl Rech Can **38**: 575–585

Li C, Dubcovsky J (2008) Wheat FT protein regulates VRN1 transcription through interactions with FDL2. Plant J Cell Mol Biol **55**: 543–554

Lieth H (2009) Salinity and Water Stress Improving Crop Efficiency. Springer, Dordrecht

Li JZ, Huang XQ, Heinrichs F, Ganal MW, Röder MS (2006) Analysis of QTLs for yield components, agronomic traits, and disease resistance in an advanced backcross population of spring barley. Genome **49**: 454–466

Linde-Laursen I, Heslop-Harrison JS, Shepherd KW, Taketa S (1997) The barley Genome and its Relationship with the Wheat Genomes. A Survey with an Internationally Agreed Recommendation for Barley Chromosome Nomenclature. Hereditas **126**: 1–16

Lin H, Wang R, Qian Q, Yan M, Meng X, Fu Z, Yan C, Jiang B, Su Z, Li J, et al (2009) DWARF27, an Iron-Containing Protein Required for the Biosynthesis of Strigolactones, Regulates Rice Tiller Bud Outgrowth. PLANT CELL ONLINE **21**: 1512–1525

Lin Q, Wang D, Dong H, Gu S, Cheng Z, Gong J, Qin R, Jiang L, Li G, Wang JL, et al (2012) Rice APC/CTE controls tillering by mediating the degradation of MONOCULM 1. Nat Commun **3**: 752

Lipka AE, Tian F, Wang Q, Peiffer J, Li M, Bradbury PJ, Gore MA, Buckler ES, Zhang Z (2012) GAPIT: genome association and prediction integrated tool. Bioinformatics **28**: 2397–2399

Liu H, Bayer M, Druka A, Russell JR, Hackett CA, Poland J, Ramsay L, Hedley PE, Waugh R (2014) An evaluation of genotyping by sequencing (GBS) to map the Breviaristatum-e (ari-e) locus in cultivated barley. BMC Genomics **15**: 104

Li X, Qian Q, Fu Z, Wang Y, Xiong G, Zeng D, Wang X, Liu X, Teng S, Hiroshi F, et al (2003) Control of tillering in rice. Nature **422**: 618–621

Li Y, Haseneyer G, Schön C-C, Ankerst D, Korzun V, Wilde P, Bauer E (2011) High levels of nucleotide diversity and fast decline of linkage disequilibrium in rye (Secale cereale L.) genes involved in frost response. BMC Plant Biol **11**: 6

Long J, Barton MK (2000) Initiation of Axillary and Floral Meristems in Arabidopsis. Dev Biol **218**: 341–353

López-Castañeda C, Richards RA (1994) Variation in temperate cereals in rainfed environments III. Water use and water-use efficiency. Field Crops Res **39**: 85–98

Lo S-F, Yang S-Y, Chen K-T, Hsing Y-I, Zeevaart JAD, Chen L-J, Yu S-M (2008) A Novel Class of Gibberellin 2-Oxidases Control Semidwarfism, Tillering, and Root Development in Rice. PLANT CELL ONLINE **20**: 2603–2618

Lukens L, Doebley J (2001) Molecular evolution of the teosinte branched gene among maize and related grasses. Mol Biol Evol **18**: 627–638

Lundqvist U, Franckowiak JD (2002) New and Revised Barley Genetic Stock Descriptions. Barley Genet Newsl **32**: 49–137

Lundqvist U, Franckowiak JD (1996) New and Revised Barley Genetic Stock Descriptions. Barley Genet Newsl 44–516

MacLeod AM, Palmer GH (1966) THE EMBRYO OF BARLEY IN RELATION TO MODIFICATION OF THE ENDOSPERM. J Inst Brew **72**: 580–589

Marquez-Cedillo LA, Hayes PM, Kleinhofs A, Legge WG, Rossnagel BG, Sato K, Ullrich SE, Wesenberg DM (2001) QTL analysis of agronomic traits in barley based on the doubled haploid progeny of two elite North American varieties representing different germplasm groups: Theor Appl Genet **103**: 625–637

Marshall C, Boyd WJR (1985) A comparison of the growth and development of biculm wheat lines with freely tillering cultivars. J Agric Sci **104**: 163–171

Mascher M, Jost M, Kuon J-E, Himmelbach A, Aßfalg A, Beier S, Scholz U, Graner A, Stein N (2014) Mapping-by-sequencing accelerates forward genetics in barley. Genome Biol **15**: R78

Mascher M, Muehlbauer GJ, Rokhsar DS, Chapman J, Schmutz J, Barry K, Muñoz-Amatriaín M, Close TJ, Wise RP, Schulman AH, et al (2013) Anchoring and ordering NGS contig assemblies by population sequencing (POPSEQ). Plant J **76**: 718–727

Mascher M, Richmond TA, Gerhardt DJ, Himmelbach A, Clissold L, Sampath D, Ayling S, Steuernagel B, Pfeifer M, D'Ascenzo M, et al (2013a) Barley whole exome capture: a tool for genomic research in the genus Hordeum and beyond. Plant J Cell Mol Biol **76**: 494–505

Mather KA, Caicedo AL, Polato NR, Olsen KM, McCouch S, Purugganan MD (2007) The Extent of Linkage Disequilibrium in Rice (Oryza sativa L.). Genetics **177**: 2223–2232

Matsumoto T, Tanaka T, Sakai H, Amano N, Kanamori H, Kurita K, Kikuta A, Kamiya K, Yamamoto M, Ikawa H, et al (2011) Comprehensive Sequence Analysis of 24,783 Barley Full-Length cDNAs Derived from 12 Clone Libraries. Plant Physiol **156**: 20–28

Matusova R, Rani K, Verstappen FWA, Franssen MCR, Beale MH, Bouwmeester HJ (2005) The Strigolactone Germination Stimulants of the Plant-Parasitic Striga and Orobanche spp. Are Derived from the Carotenoid Pathway. Plant Physiol **139**: 920–934

Mayer KFX, Martis M, Hedley PE, Simková H, Liu H, Morris JA, Steuernagel B, Taudien S, Roessner S, Gundlach H, et al (2011) Unlocking the barley genome by chromosomal and comparative genomics. Plant Cell **23**: 1249–1263

McCallum C, Comai L, Green E, Henikoff S (2000) Targeting Induced Local Lesion IN Genomes (TILLING) for plant functional genomics. Plant Physiol **123**: 439–442

McSteen P, Leyser O (2005) Shoot branching. Annu Rev Plant Biol **56**: 353–374

Merotto AJ, Mundstock C (1999) Wheat root growth as affected by soil strength. Rev Bras Ciênc Solo **23**: 197–202

Meyerowitz EM (1997) Control of Cell Division Patterns in Developing Shoots and Flowers of Arabidopsis thaliana. Cold Spring Harb Symp Quant Biol **62**: 369–375

Milhova G, Mihailov R, Tonev TK, Demirev V (2006) Correlation between traits related to lodging resistance in barley. Field Crops Stud **3**: 359–366

Minakuchi K, Kameoka H, Yasuno N, Umehara M, Luo L, Kobayashi K, Hanada A, Ueno K, Asami T, Yamaguchi S, et al (2010) FINE CULM1 (FC1) Works Downstream of Strigolactones to Inhibit the Outgrowth of Axillary Buds in Rice. Plant Cell Physiol **51**: 1127–1135

Miralles DJ, Slafer GA (2007) Sink limitations to yield in wheat: how could it be reduced? J Agric Sci **145**: 139

Mitchell JH (2010) Evaluation of reduced-tillering (tin gene) wheat lines for water limiting environments in Northern Australia. PhD Thesis. The University of Queensland, Australia.

Mitchell JH, Rebetzke GJ, Chapman SC, Fukai S (2013) Evaluation of reduced-tillering (tin) wheat lines in managed, terminal water deficit environments. J Exp Bot **64**: 3439–3451

Miyamoto N, Goto Y, Matsui M, Ukai Y, Morita M, Nemoto K (2004) Quantitative trait loci for phyllochron and tillering in rice. TAG Theor Appl Genet Theor Angew Genet **109**: 700–706

Miyoshi K, Ahn B-O, Kawakatsu T, Ito Y, Itoh J-I, Nagato Y, Kurata N (2004) PLASTOCHRON1, a timekeeper of leaf initiation in rice, encodes cytochrome P450. Proc Natl Acad Sci U S A **101**: 875–880

Mizutani M, Ohta D (2010) Diversification of P450 Genes During Land Plant Evolution. Annu Rev Plant Biol **61**: 291–315

Mori M, Nomura T, Ooka H, Ishizaka M, Yokota T, Sugimoto K, Okabe K, Kajiwara H, Satoh K, Yamamoto K, et al (2002) Isolation and characterization of a rice dwarf mutant with a defect in brassinosteroid biosynthesis. Plant Physiol **130**: 1152–1161

Morrell PL, Clegg MT (2007) Genetic evidence for a second domestication of barley (Hordeum vulgare) east of the Fertile Crescent. Proc Natl Acad Sci U S A **104**: 3289–3294

Mouchel CF, Briggs GC, Hardtke CS (2004) Natural genetic variation in Arabidopsis identifies BREVIS RADIX, a novel regulator of cell proliferation and elongation in the root. Genes Dev **18**: 700–714

Muday GK, Rahman A, Binder BM (2012) Auxin and ethylene: collaborators or competitors? Trends Plant Sci **17**: 181–195

Müller KJ, Romano N, Gerstner O, Garcia-Maroto F, Pozzi C, Salamini F, Rohde W (1995) The barley Hooded mutation caused by a duplication in a homeobox gene intron. Nature **374**: 727–730

Mussig, Shin, Altmann (2003) Brassinosteroids promote root growth in Arabidopsis. Plant Physiol 1261–1271

Nair SK, Wang N, Turuspekov Y, Pourkheirandish M, Sinsuwongwat S, Chen G, Sameri M, Tagiri A, Honda I, Watanabe Y, et al (2010) Cleistogamous flowering in barley arises from the suppression of microRNA-guided HvAP2 mRNA cleavage. Proc Natl Acad Sci **107**: 490–495

Naz A, Arifuzzaman M, Muzammil S, Pillen K, Léon J (2014) Wild barley introgression lines revealed novel QTL alleles for root and related shoot traits in the cultivated barley (Hordeum vulgare L.). BMC Genet **15**: 107

Nemhauser JL, Mockler TC, Chory J (2004) Interdependency of Brassinosteroid and Auxin Signaling in Arabidopsis. PLoS Biol **2**: e258

Nice L (2013) Characterization of a Wild Barley Multiparent Advanced Backcross Population.

Nordborg M (2000) Linkage disequilibrium, gene trees and selfing: an ancestral recombination graph with partial self-fertilization. Genetics **154**: 923–929

Norden A., Frey K. (1970) [Factors associated with lodging resistance in oats. Agron J **51**: 561–568

Ohashi J, Yamamoto S, Tsuchiya N, Hatta Y, Komata T, Matsushita M, Tokunaga K (2001) Comparison of statistical power between 2 * 2 allele frequency and allele positivity tables in case-control studies of complex disease genes. Ann Hum Genet **65**: 197–206

Oikawa T, Kyozuka J (2009) Two-Step Regulation of LAX PANICLE1 Protein Accumulation in Axillary Meristem Formation in Rice. PLANT CELL ONLINE **21**: 1095–1108

Okagaki RJ, Cho S, Kruger WM, Xu WW, Heinen S, Muehlbauer GJ (2013) The barley UNICULM2 gene resides in a centromeric region and may be associated with signaling and stress responses. Funct Integr Genomics **13**: 33–41

O'Neill DP (2002) Auxin Regulation of the Gibberellin Pathway in Pea. PLANT Physiol **130**: 1974–1982

Ookawa T, Hobo T, Yano M, Murata K, Ando T, Miura H, Asano K, Ochiai Y, Ikeda M, Nishitani R, et al (2010) New approach for rice improvement using a pleiotropic QTL gene for lodging resistance and yield. Nat Commun **1**: 132

Van Oosterom EJ, Acevedo E (1992) Adaptation of barley (Hordeum vulgare L.) to harsh Mediterranean environments. Euphytica **62**: 29–38

Orman-Ligeza B, Parizot B, Gantet PP, Beeckman T, Bennett MJ, Draye X (2013) Post-embryonic root organogenesis in cereals: branching out from model plants. Trends Plant Sci **18**: 459–467

Pacheco I, Bassi D, Eduardo I, Ciacciulli A, Pirona R, Rossini L, Vecchietti A (2014) QTL mapping for brown rot (Monilinia fructigena) resistance in an intraspecific peach (Prunus persica L. Batsch) F1 progeny. Tree Genet Genomes **10**: 1223–1242

Parkinson J, Blaxter M (2009) Expressed Sequence Tags: An Overview. *In* J Parkinson, ed, Expressed Seq. Tags ESTs. Humana Press, pp 1–12

Pasam RK, Sharma R, Malosetti M, van Eeuwijk FA, Haseneyer G, Kilian B, Graner A (2012) Genome-wide association studies for agronomical traits in a world wide spring barley collection. BMC Plant Biol **12**: 16

Pearce S, Saville R, Vaughan SP, Chandler PM, Wilhelm EP, Sparks CA, Al-Kaff N, Korolev A, Boulton MI, Phillips AL, et al (2011) Molecular characterization of Rht-1 dwarfing genes in hexaploid wheat. Plant Physiol **157**: 1820–1831

De la Pena RC, Smith KP, Capettini F, Muehlbauer GJ, Gallo-Meagher M, Dill-Macky R, Somers DA, Rasmusson DC (1999) Quantitative trait loci associated with resistance to Fusarium head blight and kernel discoloration in barley. TAG Theor Appl Genet Theor Angew Genet **99**: 561–569

Peng J, Richards DE, Hartley NM, Murphy GP, Devos KM, Flintham JE, Beales J, Fish LJ, Worland AJ, Pelica F, et al (1999) "Green revolution" genes encode mutant gibberellin response modulators. Nature **400**: 256–261

Peng S, Khush GS, Virk P, Tang Q, Zou Y (2008) Progress in ideotype breeding to increase rice yield potential. Field Crops Res **108**: 32–38

Peterson KM, Rychel AL, Torii KU (2010) Out of the Mouths of Plants: The Molecular Basis of the Evolution and Diversity of Stomatal Development. Plant Cell **22**: 296–306

Petricka JJ, Winter CM, Benfey PN (2012) Control of Arabidopsis root development. Annu Rev Plant Biol **63**: 563–590

Piffanelli P, Ramsay L, Waugh R, Benabdelmouna A, D'Hont A, Hollricher K, Jørgensen JH, Schulze-Lefert P, Panstruga R (2004) A barley cultivation-associated polymorphism conveys resistance to powdery mildew. Nature **430**: 887–891

Pirinen M, Donnelly P, Spencer CCA (2012) Including known covariates can reduce power to detect genetic effects in case-control studies. Nat Genet **44**: 848–851

Poorter H, Niklas KJ, Reich PB, Oleksyn J, Poot P, Mommer L (2012) Biomass allocation to leaves, stems and roots: meta-analyses of interspecific variation and environmental control. New Phytol **193**: 30–50

Powell AE, Lenhard M (2012) Control of Organ Size in Plants. Curr Biol **22**: R360–R367

Pozzi C, di Pietro D, Halas G, Roig C, Salamini F (2003a) Integration of a barley (Hordeum vulgare) molecular linkage map with the position of genetic loci hosting 29 developmental mutants. Heredity **90**: 390–396

Qi X, Niks RE, Stam P, Lindhout P (1998) Identification of QTLs for partial resistance to leaf rust (Puccinia hordei) in barley. Theor Appl Genet **96**: 1205–1215

Rafalski JA (2010) Association genetics in crop improvement. Curr Opin Plant Biol **13**: 174–180

Ramírez-Carvajal GA, Morse AM, Dervinis C, Davis JM (2009) The cytokinin type-B response regulator PtRR13 is a negative regulator of adventitious root development in Populus. Plant Physiol **150**: 759–771

Ramsay L, Comadran J, Druka A, Marshall DF, Thomas WTB, Macaulay M, MacKenzie K, Simpson C, Fuller J, Bonar N, et al (2011) INTERMEDIUM-C, a modifier of lateral spikelet fertility in barley, is an ortholog of the maize domestication gene TEOSINTE BRANCHED 1. Nat Genet **43**: 169–172

Rasmussen A, Beveridge CA, Geelen D (2012a) Inhibition of strigolactones promotes adventitious root formation. Plant Signal Behav **7**: 694–697

Rasmussen A, Mason MG, De Cuyper C, Brewer PB, Herold S, Agusti J, Geelen D, Greb T, Goormachtig S, Beeckman T, et al (2012b) Strigolactones suppress adventitious rooting in Arabidopsis and pea. Plant Physiol **158**: 1976–1987

Rasmusson DC (1991) A plant breeder's experience with ideotype breeding. Ideotypes Physiol Tailoring Plants Increased Prod **26**: 191–200

Rasmusson DC (1987) An Evaluation of Ideotype Breeding. Crop Sci **27**: 1140

Rebouillat J, Dievart A, Verdeil JL, Escoute J, Giese G, Breitler JC, Gantet P, Espeout S, Guiderdoni E, Périn C (2009) Molecular Genetics of Rice Root Development. Rice **2**: 15–34

Reynolds M, Dreccer F, Trethowan R (2006) Drought-adaptive traits derived from wheat wild relatives and landraces. J Exp Bot **58**: 177–186

Richards R (1988) A tiller inhibitor gene in wheat and its effect on plant growth. Aust J Agric Res **39**: 749

Richards R, Townley-Smith T (1987) Variation in leaf area development and its effect on water use, yield and harvest index of droughted wheat. Aust J Agric Res **38**: 983

Rich SM, Watt M (2013) Soil conditions and cereal root system architecture: review and considerations for linking Darwin and Weaver. J Exp Bot **64**: 1193–1208

Riefler M, Novak O, Strnad M, Schmülling T (2006) Arabidopsis cytokinin receptor mutants reveal functions in shoot growth, leaf senescence, seed size, germination, root development, and cytokinin metabolism. Plant Cell **18**: 40–54

Ringner M (2008) What is principal component analysis? Nat Biotech **26**: 303–304

Robinson D (1994) The responses of plants to non-uniform supplies of nutrients. New Phytol **127**: 635–674

Rossini L, Okagaki R, Druka A, Muehlbauer GJ (2014) Shoot and Inflorescence Architecture. *In* J Kumlehn, N Stein, eds, Biotechnol. Approaches Barley Improv. Springer Berlin Heidelberg, Berlin, Heidelberg, pp 55–80

Rostoks N, Ramsay L, MacKenzie K, Cardle L, Bhat PR, Roose ML, Svensson JT, Stein N, Varshney RK, Marshall DF, et al (2006) Recent history of artificial outcrossing facilitates whole-genome association mapping in elite inbred crop varieties. Proc Natl Acad Sci **103**: 18656–18661

Rudall PJ, Stuppy W, Cunniff J, Kellogg EA, Briggs BG (2005) Evolution of reproductive structures in grasses (Poaceae) inferred by sister-group comparison with their putative closest living relatives, Ecdeiocoleaceae. Am J Bot **92**: 1432–1443

Saisho D, Tanno K, Chono M, Honda I, Kitano H, Takeda K (2004) Spontaneous Brassinolide-insensitive Barley Mutants “uzu” Adapted to East Asia. Breed Sci **54**: 409–416

Sakamoto T, Matsuoka M (2004) Generating high-yielding varieties by genetic manipulation of plant architecture. Curr Opin Biotechnol **15**: 144–147

Sakuma S, Salomon B, Komatsuda T (2011) The Domestication Syndrome Genes Responsible for the Major Changes in Plant Form in the Triticeae Crops. Plant Cell Physiol **52**: 738–749

Salamini F, Ozkan H, Brandolini A, Schäfer-Pregl R, Martin W (2002) Genetics and geography of wild cereal domestication in the near east. Nat Rev Genet **3**: 429–441

Salim M, Todd G, Schlenhuber A (1965) Root development of wheat, oats and barley under conditions of soil moisture stress. Agron J **57**: 603–607

Sameri M, Pourkheirandish M, Chen G, Tonooka T, Komatsuda T (2011) Detection of photoperiod responsive and non-responsive flowering time QTL in barley. Breed Sci **61**: 183–188

Sawers RJH, Sheehan MJ, Brutnell TP (2005) Cereal phytochromes: targets of selection, targets for manipulation? Trends Plant Sci **10**: 138–143

Scarpella E, Rueb S, Meijer AH (2003) The RADICLELESS1 gene is required for vascular pattern formation in rice. Dev Camb Engl **130**: 645–658

Schiefelbein JW (2000) Constructing a Plant Cell. The Genetic Control of Root Hair Development. Plant Physiol **124**: 1525–1531

Schmitt J, Stinchcombe JR, Heschel MS, Huber H (2003) The adaptive evolution of plasticity: phytochrome-mediated shade avoidance responses. Integr Comp Biol **43**: 459–469

Schmitz G, Theres K (2005) Shoot and inflorescence branching. Curr Opin Plant Biol **8**: 506–511

Schulte D, Close TJ, Graner A, Langridge P, Matsumoto T, Muehlbauer G, Sato K, Schulman AH, Waugh R, Wise RP, et al (2009) The International Barley Sequencing Consortium—At the Threshold of Efficient Access to the Barley Genome. Plant Physiol **149**: 142–147

Schulze TG, McMahon FJ (2002) Genetic association mapping at the crossroads: Which test and why? Overview and practical guidelines. Am J Med Genet **114**: 1–11

Seavers GP, Wright KJ (1999) Crop canopy development and structure influence weed suppression. Weed Res **39**: 319–328

Sharman B (1942) Sharman BC (1942) Developmental anatomy of the shoot of Zea mays L. Ann Bot 6:245-282. Ann Bot **6**: 245–282

Sharp RE, Poroyko V, Hejlek LG, Spollen WG, Springer GK, Bohnert HJ, Nguyen HT (2004) Root growth maintenance during water deficits: physiology to functional genomics. J Exp Bot **55**: 2343–2351

Shashidhar HE (2012) PVC tubes to characterize roots and shoots to complement field plant productivity studies. Methodol. Root Drought Stud. Rice

Shitsukawa N, Kinjo H, Takumi S, Murai K (2009) Heterochronic development of the floret meristem determines grain number per spikelet in diploid, tetraploid and hexaploid wheats. Ann Bot **104**: 243–251

Siddique KHM, Kirby EJM, Perry MW (1989) Ear: Stem ratio in old and modern wheat varieties; relationship with improvement in number of grains per ear and yield. Field Crops Res **21**: 59–78

Skinner RH, Nelson CJ (1992) Estimation of Potential Tiller Production and Site Usage During Tall Fescue Canopy Development. Ann Bot **70**: 493–499

Slafer GA (2003) Genetic basis of yield as viewed from a crop physiologist's perspective. Ann Appl Biol **142**: 117–128

Slafer GA, Abeledo LG, Miralles DJ, Gonzalez FG, Whitechurch EM (2001) Photoperiod sensitivity during stem elongation as an avenue to raise potential yield in wheat. Euphytica **119**: 191–197

Slatkin M (2008) Linkage disequilibrium--understanding the evolutionary past and mapping the medical future. Nat Rev Genet **9**: 477–485

Sreenivasulu N, Schnurbusch T (2012) A genetic playground for enhancing grain number in cereals. Trends Plant Sci **17**: 91–101

Stadler LJ (1928) MUTATIONS IN BARLEY INDUCED BY X-RAYS AND RADIUM. Science **68**: 186–187

Steffens B, Wang J, Sauter M (2006) Interactions between ethylene, gibberellin and abscisic acid regulate emergence and growth rate of adventitious roots in deepwater rice. Planta **223**: 604–612

Stepanova AN, Alonso JM (2009) Ethylene signaling and response: where different regulatory modules meet. Curr Opin Plant Biol **12**: 548–555

Stracke S, Haseneyer G, Veyrieras J-B, Geiger HH, Sauer S, Graner A, Piepho H-P (2009) Association mapping reveals gene action and interactions in the determination of flowering time in barley. Theor Appl Genet **118**: 259–273

Studer A, Zhao Q, Ross-Ibarra J, Doebley J (2011) Identification of a functional transposon insertion in the maize domestication gene tb1. Nat Genet **43**: 1160–1163

Szucs P, Skinner JS, Karsai I, Cuesta-Marcos A, Haggard KG, Corey AE, Chen THH, Hayes PM (2007) Validation of the VRN-H2/VRN-H1 epistatic model in barley reveals that intron length variation in VRN-H1 may account for a continuum of vernalization sensitivity. Mol Genet Genomics MGG **277**: 249–261

Tabuchi H, Zhang Y, Hattori S, Omae M, Shimizu-Sato S, Oikawa T, Qian Q, Nishimura M, Kitano H, Xie H, et al (2011) LAX PANICLE2 of Rice Encodes a Novel Nuclear Protein and Regulates the Formation of Axillary Meristems. PLANT CELL ONLINE **23**: 3276–3287

Takahashi H (1997) Hydrotropism: the current state of our knowledge. J Plant Res **110**: 163–169

Takahashi R, Yasuda S (1971) Genetics of earliness and growth habit in barley. Barley Genetics II, Proc. Second Int. Barley Genetics Symp., Pullman, 1969. (Ed. R. A. Nilan). p. 388-408. Barley Genet. II Proceeding Second Int. Barley Genet. Symp. Washington State University Press, Pullmann, pp 388–408

Takeda T, Suwa Y, Suzuki M, Kitano H, Ueguchi-Tanaka M, Ashikari M, Matsuoka M, Ueguchi C (2003) The OsTB1 gene negatively regulates lateral branching in rice. Plant J **33**: 513–520

Taketa S, Amano S, Tsujino Y, Sato T, Saisho D, Kakeda K, Nomura M, Suzuki T, Matsumoto T, Sato K, et al (2008) Barley grain with adhering hulls is controlled by an ERF family transcription factor gene regulating a lipid biosynthesis pathway. Proc Natl Acad Sci U S A **105**: 4062–4067

Talamè V, Bovina R, Sanguineti MC, Tuberosa R, Lundqvist U, Salvi S (2008) TILLMore, a resource for the discovery of chemically induced mutants in barley: A new TILLING resource in barley. Plant Biotechnol J **6**: 477–485

Tanksley SD, Ganal MW, Martin GB (1995) Chromosome landing: a paradigm for map-based gene cloning in plants with large genomes. Trends Genet **11**: 63–68

Tanksley SD, McCouch SR (1997) Seed banks and molecular maps: unlocking genetic potential from the wild. Science **277**: 1063–1066

Tenaillon MI, Sawkins MC, Long AD, Gaut RL, Doebley JF, Gaut BS (2001) Patterns of DNA sequence polymorphism along chromosome 1 of maize (Zea mays ssp. mays L.). Proc Natl Acad Sci U S A **98**: 9161–9166

The International Barley Genome Sequencing Consortium (2012) A physical, genetic and functional sequence assembly of the barley genome. Nature **491**: 711–716

The R development Core Team (2008) Development Core Team, R: A language and environment for statistical computing. R Foundation for Statistical Computing, Vienna, Austria. ISBN 3-900051-07-0.

Thomas WTB, Powell W, Wood W (1984) The chromosomal location of the dwarfing gene present in the spring barley variety golden promise. Heredity **53**: 177–183

Tian H, De Smet I, Ding Z Shaping a root system: regulating lateral versus primary root growth. Trends Plant Sci **19**: 426–431

Tommasini L, Schnurbusch T, Fossati D, Mascher F, Keller B (2007) Association mapping of Stagonospora nodorum blotch resistance in modern European winter wheat varieties. TAG Theor Appl Genet Theor Angew Genet **115**: 697–708

Tomoshiro T, Mitsunori O, Waichi A (1983) Comparison of the formation of dry substance by the old and new type of rice cultivars. Jpn J Crop Sci **52**: 299–305

Tondelli A, Xu X, Moragues M, Sharma R, Schnaithmann F, Ingvardsen C, Manninen O, Comadran J, Russell J, Waugh R, et al (2013) Structural and Temporal Variation in Genetic Diversity of European Spring Two-Row Barley Cultivars and Association Mapping of Quantitative Traits. Plant Genome **6**: 0

Tong H, Jin Y, Liu W, Li F, Fang J, Yin Y, Qian Q, Zhu L, Chu C (2009) DWARF AND LOW-TILLERING, a new member of the GRAS family, plays positive roles in brassinosteroid signaling in rice. Plant J **58**: 803–816

Trevaskis B (2006) HvVRN2 Responds to Daylength, whereas HvVRN1 Is Regulated by Vernalization and Developmental Status. PLANT Physiol **140**: 1397–1405

Tsuchiya T (1976) Allelism Testing in Barley. II. Allelic Relationships of Three Uzu Genes1. Crop Sci **16**: 496

Turner A (2005) The Pseudo-Response Regulator Ppd-H1 Provides Adaptation to Photoperiod in Barley. Science **310**: 1031–1034

Turner SD (2014) qqman: an R package for visualizing GWAS results using Q-Q and manhattan plots.

Ullrich SE, ed (2010) Significance, Adptation, Production and Trade of Barley. Barley Prod. Improv. Uses. Wiley-Blackwell, Oxford, UK, p 3

Umehara M, Hanada A, Yoshida S, Akiyama K, Arite T, Takeda-Kamiya N, Magome H, Kamiya Y, Shirasu K, Yoneyama K, et al (2008) Inhibition of shoot branching by new terpenoid plant hormones. Nature **455**: 195–200

VanRaden PM (2008) Efficient Methods to Compute Genomic Predictions. J Dairy Sci **91**: 4414–4423

Waddington SR, Cartwright PM, Wall PC (1983) A Quantitative Scale of Spike Initial and Pistil Development in Barley and Wheat. Ann Bot **51**: 119–130

Wang G, Schmalenbach I, von Korff M, Léon J, Kilian B, Rode J, Pillen K (2010) Association of barley photoperiod and vernalization genes with QTLs for flowering time and agronomic traits in a BC2DH population and a set of wild barley introgression lines. Theor Appl Genet **120**: 1559–1574

Wang Y, Li J (2008) Molecular Basis of Plant Architecture. Annu Rev Plant Biol **59**: 253–279

Wang Y, Li J (2006) Genes controlling plant architecture. Curr Opin Biotechnol **17**: 123–129

Wang Z, Gerstein M, Snyder M (2009) RNA-Seq: a revolutionary tool for transcriptomics. Nat Rev Genet **10**: 57–63

Weatherwax P (1923) The story of the maize plant. University of Chicago Press

Weber H (2002) Fatty acid-derived signals in plants. Trends Plant Sci **7**: 217–224

Welander NT, Ottosson B (1997) Influence of photosynthetic photon flux density on growth and transpiration in seedlings of Fagus sylvatica. Tree Physiol **17**: 133–140

Werner T (2003) Cytokinin-Deficient Transgenic Arabidopsis Plants Show Multiple Developmental Alterations Indicating Opposite Functions of Cytokinins in the Regulation of Shoot and Root Meristem Activity. PLANT CELL ONLINE **15**: 2532–2550

Werner T, Motyka V, Laucou V, Smets R, Van Onckelen H, Schmülling T (2003a) Cytokinin-Deficient Transgenic Arabidopsis Plants Show Multiple Developmental Alterations Indicating Opposite Functions of Cytokinins in the Regulation of Shoot and Root Meristem Activity. Plant Cell Online **15**: 2532–2550

Werner T, Motyka V, Laucou V, Smets R, Van Onckelen H, Schmülling T (2003b) Cytokinin-Deficient Transgenic Arabidopsis Plants Show Multiple Developmental Alterations Indicating Opposite Functions of Cytokinins in the Regulation of Shoot and Root Meristem Activity. Plant Cell Online **15**: 2532–2550

Whipple CJ, Kebrom TH, Weber AL, Yang F, Hall D, Meeley R, Schmidt R, Doebley J, Brutnell TP, Jackson DP (2011) grassy tillers1 promotes apical dominance in maize and responds to shade signals in the grasses. Proc Natl Acad Sci **108**: E506–E512

Wicker T, Taudien S, Houben A, Keller B, Graner A, Platzer M, Stein N (2009) A whole-genome snapshot of 454 sequences exposes the composition of the barley genome and provides evidence for parallel evolution of genome size in wheat and barley. Plant J Cell Mol Biol **59**: 712–722

Wilkinson MD, Haughn GW (1995) UNUSUAL FLORAL ORGANS Controls Meristem Identity and Organ Primordia Fate in Arabidopsis. Plant Cell Online **7**: 1485–1499

Winham SJ, Cuellar-Barboza AB, Oliveros A, McElroy SL, Crow S, Colby C, Choi D-S, Chauhan M, Frye M, Biernacka JM (2014) Genome-wide association study of bipolar disorder accounting for effect of body mass index identifies a new risk allele in TCF7L2. Mol Psychiatry **19**: 1010–1016

Woll K, Borsuk L, Stransky H, Nettleton D, Shnable P, Hocnholdinger F (2005) Isolation, characterization, and pericycle-specific transcriptome analyses of the novel maize lateral and seminal root initiation mutant rum1. Plant Physiology 139: 1255–1267. Plant Physiol 1255–1267

Würschum T, Langer S, Longin CF, Korzun V, Akhunov E, Ebmeyer E, Schachschneider R, Schacht J, Kazman E, Reif J (2013) Population structure, genetic diversity and linkage disequilibrium in elite winter wheat assessed with SNP and SSR markers. Theor Appl Genet **126**: 1477–1486

Xu C, Wang Y, Yu Y, Duan J, Liao Z, Xiong G, Meng X, Liu G, Qian Q, Li J (2012) Degradation of MONOCULM 1 by APC/CTAD1 regulates rice tillering. Nat Commun **3**: 750

Yan J, Shah T, Warburton ML, Buckler ES, McMullen MD, Crouch J (2009) Genetic Characterization and Linkage Disequilibrium Estimation of a Global Maize Collection Using SNP Markers. PLoS ONE **4**: e8451

Yan L, Fu D, Li C, Blechl A, Tranquilli G, Bonafede M, Sanchez A, Valarik M, Yasuda S, Dubcovsky J (2006) The wheat and barley vernalization gene VRN3 is an orthologue of FT. Proc Natl Acad Sci **103**: 19581–19586

Yan L, von Zitzewitz J, Skinner JS, Hayes PM, Dubcovsky J (2005) Molecular characterization of the duplicated meristem identity genes HvAP1a and HvAP1b in barley. Genome **48**: 905–912

Yoshida A, Ohmori Y, Kitano H, Taguchi-Shiobara F, Hirano H-Y (2012) ABERRANT SPIKELET AND PANICLE1, encoding a TOPLESS-related transcriptional co-repressor, is involved in the regulation of meristem fate in rice: Function of the TOPLESS-like gene in rice. Plant J **70**: 327–339

Yu J, Pressoir G, Briggs WH, Vroh Bi I, Yamasaki M, Doebley JF, McMullen MD, Gaut BS, Nielsen DM, Holland JB, et al (2006) A unified mixed-model method for association mapping that accounts for multiple levels of relatedness. Nat Genet **38**: 203–208

Yunusa IAM, Sedgley RH (1992) Reduced Tillering Spring Wheats for Heavy Textured Soils in a Semi-arid Mediterranean Environment. J Agron Crop Sci **168**: 159–168

Zadocks JC, Chang TT, Konzak CF (1974) A decimal code for the growth stages of cereals. Weed Res **14**: 415–421

Zazimalova E, Murphy AS, Yang H, Hoyerova K, Hosek P (2010) Auxin Transporters--Why So Many? Cold Spring Harb Perspect Biol **2**: a001552–a001552

Zhang D, Bai G, Zhu C, Yu J, Carver BF (2010) Genetic Diversity, Population Structure, and Linkage Disequilibrium in U.S. Elite Winter Wheat. Plant Genome J **3**: 117

Zhang P (2005) MetaCyc and AraCyc. Metabolic Pathway Databases for Plant Research. PLANT Physiol **138**: 27–37

Zhang S-W, Li C-H, Cao J, Zhang Y-C, Zhang S-Q, Xia Y-F, Sun D-Y, Sun Y (2009) Altered Architecture and Enhanced Drought Tolerance in Rice via the Down-Regulation of Indole-3-Acetic Acid by TLD1/OsGH3.13 Activation. PLANT Physiol **151**: 1889–1901

Zhou M, Johnson P, Zhou G, Li C, Lance R (2012) Quantitative Trait Loci for Waterlogging Tolerance in a Barley Cross of Franklin × YuYaoXiangTian Erleng and the Relationship Between Waterlogging and Salinity Tolerance. Crop Sci **52**: 2082

Zhu C, Gore M, Buckler ES, Yu J (2008) Status and Prospects of Association Mapping in Plants. Plant Genome J **1**: 5

Zhu X-G, Long SP, Ort DR (2010) Improving Photosynthetic Efficiency for Greater Yield. Annu Rev Plant Biol **61**: 235–261

Von Zitzewitz J, Szucs P, Dubcovsky J, Yan L, Francia E, Pecchioni N, Casas A, Chen THH, Hayes PM, Skinner JS (2005) Molecular and structural characterization of barley vernalization genes. Plant Mol Biol **59**: 449–467